SEMICOVALENT SYNTHESIS OF MOLECULARLY IMPRINTED POLYMERS FOR CHOLESTEROL AND ENGINEERING OF METAL BINDING POLYMERS FOR BIOLOGICAL AND BIOPHYSICAL STUDIES

SOMCHAI BOONPANGRAK

**A THESIS SUBMITTED IN PARTIAL FULFILLMENT
OF THE REQUIREMENTS FOR
THE DEGREE OF DOCTOR OF PHILOSOPHY
(MEDICAL TECHNOLOGY)
FACULTY OF GRADUATE STUDIES
MAHIDOL UNIVERSITY
2006**

ISBN 974-04-7526-4

Thesis
entitled

SEMICOVALENT SYNTHESIS OF MOLECULARLY IMPRINTED POLYMERS FOR CHOLESTEROL AND ENGINEERING OF METAL BINDING POLYMERS FOR BIOLOGICAL AND BIOPHYSICAL STUDIES

Somchai Boonpangrak
.....
Mr. Somchai Boonpangrak
Candidate

Virapong P.
.....
Assoc. Prof. Virapong Prachayasittikul
Ph.D.(Microbiology)
Major-Advisor

Srisurang Tantimavanich
.....
Assoc. Prof. Srisurang Tantimavanich
Ph.D.(Microbiology)
Co-Advisor

C. Isarankura
.....
Asst.Prof. Chartchalerm Isarankura Na Ayudhya
Ph.D.(Medical Technology)
Co-Advisor

Svasti
.....
Prof. M.R. Jisnuson Svasti
Ph.D.
Dean
Faculty of Graduate Studies

Virapong P.
.....
Assoc. Prof. Virapong Prachayasittikul
Ph.D.
Chair
Doctor of Philosophy Programme in
Medical Technology
Faculty of Medical Technology

Thesis
entitled

SEMICOVALENT SYNTHESIS OF MOLECULARLY IMPRINTED POLYMERS FOR CHOLESTEROL AND ENGINEERING OF METAL BINDING POLYMERS FOR BIOLOGICAL AND BIOPHYSICAL STUDIES

was submitted to the Faculty of Graduate Studies, Mahidol University
for the degree of Doctor of Philosophy (Medical Technology)
on
July 17, 2006

Somchai Boonpangrak
.....
Mr. Somchai Boonpangrak
Candidate

Virapong P.
.....
Assoc.Prof.Virapong Prachayasittikul,
Ph.D.
Chair

Somsak Ruchirawat
.....
Prof.Somsak Ruchirawat,
Ph.D.
Member

Srisurang Tantimavanich
.....
Assoc.Prof.Srisurang Tantimavanich,
Ph.D.
Member

Ratana Lawung
.....
Ratana Lawung,
Ph.D.
Member

C. Isarankura
.....
Asst.Prof.Chartchalerm Isarankura Na Ayudhya,
Ph.D.
Member

Jisnuson Svasti
.....
Prof. M.R. Jisnuson Svasti,
Ph.D.
Dean
Faculty of Graduate Studies
Mahidol University

Somchai
.....
Assoc.Prof.Chatchai Sornchai,
M.D.
Dean
Faculty of Medical Technology
Mahidol University

ACKNOWLEDGEMENTS

I would like to thank Associate Professor Dr. Virapong Prachayasittikul, my advisor, for giving me constant advice throughout this study, teaching me how to make myself happy and never ending of love to me. I would also like to thank to Assistant Professor Dr. Chartchalerm Isarankura Na Ayudhya, my co-advisor for his valuable advice. I am grateful to Associate Professor Dr. Srisurang Tantimavanich, Dr. Rattana Lawang and Prof. Dr. Somsak Ruchirawat for their comments, suggestions and as my examination committee.

I am grateful to all of those of the Department of Pure and Applied Biochemistry, Chemical center, Lund University especially, Professor Dr. Leif Bülow and Dr. Lei Ye for giving me opportunity to work in the department and their support. I wish to thank to all members of the department particularly, imprinting groups and Ingrid Nelsson for their warm welcome and help.

I also want to thank members of the Faculty of Medical Technology, Mahidol University for their assistance and friendliness.

Particular acknowledgments go to the Thailand Research Fund for granting me the Royal Golden Jubilee Ph.D Scholarship throughout the Ph.D. program.

I am grateful to all of those of my research group as well as all my colleagues and friends for friendship and moral support. Special thanks are also convey to Mr. Benjapol Samranthin for his helpful assistances and cheering me up.

Finally, I am very grateful to my family, Papa, Mama, my sisters and all of my teachers who provide teaching along the milestone of my life. Thanks all for never-ending of love and understanding.

Somchai Boonpangrak

SEMICOVALENT SYNTHESIS OF MOLECULARLY IMPRINTED POLYMERS FOR CHOLESTEROL AND ENGINEERING OF METAL BINDING POLYMERS FOR BIOLOGICAL AND BIOPHYSICAL STUDIES

SOMCHAI BOONPANGRAK 4136468 MTMT/D

Ph.D. (MEDICAL TECHNOLOGY)

THESIS ADVISORS: VIRAPONG PRACHAYASITTIKUL (Ph.D.), CHARTCHALERM ISARANKURA NA AYUDHYA (Ph.D.), SRISURANG TANTIMAVANICH (Ph.D.)

ABSTRACT

This thesis reports the construction of molecularly imprinted polymers designed to recognize of cholesterol by using the molecular imprinting technique. Semicovalent imprinting in combination with either precipitation polymerization or nitroxide mediated radical polymerization was used. For the former, the results reveal the cholesterol imprinted microsphere polymer prepared by divinyl benzene (DVB) as a cross linker was larger, had a more defined spherical shape and a higher imprinting effect (3 times) than that prepared by ethylene glycol dimethacrylate (EDMA). Because of the small particle size of DVB based microsphere polymers, template removal from imprinted polymer microspheres was easily performed upon hydrolysis. For the latter, the binding capability of the nitroxide-based polymer MIP(NMP)-H (hydrolyzed) to cholesterol was approximately 6 and 3 times higher than those of the two controls of MIP(NMP)-UH (unhydrolyzed) and the NIP(NMP)-H, respectively. The specific cholesterol binding of the MIP(NMP)-H was almost 60% higher than that of benzoyl peroxide based polymers (MIP(BPO)-H) and template removal of cholesterol polymer prepared by nitroxide was much more efficient than using the BPO as radical generator. However, results obtained from the binding isotherm of both polymers indicated the heterogeneity of binding sites. The K_d at high affinity site was $5.2 \pm 0.3 \times 10^{-6}$ M for the DVB based-microsphere polymers and $4.5 \pm 1.2 \times 10^{-6}$ M for the nitroxide-based polymers.

Using chimeric green fluorescent protein carrying metal-binding regions, particularly cadmium binding peptides (CdBP), as tools for studying intracellular protein localization was also an objective. Three chimeric proteins designated as H6CdBP4GFP, H6GFP and CdBP4GFP were used to explore the association of cadmium binding protein with both cellular and artificial lipid membranes. At the cellular level, the chimeric GFP carrying cadmium binding peptides promoted the association of chimeric GFP to lipid membrane. Fluorescence of cells expressing chimeric H6GFP was approximately 3 times higher than that of cells expressing native GFP, while the fluorescence of cells expressing cadmium binding proteins CdBP4GFP and H6CdBP4GFP was about 1.6 times lower than that of native GFP. For artificial lipid membrane, small amounts of chimeric H6CdBP4GFP were found to incorporate in liposome. In monolayer, the H6CdBP4GFP was incorporated onto lipid monolayer at low interfacial pressure and caused an increase in fluidity and expansion of the surface area of lipid molecule. These effects were much more pronounced than that of the H6GFP. The epifluorescent microscopy shows that the H6CdBP4GFP preferentially binds to fluid phase areas and defect parts of the lipid monolayers. These findings demonstrate that the hydrophobicity of the GFP constructs is mainly influenced by the fusion partner.

In conclusion, the construction was successful and opens up the possibility of applying precipitation polymerization and nitroxide mediated polymerization in the molecular imprinting field where set up of an alternative cholesterol determination can further be implemented. For example, the imprinted polymers could be incorporated onto the quartz crystal microbalance and applied for real-time monitoring of cholesterol molecules. In addition, the effect of cadmium binding peptide to GFP on association to lipid membrane opens up a high possibility of developing a fluorescent membrane-based metal sensor in the future.

KEYWORDS: CHOLESTEROL/ SEMICOVALENT IMPRINTING / PRECIPITATION POLYMERIZATION/ NITROXIDE MEDIATED POLYMERIZATION/ GREEN FLUORESCENT PROTEIN/ METAL BINDING PEPTIDE

129 P. ISBN 974-04-7526-4

การสังเคราะห์พอลิเมอร์รอยประทับสำหรับคอเลสเตอรอลโดยวิธีกึ่งพันธะโควาเลนต์และการสังเคราะห์พอลิเมอร์จับจำเพาะกับโลหะเพื่อใช้ในการศึกษาทางชีววิทยาและชีวฟิสิกส์ (SEMICOVALENT SYNTHESIS OF MOLECULARLY IMPRINTED POLYMERS FOR CHOLESTEROL AND ENGINEERING OF METAL BINDING POLYMERS FOR BIOLOGICAL AND BIOPHYSICAL STUDIES)

สมชาย บุญเพ็งรักษ์ 4136468 MTMT/D
ปร.ด. (เทคนิคการแพทย์)

คณะกรรมการควบคุมวิทยานิพนธ์: วีระพงศ์ ปรัชชญาสิทธิกุล, Ph.D., ฉัตรเฉลิม อิศรางกูร ณ อยุธยา, ปร.ด, ศรีสุรางค์ ตันติมาวานิช, ปร.ด.

บทคัดย่อ

วิทยานิพนธ์ฉบับนี้รายงานการสร้างพอลิเมอร์รอยประทับที่ออกแบบให้สามารถจดจำคอเลสเตอรอลโดยใช้เทคนิคการสร้างรอยประทับโมเลกุล ด้วยวิธีกึ่งพันธะโควาเลนต์ร่วมกับการสร้างพอลิเมอร์ด้วยวิธีตกตะกอนหรือการสร้างพอลิเมอร์โดยใช้ไนตรอกไซด์ โดยวิธีแรก ผลที่ได้จากการเตรียมพอลิเมอร์สำหรับคอเลสเตอรอลแบบเม็ดกลมโดยใช้ ไดไวนิลเบนซิน (DVB) เป็นตัวเชื่อมจะได้เม็ดพอลิเมอร์ที่ใหญ่กว่า มีความเป็นเม็ดกลมและคุณสมบัติจับจำเพาะมากกว่าพอลิเมอร์ที่เตรียมจากเอทิลีนไกลคอลไดเมทอะไครเลต (EDMA) อนึ่งผลจากการมีขนาดเม็ดที่เล็กของพอลิเมอร์ที่เตรียมจาก DVB ส่งผลให้การสกัดคอเลสเตอรอลออกจากพอลิเมอร์สามารถกระทำได้ง่าย ส่วนวิธีที่สองจะพบว่า ความสามารถในการจับกับคอเลสเตอรอลของพอลิเมอร์ที่เตรียมโดยไนตรอกไซด์ (MIP(NMP)-H (hydrolyzed)) คิดเป็น 6 และ 3 เท่ามากกว่าพอลิเมอร์ควบคุมคือ MIP(NMP)-UH (unhydrolyzed) และ NIP(NMP)-H ตามลำดับ นอกจากนั้นค่าการจับจำเพาะต่อคอเลสเตอรอลของ MIP(NMP)-H จะมีมากกว่าพอลิเมอร์ที่เตรียมโดยใช้เบนโซอิลเปอร์ออกไซด์ (MIP(BPO)-H) โดยคิดเป็นประมาณ 60% รวมไปถึงการสกัดคอเลสเตอรอลออกจากพอลิเมอร์ที่เตรียมจากไนตรอกไซด์ก็มีประสิทธิภาพมากกว่าพอลิเมอร์ที่เตรียมโดยเบนโซอิลเปอร์ออกไซด์ (BPO) เป็นตัวเริ่มปฏิกิริยา อย่างไรก็ตามผลของการจับคอเลสเตอรอล (binding isotherm) ของพอลิเมอร์ทั้งคู่แสดงให้เห็นถึงความหลากหลายของตัวจับจำเพาะ (heterogeneity of binding site) ค่าคงที่ของการแยกจากกัน (K_d) ของตัวจับจำเพาะที่มีความสามารถจับสูง (high affinity site) คือ $5.2 \pm 0.3 \times 10^{-6}$ M สำหรับพอลิเมอร์แบบเม็ดกลมและ $4.5 \pm 1.2 \times 10^{-6}$ M สำหรับพอลิเมอร์ที่เตรียมโดยใช้ไนตรอกไซด์

วัตถุประสงค์หลักอีกประการหนึ่งของวิทยานิพนธ์มุ่งเน้นที่ การใช้โปรตีนลูกผสมระหว่างโปรตีนเรืองแสงสีเขียวที่มีส่วนของเปปไทด์ที่มีความสามารถในการจับโลหะโดยเฉพาะเปปไทด์ที่สามารถจับกับแคดเมี่ยม (CdBP) เพื่อเป็นเครื่องมือสำหรับศึกษาตำแหน่งของโปรตีนภายในเซลล์ กล่าวคือโปรตีนลูกผสม 3 ชนิดได้แก่ H6CdBP4GFP, H6GFP และ CdBP4GFP ถูกนำมาใช้เพื่อประเมินกลไกการทำปฏิกิริยาระดับโมเลกุลของโปรตีนที่สามารถจับกับแคดเมี่ยมกับเมมเบรนทั้งในระดับเซลล์และเมมเบรนจำลอง ในระดับเซลล์โปรตีนลูกผสมสีเขียวที่มีเปปไทด์ที่สามารถจับแคดเมี่ยมส่งผลให้เกิดการจับกันระหว่างโปรตีนลูกผสมสีเขียวและ ผนังเซลล์เมมเบรน ในขณะที่การเรืองแสงของเซลล์ที่แสดงออกโปรตีนลูกผสมชนิด H6GFP คิดเป็นประมาณ 3 เท่ามากกว่าเซลล์ที่แสดงออก GFP ในขณะที่การเรืองแสงของเซลล์ที่แสดงออกโปรตีนที่สามารถจับกับแคดเมี่ยม (CdBP4GFP และ H6CdBP4GFP) จะน้อยกว่าชนิด GFP ประมาณ 1.6 เท่า สำหรับการศึกษาโดยใช้เมมเบรนจำลอง โปรตีนลูกผสมชนิด H6CdBP4GFP สามารถแทรกเข้าไปในลิโปโซม (liposome) ได้เพียง 5-10 % เท่านั้น ในขณะที่เมื่อทดสอบกับเมมเบรนชั้นเดียว (monolayer) จะพบว่า H6CdBP4GFP ถูกแทรกเข้าไปบนเมมเบรนที่ความดันต่ำและเป็นผลทำให้เกิดการหลอมเหลวและการขยายตัวของพื้นที่ผิวของโมเลกุลไขมันซึ่งผลนี้ชัดเจนมากกว่าผลที่เกิดจาก H6GFP ส่วนผลจาก epifluorescent microscopy บ่งชี้ว่า H6CdBP4GFP ชอบที่จะจับกับพื้นที่หลอมเหลวและพื้นที่บกพร่องของเมมเบรนจำลองชั้นเดียว การศึกษาครั้งนี้แสดงให้เห็นถึงว่าการต่อเชื่อมเปปไทด์ชนิดต่างๆเข้ากับโปรตีนเรืองแสงมีผลกระทบต่อคุณสมบัติการชอบจับกับลิปิด (hydrophobicity) ตลอดจนตำแหน่งของโปรตีนที่พบภายในเซลล์ (protein localization) อีกด้วย

โดยสรุป การสร้างพอลิเมอร์ประสบความสำเร็จและเปิดโอกาสของความเป็นไปได้ในการประยุกต์การเตรียมพอลิเมอร์ด้วยวิธีตกตะกอนและด้วยวิธีการใช้ไนตรอกไซด์ในวงการของการสร้างรอยประทับโมเลกุลและสามารถที่จะนำไปสู่การพัฒนาวิธีทางเลือกสำหรับการตรวจคอเลสเตอรอลต่อไป ตัวอย่างเช่นการนำพอลิเมอร์ไปติดอยู่บน quartz crystal microbalance เพื่อนำไปใช้ตรวจติดตามคอเลสเตอรอลแบบ real time ในส่วนของผลของเปปไทด์ที่สามารถจับกับ แคดเมี่ยมได้ต่อโปรตีนเรืองแสงสีเขียวที่มีต่อเมมเบรนนั้นแสดงให้เห็นถึงศักยภาพในการพัฒนาฟลูออเรสเซนต์เมมเบรนเซ็นเซอร์สำหรับตรวจวิเคราะห์โลหะในอนาคต

129 หน้า ISBN 974-04-7526-4

CONTENTS

CONTENTS (continued)

CONTENTS (continued)

CONTENTS (continued)

LIST OF TABLES

LIST OF FIGURES

Page

LIST OF FIGURES (continued)

LIST OF ABBREVIATIONS

CHD	Coronary heart disease
CAD	Coronary artery disease
LDL	Low density lipoprotein
ROS	Reactive oxygen species
SEM	Scanning electron microscope
MI	Myocardial infraction
HDL	High density lipoprotein
VLDL	Very low density lipoprotein
g	gram
kg	kilogram
IDL	Intermediate density lipoprotein
L-B	Liebermann–Burchard
nm	nanometer
et .al.	Et alii
L	Litre
mg	milligram
mmol	millimolar
Amax	Absorption maxima
HPLC	High performance liquid chromatography
GLC	Gas-liquide chromatography
F-C-T	Functional monomer- cross linker-template
DMSO	Dimethylsulfoxide
THF	Tetrahydrofuran
MeOH	Metanol
EDMA	Ethylene glycerool dimethacrylate
DVB	Divinyl benzene
Chol	Cholesterol
MAA	Methacrylic acid
EtOH	Ethanol
CVPC	Cholesteryl 4-(vinyl) phenyl carbonate

LIST OF ABBREVIATIONS (continued)

DCM	Dichloromethan
µm	micrometer
NMP	Nitroxide mediated polymerization
GFP	Green fluorescent protein
Ser	Serine
Tyr	Tyrosine
Gly	Glycine
C	Degree Celsius
MIPs	molecularly imprinted polymers
AIBN	azobis-isobutyronitrile
mL	milliliter
nM	nanomolar
K_D	Dissociation constant
*B*max	maximum binding
µmol	micromole
B	Bound
F	Free
ATRP	Atom-transfer radical polymerization
RAFT	Reversible association fragmentation polymerization
TEMPO	2,2,6,6-tetramethyl-1-piperidinyloxy
BPO	Benzoyl peroxide
pM	picomolar
Cd	Cadmium
KDa	Kilodalton
DPPC	1,2-Dipalmitoyl-sn-glycero-3-phosphocholine
DOPC	1,2-dioleoyl-sn-glycero-3-phosphocholine
IMAC	Immobilized metal affinity chromatography
MLVs	Multilamella vesicles
TCA	Trichloroacetic acid
mN	millinewton

LIST OF ABBREVIATIONS (continued)

m	meter
min	minute
SDS	Sodium dodecyl sulphate
PAGE	Polyacrylamide gel electrophoresis
DPPS	1,2-dipalmitoyl-sn-glycero-3-phosphoserine
DPPG	l,2-dipalmitoyl-sn-glycero-3-(phospho-rac-(1-glycerol))
DPPA	1,2-dipalmitoyl-sn-glycero-3-phosphate
DOPS	1,2-dioleoyl-sn-glycero-3-(phospho-L-serine)
lc	liquid condensed
le	liquid expanded
Cys	Cysteine

PUBLICATIONS DERIVED FROM THIS STUDY

1. Molecularly imprinted polymer microspheres prepared by precipitation polymerization using a sacrificial covalent bond.
   J. Appl. Polym. Sci. 2006; 99:1390-1398
2. Preparation of molecularly imprinted polymers using nitroxide-mediated living radical polymerization.
   Biosens Bioelectrons 2006 May 22 (E-ahead of print)
3. Construction of molecularly imprinted polymers for cholesterol by semi-covalent imprinting approach and nitroxide mediated radical polymerization.
   Thammasat Int. J.Sc. Tech. 2005; 10(4): 1-6
4. Lipid-membrane affinity of chimeric metal-binding green fluorescent protein.
   J. Membrane Biol. 2004; 200: 47–56
5. Co-expression of zinc binding motif and GFP as a cellular indicator of metal ions mobility.
   Int. J. Biol. Sci. 2005; 1(4): 146-151
6. Engineering and characterization of chimeric vitreoscilla hemoglobin and green fluorescent protein *(in preparation)*.

CHAPTER 1
INTRODUCTION

Cholesterol is an important biological substance for human life. It is a precursor for synthesis of bile acid, steroid hormone and vitamin D. It is also a component of cell membrane. However, upon an imbalance between intake and body metabolic consumption, cholesterol is a bioparameter to be considered as one of the predispose factors for cardiovascular diseases. Elevated level of serum cholesterol of an individual is accounted for an increase risk of coronary heart disease (CHD) (1). CHD is the most common type of heart disease and the major leading cause of death in the United States and many other countries. In the United States, an estimated of 50 % of the adult deaths annually are attributed to CHD (2). Hence, determination of blood cholesterol is commonly required for routine annual check up to assess risk among the multifactorial predisposition toward cardiovascular abnormality (3-5).

For almost a century, serum cholesterol has been determined by chemical method, such as the Liberman-burchard (6) and the method of Zlatkis et al (7). In recent decades, enzymatic methods have replaced the chemical assay in clinical laboratory due to the specificity and the ease of handling (8). However, in many circumstances, disadvantages arise because of the multiple steps of the assay, the involvement of carcinogenic or toxic substance and short shelf-life of reagents. Thus, many other settings have been explored to derive as alternative method for cholesterol determination. For instances, high performance liquid chromatography (9), gas liquid chromatography (10), flow injection potentiometry (11) and refloton (12). Molecular imprinting is also a good choice of potential to denote to develop a molecularly differentiated cholesterol assay in the blood (13).

In recent year, molecular imprinting is a newly developed methodology, which provides molecular assemblies of desired structure and property. The technique composed of preorganization of functional monomer to the template molecule by covalent or non-covalent interaction. Then, polymerization of supramolecular assembly in the presence of excess amount of cross linker is performed. Finally, removal of the template molecule from the polymer is done resulting in specific functional groups within the cavity of the polymer that act as receptor for many applications (14-17). This includes molecular separation, molecular sensing for analysis and selective catalysis (18, 19). The molecular

imprinting of cholesterol has firstly been reported since 1995 by Whitcombe et al (13). After that, many groups have independently constructed molecularly imprinted polymers (MIPs) for cholesterol by using various methods of preparation such as bulk polymerization, suspension polymerization and core-shell emulsion polymerization (13, 20-28). Although MIPs are advantageous over biological polymers on the high stability and cost saving, however, limitation is occurred due to the polydispersion of polymer and heterogeneity of binding site distribution. Such disparity of binding site as well as binding site distribution in an individual preparation affect the binding capacity of MIPs. Thus imprinting factors of MIPs has been found varied (13, 20-28). This apparently holds back the development of MIPs toward routine sensors for clinical chemistry. Therefore, the first part of this thesis has been aimed to maximize the preparation of MIPs by using precipitation polymerization to facilitate the more uniform and monodispersion of polymers. A new chemical process of nitroxide-mediated living radical polymerization is also introduced.

In recent years, molecular imprinting has been very attractive to variety of researchers. The art of creating tailored recognition site for binding avidity or site of organic synthesis is utmost a treasured point of applications. However, limitations of MIPs have to be noted that polymers provide poor binding kinetic in the aqueous system along with the probably biological toxic halting an application of MIPs *in vivo* system. In this facet, biopolymers or engineering proteins with tailoring specific avidity elicit more advantages. Therefore, the second part of this thesis is aimed for biological and cellular studies using a series of chimeric genetically engineered of metal binding green fluorescent protein (GFP). As being reported from our lab, difference of metal binding polymers give rise to various localization of cellular compartment of fusion chimeric proteins while role playing in the cells of such series of metal binding protein remain to be explored (29-34). A set of chimeric metal binding GFPs (Cadmium binding GFP, H6-cadmium binding GFP, H6-GFP) are then prepared. Interaction of metal binding proteins to synthetic lipid monolayers and whole *E. coli* is then performed.

The objectives of this study are:

1. To construct molecular imprinting polymer for cholesterol by using semi-covalent imprinting strategy along with nitroxide mediated radical polymerization and precipitation polymerization.
2. To characterize and investigate the molecular imprinting for cholesterol prepared by semi-covalent imprinting strategy along with nitroxide mediated radical polymerization and precipitation polymerization.
3. To construct chimeric hexahistidine and four repetitive cadmium binding regions to green fluorescent protein by using gene fusion technology.
4. To explore the effect of fusion protein partner, hexahistidine and four repetitive cadmium binding sequences, to the localization and activity of chimeric metal binding green fluorescent protein.
5. To study the effect of metal-binding motif on metal ion mobility in *E. coli* cells by co-expression of membrane-integrated metal-binding peptide and cellular GFP or hexahistidine-tagged GFP.

CHAPTER 2
LITERATURE REVIEW

1. Coronary Heart Disease

Coronary heart disease (CHD), also called coronary artery disease (CAD), occurs when the arteries that supply blood to the heart muscle (coronary arteries) become hardened and narrowed. The buildup of plaque on the inner walls or lining of the arteries is accounted for the loss of elasticity and narrowing of blood vessels (atherosclerosis). Blood flow to the heart is reduced as plaque narrows the coronary arteries. This decreases the oxygen supply to the heart muscle developing angina and consequently heart attack. Angina is chest pain or discomfort that occurs when the heart is not getting enough blood. A heart attack happens when a blood clot suddenly cuts off most or all blood supply to part of the heart. This can cause myocardial infraction and permanent damage to the heart muscle. Over time, CHD can weaken the heart muscle and contribute to heart failure and arrhythmias on which the heart is unable to pump blood to the rest of the body effectively. Heart failure does not mean that heart has stopped or is about to stop working. But it refers the failing of myocardial function to pump blood to the body while arrhythmias are changes in the normal rhythm of the heartbeats (35).

1.1 Atherosclerosis

Atherosclerosis, a progressive disease, is generally characterized by the accumulation of lipids, fibrous elements and inflammatory cells within the arterial wall. Initiation of atherosclerosis begins with endothelial injury or dysfunction that is characterized by enhancing of endothelial permeability and LDL deposition in the intima (36-38). Excess of LDL accumulation will consequently induce lesion as a result of oxidative modification with reactive oxygen species (39). LDL is highly oxidized by the action of ROS produced by endothelial cells and macrophages. The overlying endothelial cells are activated by the minimally oxidized LDL to produce a number of pro-inflammatory molecules, including adhesion molecules, chemotactic proteins (e.g., MCP-1) and growth factors (e.g., macrophage colony stimulating factor (M-CSF)) (40, 41). Adhesion molecules, such as

ICAM-1, P-selectin, E-selectin, PECAM-1 and VCAM-1, and chemotactic factors, attract binding of monocytes to the endothelium of the arterial wall, and this induces the entry of monocytes into the arterial intima (42, 43). The cytokine M-CSF contributes to the proliferation and differentiation of macrophages, and stimulates the expression of scavenger receptors (44). Macrophages bind to highly oxidized LDL particles through scavenger receptors and form foam cells that constitute a fatty streak, the early lesions of atherosclerosis. Fibrous plaques are formed when smooth muscle cells (SMC) in the intima proliferate and migrate to the extracellular matrix. SMC migration and proliferation as well as extracellular matrix production are stimulated by several risk factors, such as homocysteine and angiotensin II (45). The interaction of CD40 and CD40 ligand on endothelial cells and SMCs, macrophages and T lymphocytes within human atherosclerotic lesions, promotes the development of an advanced lesion (46). Various proteases produced by macrophages degrade the extracellular matrix, which may make a fibrous cap thin and weak. Further inflammation may trigger the plaque to rupture, and this can lead to thrombosis, acute coronary events, MI or stroke (47).

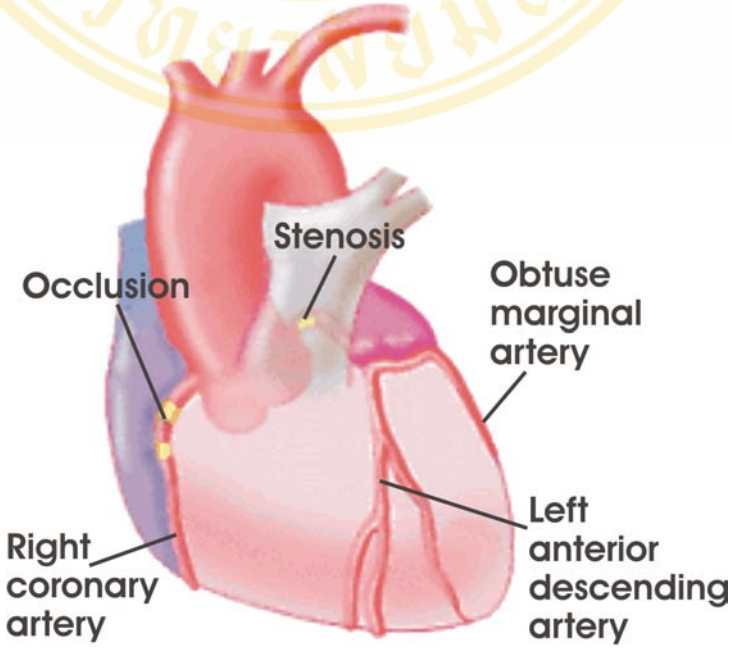

Figure 2.1 Heart with coronary artery disease (48)

1.2 Risk factor associated with coronary heart disease

Although the basic cause of CAD is unknown, scientists have identified several factor associated with a distinct increase chance to develop a heart attack (see table 2.1) (37, 49). The risk factors are identified as primary and secondary. Some risk factors are unavoidable, such as racial, gender and genetic susceptibility while many are behavior dependent. Particularly important among these are high blood pressure, cigarette smoking, and high serum cholesterol, or more significantly, evaluated LDL cholesterol. Approximately, 50% of persons who experience heart attacks have one or more of these three risk factors. According to Framingham data, there is a clear gradient of CHD incidence rate in relation to serum HDL-cholesterol concentrations. Importantly, additional risk factors are lipoproteins (a) [Lp (a)], oxidized LDL, small lipoprotein particle size (or dense LDL), fibrinogen, homocysteine, specific apolipropotein (A-I, B, E isoforms), triglyceride-poor remnant lipoproteins and stress (50-55). No degree of risk has yet been assigned to these factors. Other possible factors whose relative importance is still being established include hypertriglyceridemia, level of physical activity and personality types.

Table 2.1 Primary and secondary risk factors associated with CHD (56)

Primary and secondary risk factors associated with coronary heart disease	
Primary	**Secondary**
- Genetic predisposition of CHD - Family history of premature CHD in first degree relatives (<45 years for males,<55 years for females) - Hypertension - Cigarette smoking - Evaluated total cholesterol (LDL cholesterol) - Decrease HDL cholesterol - Evaluated triglycerides (VLDL cholesterol, remnant lipoproteins) - Increase age - Male gender	- Lack of exercise - Obesity - Stress - Diabetes mellitus - Evaluated lipoprotein (a) - Evaluated homocysteine - Evaluated intermediate-density lipoproteins - Renal failure patients receiving hemodialysis - Postmenopausal state - Certain thrombogenic disorder

2. Cholesterol

Cholesterol is a sterol compound that is found in all animal tissues and serves many important physiological functions, including synthesis of bile acids, steroid hormones, vitamin D, and cell membranes (57, 58).The human liver makes its own cholesterol by using acetyl-CoA as a precursor, and animal-derived foods are a dietary source. Cholesterol is present in tissues and in plasma either as free cholesterol or as a storage form, combine with fatty acid as cholesterol ester. In the liver, cholesterol molecules bind to protein molecules to form lipoproteins such as low density lipoprotein (LDL), and high density lipoprotein (HDL) that can travel through the bloodstream. Although cholesterol is an important in human life, the high cholesterol also appears to be involved in atherosclerosis of vital artery, causing cerebrovascular, coronary, and peripheral vascular disease (59). Therefore, cholesterol measurement is one of the most common laboratory tests used for disease diagnosis, prevention, monitoring, therapy and health promotion.

Cholesterol is a solid alcohol that composes of 27 carbon atoms and a tetracyclic perhydrocyclopentanophenanthrene. The structure of cholesterol is a polar head group (hydroxyl at C-3) and a non polar hydrocarbon body (the steroid nuclease and carbon side chain at C-17).The chemical formula of cholesterol is $C_{27}H_{46}O$ and molecular weight is about 386 dalton (60-62). Normally, cholesterol in the body can be classified into two forms, free and esterified form. Free cholesterol is a component of cell membrane while cholesterol esters predominate in serum and transport by lipoprotein.

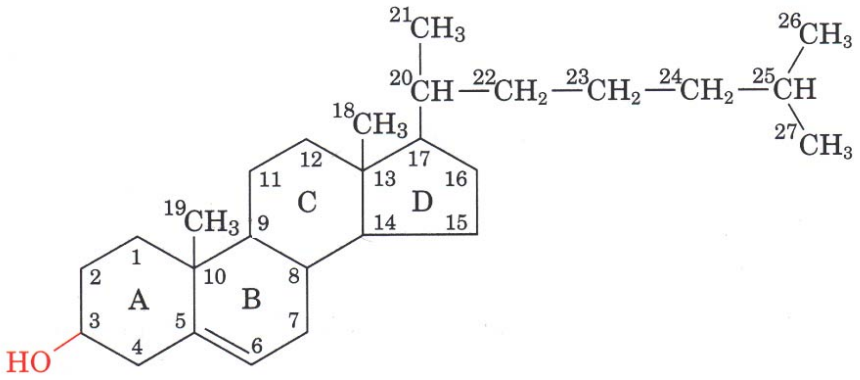

Figure 2.2 Cholesterol molecule (63)

Cholesterol uptakes in the body come from two sources: diary diet and autosynthesis. Normal human body contains cholesterol about 2 g/kg of body weight; whereas about 2 % of cholesterol is renewed each day (64). Cholesterol transportation is carried out by lipoprotein to target tissue and metabolic pathway for maintaining homeostasis. For cholesterol excretion, bile salts (bile acid) are the major excretion of cholesterol, which was emulsified in the small intestine as lipid and excretes in feces. However, before excreting as bile salts, the body can recycle and uses it several times.

2.1 Cholesterol absorption

Cholesterol containing food such as egg, meat, seafood and whole fat dietary product was digested and absorbed in the intestine (61, 65). The pancreatic enzyme degrades dietary lipid to free fatty acid, monoglycerides, glycerols, phospholipids and free cholesterol. These products combine with bile salts to mix micells that pass through the water layer and are absorbed by the brush border of enterocyte. Maximum absorption of cholesterol is occurred at the middle and terminal ilium. After absorption, the lipids are resynthesized in the enterocyte by combination with the apolipoproteins into a large micelle called chylomicrons. The chylomicrons are transported to the cell membrane and enter the circulation via the intestinal lymphatic system (62). Liver can use chylomicron to synthesize other lipoprotein such as HDL, LDL, IDL and VLDL.

2.2 Synthesis of cholesterol

For cholesterol synthesis in body, the liver is a major organ for this function. In addition, cholesterol can also be synthesized by other tissue such as intestine. Liver can be produce cholesterol about 1.5 g/d, while the extrahepatic tissue can produce 0.5 g/d (66). Like the long-chain fatty acids, cholesterol is made from acetyl CoA, but the acetyl groups are linked together in a different way (67). The first stage in cholesterol biosynthesis leads to the intermediate mevalonic acid. In the next step of reactions, three phosphate groups are attached to mevalonate, following which the phosphorylated mevalonate so formed loses a carboxyl group and a pair of hydrogen atoms to yield A3-isopentenyl pyrophosphate, an activated form of an isoprene unit. Six isopentenyl groups are then joined together to yield the hydrocarbon squalene which has 30 carbon atoms, 24 in the chain and 6 in the form of methyl-group branches. Squalene was first isolated from the liver of sharks *(Squalus).* In the third steps of reactions in cholesterol biosynthesis, squalene undergoes a series of complex enzymatic reactions in which its linear structure is folded and cyclized to form

lanosterol, which has the four condensed rings characteristic of steroids. Lanosterol is finally converted, after a fourth set of reactions, into cholesterol.

Elucidation of this biosynthetic pathway, one of the most complex known, was rewarded in 1961 by Nobel prizes to Konrad Bloch, Feodol Lynen, and John Cornforth (67). The enzymes involved in cholesterol biosynthesis, and their regulations have been reviewed (68). The rate of cholesterol biosynthesis is altered not only by tissue levels of cholesterol and other steroids but also by fasting, diurnal variations in food intake, and by diseases such as cancer. Faulty regulation of cholesterol biosynthesis is one of the factors involved in the pathological process of atherogenesis, the formation of attacks or strokes by depriving the tissue of an adequate supply of oxygen.

2.3 Cholesterol esterification

Major cholesterol in the body is conjugated with fatty acid to form cholesterol ester. Cholesterol ester in the circulation appears about 75 % of total cholesterol (69). Lecithin-cholesterol acyltransferase (LCAT) that is synthesized in liver catalyzes the reaction of esterifies cholesterol in the serum (61). High density lipoprotein (HDL) obtained free cholesterol by extracting free cholesterol from peripheral tissues and converts free cholesterol to cholesterol ester by the action of LCAT. While acyl-cholesterol acyltransferase (ACAT) catalyzes reaction of esterified cholesterol within the cell, it is an energy-requiring pathway. The initial reaction involves activation of fatty acid with thio coenzyme A (CoASH) to form an acyl CoA that in turn react with free cholesterol to cholesterol ester form.

2.4 Cholesterol transportation

Cholesterol is transported through the body by lipoprotein particle. In human blood circulation, there are five lipoprotein particles; chylomicron, very low density lipoprotein (VLDL), intermediate density lipoprotein (IDL), low density lipoprotein (LDL) and high density lipoprotein (HDL). The cholesterol component of chylomicron, VLDL, IDL, LDL and HDL are 4-8 %, 15-25%, 30 %, 42-50%, and 15-21 % respectively (57). Moreover, flowing of cholesterol in circulation divided into two ways, exogenous and endogenous pathway.

For exogenous pathway, dietary lipids are a basic of chylomicron particles in blood circulation. Chylomicron particles are triglyceride rich and contain less amount of cholesterol. When chylomicron paticles reach the capillary of adipose tissue or muscle,

apolipoprotein C II (Apo C II) in chylomicrons activate lipoprotein lipase (LPL). This enzyme hydrolyzes triglycerides in chylomicron and release fatty acid to the tissue and glycerol to the liver. The loss of triglyceride converts chylomicrons to small particles known as chylomicron remnants. Chylomicron remnants are ingested by hepatocytes via chylomicron remnant receptor (57, 61).

Endogenous lipids are synthesized within the body, rather than originating from dietary sources. Liver is the main cycle in endogenous cholesterol process. A proportion of hepatic cholesterol is incorporated into VLDL which is secreted into bloodstream. The VLDL assembles rich triglyceride, less cholesterol and apolipoprotein B-100 (Apo B-100), apolipoprotein C (Apo C) and apolipoprotein E (Apo E). The processing of VLDL is as same as chylomicron particles. When the VLDL reaches the capillary of adipose tissue or muscle, it is cleaved by lipoprotein lipase that is process extracted most of triglyceride resulting in molecule calls IDL (VLDL remnants). However, it retains Apo B-100 and Apo E around two of the three of VLDL particles. The IDL rapidly converts to LDL by remove of the remains triglycerides and Apo E.

LDL is removed from plasma by binding to the cell surface receptors and degraded delivering its load of cholesterol to the cell. The most important receptor is known as the LDL receptor (70). Most of the LDL receptor is found in the liver, although a proportion of the uptake of plasma LDL is via LDL receptor in extrahepatic tissues. The uptake of LDL by extrahepatic tissues is not essential and most extrahepatic tissue cannot catabolise cholesterol. Thus, as cell and cell membrane undergo normal metabolic turnover, there must exist a mechanism for the elimination of cholesterol, which would otherwise accumulate in the cell. This is achieved by the delivery of cholesterol from cell membrane to plasma HDL in the first step of a pathway known as reveres cholesterol transport (71). The HDL particles have opposite function to LDL particles that take up free cholesterol from hepatic tissue and other lipoprotein to liver. Nascent HDL (discoidal particle) synthesizes in hepatocyte and small intestine. It consists of very little esterified cholesterol and the large of apoliproprotein AI (Apo AI).The cholesterol that is transferred from cell membrane to HDL is esterified by plasma enzyme, LCAT. A part of cholesterol ester of spherical HDL is subsequently transferred by cholesterol ester transfer protein (CEPT) to VLDL, IDL and LDL particles. HLD is delivered to the liver by three pathways. First, cholesterol esters are selectively taken from HDL, probably by the hepatic HDL receptor. Second, cholesterol ester are transferred from HDL to apoprotein B 100 lipoprotein, a process mediates by cholesterol ester transfer protein, then take up by the liver through

receptor for these lipoproteins. Finally, HDL apoprotein E can be recognized by the hepatic remnant receptor (72). The exogenous and endogenous pathways of cholesterol are shown below.

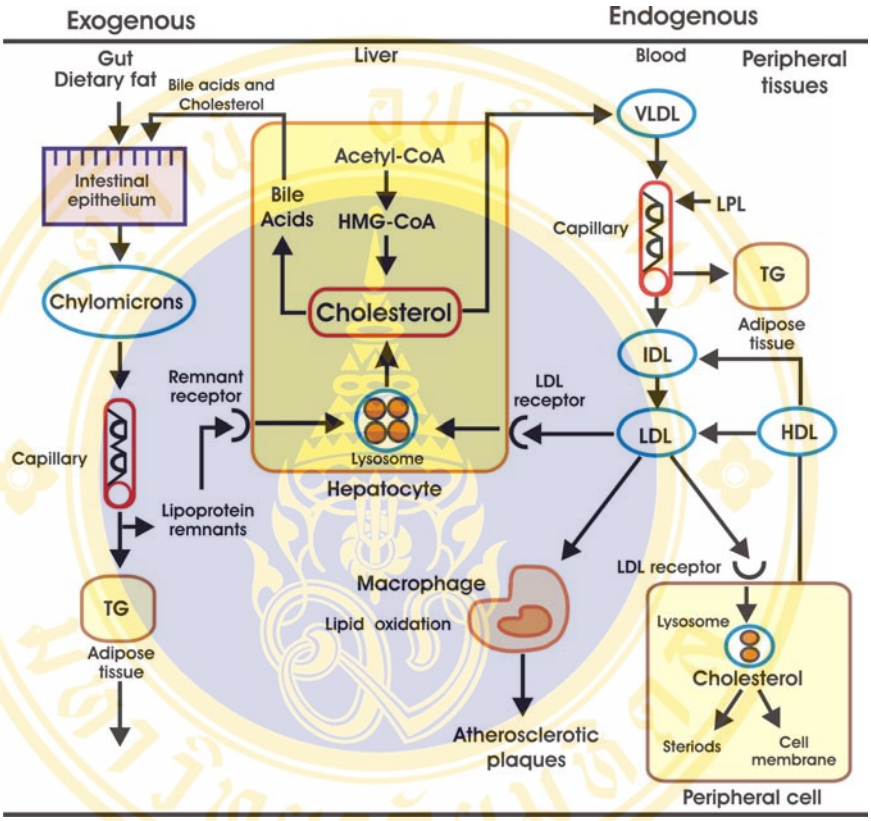

Figure 2.3 Exogenous and endogenous pathways of cholesterol (73)

2.5 Cholesterol catabolism

Approximately one third of the daily production of cholesterol is catabolized into bile acids. Bile acids synthesis averages 200 to 400 mg/day. The primary bile acids, cholic and chenodeoxycholic, are conjugated with either glycine or tuarine and enter to the bile canaliculi. After reaching the small intestine, they play an active part in cholesterol and fat absorption. Some of the bile acids are deconjugated and converted by bacteria in the intestine to secondary bile acid, which are reabsorbed and returned to the liver via the portal vein. Deconjugation of cholic acid is deoxycholic acid while chenodeoxycholic acid is lithocholic acid. At least 90% of bile acid absorption, except lithocholic acid, is secreted with feces (61), (74).

3. Cholesterol Determination

Currently, cholesterol determination is based on two major principles: the chemical and enzymatic methods. Chemical method is the indirect assay; sample must be treated with solvent or uses other isolation techniques. Thus, the assay is complex and unsuitable to perform. While enzymatic method does not require fractionation of the sample before measurement. Therefore, the assay is simple, convenient and suitable for automation. In general, cholesterol detection step can be classified into four classes such as single, two three and four step method. In addition, method of cholesterol analysis will also be classified based upon the principle of chemical reaction (Liebermann–Burchard, iron–salt–acid and p-toluenesulfonic acid) and enzyme reaction. However, other principle methods have also been established for cholesterol determination. All of them will be described below.

3.1 Classification of cholesterol detection step

3.1.1 Single-step detection

In these direct assays there is no sample preparation, that is, no isolation and purification of the steroid or steroids. Thus direct procedures are those carried out on serum or plasma samples without any prior solvent extraction steps. These methods are simple and rapid and require little manipulation of the sample, and therefore are suitable for automation. However, depending on the chemical reaction, these procedures are likely to exhibit both positive and negative errors resulting from the presence of proteins; bilirubin; hemoglobin; vitamins A, C, and D; steroid hormones; uric acid; turbidity; and differences in chromogenicity of free cholesterol and ester cholesterol. Many automated procedures are based on direct methods. They are usually based on such acceptable methods as Zlatkis et al.(7)**,** Huang et al (75)**,** Pearson et al (76)and enzymatic procedures (77, 78).

3.1.2 Two-step detection

In two-step assays an organic-phase extraction step is introduced before measurement of cholesterol and other chemically related steroids. This pretreatment step removes many nonspecific chromogens that might interfere with the assay; the relative chromogenic response of each interfering substance is dependent on the chemistry involved. Since no saponification step is involved in these methods, the deleterious effect of differential color response between free and ester cholesterol still remains, especially in Liebermann–

Burchard reactions. However, for most routine clinical work, this two-step procedure has been well accepted; the values obtained correspond closely with that of the Abell et al. (79) method. The correlation is even closer when a calibration factor is added to correct for free and ester cholesterol differential color development. The methods of Zak and Ressler, (80) Carr and Drekter, (81) Bloor, (82) and Chiamori and Henry (83) are examples of two-step procedures.

3.1.3 Three-step detection

Three-step procedures involve, in addition to extraction of cholesterol, a saponification step that hydrolyzes the fatty-acid moiety from the cholesterol ester. Consequently one measures only free cholesterol. The method of Abell et al. (79) belongs in this classification and has now been considered a reference method. Some modifications have been added to improve the accuracy and precision of the measurement.

3.1.4 Four-step detection

Four-step methods go a step further than the three-step method of extraction, saponification, and color development. The total extractable steroids are purified for cholesterol determination by the addition of a saponin, digitonin. The reactive site on the C-3 position on the cyclopentanoperhydrophenanthrene ring in cholesterol is a hydroxyl group that is esterified by the digitonin. This causes the complex to be precipitated. The addition of the digitonin step also eliminates the effect of interfering nonspecific chromogen constituents. Empirically, four-step procedures should be more accurate and precise than any other procedure, with the possible exception of enzymatic cholesterol determinations. However, unless extreme precautions are taken, multiple steps may also mean multiple errors. For instance, whereas digitonin precipitation enhances the accuracy of the method, the digitonin must be completely decomposed and removed or it will cause additional color development and thus positive error.

The Schoenheimer and Sperry (84) and Sperry and Webb (85) methods are four-step procedures that have, in the past, been considered reference methods for cholesterol determinations. These two methods also employ Liebermann–Burchard reagents. Although the Abell et al**.** (79) method may be more tailored to serum or plasma cholesterol analysis, four-step methods may be more suitable for tissue extracts, (86) since certain tissues may have appreciable non cholesterol and cholesterol esters that may contribute to the inaccuracy of the final development of color.

3.2 Methods of cholesterol analysis

Literally hundreds of cholesterol analysis methods have been published, usually as modifications of the following reactions: Liebermann–Burchard, iron–salt–acid, *p*-toluenesulfonic acid and enzymatic method. Therefore, those methods will be described in more detail.

3.2.1 Chemical method

3.2.1.1 Liebermann–Burchard Reaction

The history of this famous organic compound goes back to the 19th century. Liebermann, (87) in 1885, first described the color reaction of sulfuric acid with a solution of cholesterol in acetic anhydride. Four years later, in 1889, Burchard (88) reported that a more intense blue-green color is produced when acetic anhydride and sulfuric acid are added to a solution of cholesterol in chloroform. Since that time, this "Liebermann–Burchard reaction" has been widely used as a colorimetric reaction for the estimation of cholesterol in biological fluids (89).

Among the non-enzymatic colorimetric reactions for cholesterol, the Liebermann–Burchard (L-B) procedure is perhaps the most widely used. The L-B reaction generally is carried out in a strong acid medium—sulfuric acid, acetic acid, and acetic anhydride. Mechanism of Liebermann–Burchard reaction involves the protonation of hydroxyl group in cholesterol. Sulfuric acid initiated color reaction of dehydrated cholesterol to carbocation 3,5-cholestadiene. Serial oxidation of this carbocation with the excess of sulfuric acid yields a cholest-hexene sulfonic acid chromophoric compound as blue-green color. The blue-green color is measured at maximum wavelength at 630 nm. The Liebermann–Burchard reaction had the widest application in the past for cholesterol determination. However, the disadvantages of Liebermann–Burchard method were unstable color product and rigorous exclusion of moisture (58). Although, the Liebermann–Burchard reaction are very non-specific, but it can be applied directly to serum for cholesterol determination. The application of Liebermann–Burchard have been reported for cholesterol determination by Abell et al.(79). Abell et al suggested the method for cholesterol determination that involved a sponification of cholesterol ester in serum or plasma with alcoholic potassium hydroxide. Free cholesterol was extracted with petroleum ether and an aliquot extraction was evaporated to dryness. Total cholesterol is determined by Liebermann–Burchard reaction. This procedure was widely accepted as the reference method for total cholesterol.

Currently, the Lipid Standardization of the Center for Disease Control (CDC) proposed the reference method that modified Abell et al's procedure (90). The method uses hexane that substitute to petroleum ether in the extraction of free cholesterol.

3.2.1.2 Iron–salt–acid reaction

In 1953, Zlatkis and Boyle (7) proposed a new colorimetric procedure for cholesterol, dependent on the color produced when a solution of ferric chloride in concentrated sulfuric acid is added to a solution of cholesterol in glacial acetic acid. The color developed in this reaction is more intense and more stable than that developed in the Liebermann–Burchard reaction. This reaction involves acetic acid–sulfuric acid in the absence of acetic anhydride. In this reaction, however, Fe^{3+} must be added to obtain the desired chromogen. As in the L-B procedure, the initial step is the protonation of the OH group in the cholesterol molecule and subsequent loss of water to form the carbocation (3,5-cholestadiene). Serial oxidation of this allylic carbocation by Fe^{3+} yields a tetraenylic cation with resulting in red color an absorbance maximum of 563 nm. The iron–salt–acid procedures are about 7 fold more sensitive than the L-B methods. This increased sensitivity may be attributed largely to the stabilizing effect on enyliccation formation at higher H_2SO_4 concentrations. In general, increasing the H_2SO_4 concentration would be expected to improve the stability of each of the carbocations formed in the stepwise oxidation of the sterol, thereby making it much more likely for one to observe carbocation formation in the iron-salt-acid reaction than in the L-B reaction. Measurements of serum cholesterol by the $FeCl_3$–H_2SO_4 reaction were automated by Levine and Zak (91) and by Block and co-workers.(92).

In 1969, a "micromethod" for serum cholesterol, which requires only 20 µl of serum, was described by Jordan and Knoblock. (93) In this technique, cholesterol is precipitated as a dextran sulfate complex to avoid interference from bilirubin. The precipitate is dissolved in glacial acetic acid, and ferric chloride reagent is then added. Even greater sensitivity can be achieved by fluorometric detection of the ferric chloride–sulfuric acid chromogen (94). An automated fluorometric technique for serum cholesterol was described by Robertson and Cramp (95).

3.2.1.3 *p*-toluenesulfonic acid reactions

These methods are based on reactions of cholesterol with *p*-toluenesulfonic acid (p-TSA), acetic anhydride, glacial acetic acid, and H_2SO_4 (76).

The limitation of the chemical method is sensitivity to interference and corrosive agent. In addition, bilirubin is one of the major interfering substances especially for the Liebermann–Burchard reaction. The easy conversion of bilirubin to biliverdin by Liebermann–Burchard reagent increases the measurable spectral absorbance in the region of the measurement wavelength of cholesterol reaction. Therefore, chemical method for cholesterol determination is replaced by the enzymatic method that composes of cholesterol esterase and cholesterol oxidase. The use of enzymes improves specificity without pretreatment and includes reagents that are less corrosive. For the reaction process, cholesterol esterase hydrolyzes cholesterol ester to free cholesterol. In the next step, cholesterol oxidase causes the oxidation of free cholesterol to cholest-4-en-3-one and hydrogen peroxide (H_2O_2). Then, H_2O_2 can be used to quantify the amount of cholesterol by peroxidase- substrate system.

3.2.2 Enzymatic reactions

Developments over the past 10 years in clinical chemistry have been geared toward more rapid, direct analyses of serum or whole blood. Pretreatment of samples increases the possibility for error and increases turnaround time. These demands have led to the most important development in cholesterol measurements, which is the introduction of enzymatic techniques.

Enzymatic techniques for determining cholesterol have emerged to compete with the classical Liebermann–Burchard reaction and have become the most popular method for cholesterol analysis. The original work used preliminary alkaline saponification of the sample to produce only free cholesterol. (80, 81, 96). In the next step, cholesterol oxidase, an enzyme specific for cholesterol, was added. This caused the breakdown of cholesterol to cholest-4-en-3-one and hydrogen peroxide, after that, several different reaction systems have been used to produce a final chromogen.

Subsequent developments led to the technique of enzymatic hydrolysis of cholesterol esters by employing cholesterol esterase (77). The commercial kits on the market now offer a total enzymatic procedure, utilizing the enzyme cholesterol esterase to replace the chemical saponification. Cholesterol esterase is specific for cholesterol esters, splitting the esters into free cholesterol and free fatty acids. Following is the cholesterol oxidase reaction by which cholesterol was then oxidized. The amount of color produced is directly proportional to the amount of serum cholesterol.

The most common enzymatic method employs the Trinder's reaction which includes

three steps. The first step in the enzymatic methods for cholesterol uses the enzyme cholesterol esterase to hydrolyze the cholesterol esters present in the serum to free cholesterol and free fatty acids:

Cholesterol esters + H_2O + Cholesterol esterase → Cholesterol + Free fatty acids (1)

As discussed previously, the second step uses the enzyme cholesterol oxidase in the presence of oxygen to oxidize the cholesterol (both the free cholesterol found in the serum and the free cholesterol generated in step 1) to cholest-4-en-3-one and hydrogen peroxide:

Cholesterol + O_2 +Cholesterol oxidase → Cholest-4-en-3-one + H_2O_2 (2)

In this reaction cholesterol concentration can be determined by amperometric measurement of the rate of oxygen depletion.

Other assays make use of the ability of hydrogen peroxide to oxidize compounds to produce colored species that can be measured spectrophotometrically:

$2H_2O_2$ + 4-Aminophenazone (Phenol) +Peroxidase → Quinoneimine dye+$4H_2O$ (3)

The reaction (3) (Trinder's reaction), which forms the quinoneimine dye (absorbance maximum 500 to 525 nm), is the basis of the majority of the methods currently on the market (8, 97). In addition, hydrogen peroxide can be quantified by titanium (IV) and xylenol (96), *o*-dianisidine-peroxidase chromogen (98), N, N- Diethylaniline hydrogen chloride peroxidase chromogen (99), Phenol- aminoantipyrine-peroxidase (77), 2,2'-azino-di-3 [ethyl-benzthiazolin sulfonic acid] (ABTS) (Majkic N 1977), electrochemical(100) and fluorometric (101).

For a variety of cholesterol determination with enzymatic method, the analytical reaction of the reaction based upon the two molecules such as oxygen and hydrogen peroxide. In 1976, Noma et al. describes a new oxygen electrode for cholesterol determination. The method use polarlographic oxygen analyzer with circuit modifies to record simultaneously amount and rate of oxygen consumption in the absolutely specific oxidation of free cholesterol. The advantages of this method are rapidity and insensitivity to bilirubin and ascorbic acid (102).

In 1973, Richmond et al (96) used sodium hydroxide for hydrolysis of cholesterol ester to free cholesterol. Free cholesterol was oxidized by cholesterol oxidase to produce hydrogen peroxide (H_2O_2). H_2O_2 chelation with titanium and xylenol orange gave a complex measuring at 550 nm. This method used stable reagent that did not require protein precipitation.

In 1974, Allian et al (77), propose the method using three enzymes including cholesterol ester, cholesterol oxidase and peroxidase. H_2O_2 generated from oxidation of free cholesterol by cholesterol oxidase was measured by the oxidative coupling of 4-aminoantipyrine/phenol in the present of peroxidase. The chromogens absorbance was measured at 500 nm. This method has widely been used for serum cholesterol determination because it is rapid, specific, non consumption time. Evaluated of enzymatic method of Allian et al in the Abbot ABC-100 analyzer by Witte et al reveal good agreement to the manual procedure of Abell et al (8). Therefore, this method is a good alternative for cholesterol determination because the easy operation, acceptable accuracy, precision and specificity. However, bilirubin 1mg/dl gave slightly positive interference. In the same year, Tarbutton and Gunther (98) introduced the method using *o*-dianisidine-peroxidase chromogen. The assay is based on complete enzymatic method. Hydrogen peroxide reduction with *o*-dianisidine in the presence of peroxidase yields a color product which can be measures at 450 nm. The disadvantage of *o*-dianisidine is carcinogenic substance (99)

In 1975, Huang et al (101) suggested a fluorometric enzymatic method for cholesterol determination. Homovanelic acid, in the presence of peroxidase, oxidizes the hydrogen peroxide to 2,2'-dyhydroxy-3,3- dimethoxy-biphenyl-5,5'-diacetic acid providing fluorescence. This method is a specific, precise, accurate, and rapid. The results were consistent to those obtains by the Liebermann–Burchard reaction and other colorimetric enzymatic method.

In 1976, Pesce and Bodourian (78) measured cholesterol in serum by the enzymatic rate method. The production of the oxidation of cholesterol, hydrogen peroxide, reacts with methanol in the presence of catalase to produce formaldehyde. Formaldehyde reacted with acethylacetone and ammonium ion to form 3,5-diacyl-1,4-dihydrolutidine. The rate of increasing in absorbance of the dihydrolutidine product was measured at wavelength of 405 nm. The change in absorbance between 4 and 10 minute was used to calculate cholesterol concentration. The presence of hemoglobin up to 1g/L, bilirubin up to 200 mg/L or ascorbic acid could interfere serum cholesterol detection.

In 1977, Pesce and Bodourian (103) applied the method of Allian et al for the cholesterol determination by using centrifugal analyzer. Cholesterol is measured by mixing 5 microliters of sample with 350 microliters of a reagent consist of phenol, 4-aminoantipyrine, cholesterol esterase, cholesterol oxidase and peroxidase. After 21 minutes, the quinoneimine is measured at 520 nm. Lipemic sera, sample containing uric acid (up to

200 mg/L) and hemoglobin (up to 1 g/L) gave no interference for this method. In addition, Huang et al (100) described electrochemical method for cholesterol determination. Cholesterol esterase and cholesterol oxidase are immobilized with layer in groove of polarorganic oxygen analyzer. The reaction mixtures pass the enzyme layer in groove. Thus, enzyme transforms cholesterol ester in the serum to hydrogen peroxide. Hydrogen peroxide is measured by amperometric at + 0.60 voltages (V) versus a standard calamel electrode. Result of this study correlate well with those obtains for the method of Abell'et al.

Majkic and Berkes in 1977 (104) measured hydrogen peroxide by the oxidation of ABTS. ABTS allowed the direct calculation of cholesterol concentrations by measured absorbance change at 410 nm. This procedure is rapid, specific reproducible and applicable to measurement of free and etherified cholesterol concentration. In 1978, Rautela et al (99) presented complete automation of enzymatic method for cholesterol determination in Du Pont's Automatic Clinical Analyzer. Hydrogen peroxide reacts with N, N- Diethylaniline hydrogen chloride and 4-aminoantipyrine in present of peroxidase.

In 1979, Deacon et al (105) compared the enzymatic method with chemical method for the cholesterol determination. Cholesterol ester is hydrolyzed by cholesterol esterase. While free cholesterol is oxidized by cholesterol oxidase and used chromogenic system that consists of peroxidase/phenol/4-aminoantipyridine for determination of cholesterol concentration. For chemical method, cholesterol ester was hydrolyzed by potassium hydroxide. The product of sponification was neutralized and used for color generation. The yields of chemical hydrolysis were lower than enzymatic method about 10 %. Moreover, enzymatic method is simple and provides greater potential for cholesterol determination than chemical method.

In 1983, Degg et al (106) described the rapid kinetic for cholesterol determination based on the method of Allian et al. In this study, the addition of competitive inhibitor (3,4-dichlorophenol) increase of Michaelis constant of cholesterol oxidase that extends the linearity of cholesterol concentration range from 20.7 to 25.9 mmol/L. This method is suitable for automation of kinetic method and use in routine clinical laboratory.

The advantages of enzymatic method such as specificity and one step determination of cholesterol over the chemical method is presented. The enzymatic method that composed of cholesterol esterase, cholesterol oxidase and peroxidase, is become a popular and widely used. Hence, the development for the cholesterol determination using automation system has been established so far based on enzymatic reaction.

3.2.3 Other detection methods for cholesterol

Although cholesterol determination is mainly based on two principles: chemical and enzymatic method. Many scientists have attempted to develop others method for cholesterol determination. Some methods are based on the principle of enzymatic reactions and incorporated to sensor unit such as using amperometric and electrochemical principle (107), (108) for detection instead of color system. In addition, cholesterol determination with enzymatic method can be used either fluorescent or chemiluminescent substrate instead color substrate for detection (109, 110). Moreover, a variety of principles have been introduced as a alternative method for cholesterol determination. For instances, high performance liquid chromatography (HPLC) (9, 111, 112), gas-liquide chromatography (GLC) (10, 113), mid-infrared (114), flow injection potentiometry (11), enzyme thermister (115), refloton (12) and molecular imprinting (13).

Molecular imprinting is emerging technique in recent years that used for creating a cavity specific for cholesterol. The first pioneer of imprinted polymer construction for cholesterol is Whitcombe et al in 1995. This technique based on the molecular assembly of template functional monomer and cross-linker to create a size and shape specific binding pocket for template molecule. This technique rapidly became widely used. Therefore, there are many scientific papers have been published so far for cholesterol detection using molecular imprinting technique. All of the cholesterol imprinted polymers was summarized in table 2.3.

Table 2.2 Summary of chemical and enzymatic reaction for cholesterol detection (56).

1. Liebermann–Burchard (L-B); one-, two-, three-, or four-step method **Principle of analysis:** Cholesterol extracted and reacted with strong acid (sulfuric acid) and acetic anhydride to form colored cholestahexaene–sulfonic acid molecule (Amax, 410 nm); nonesterified cholesterol precipitated by digitoxin, and remaining cholesterol measured and free cholesterol calculated; Total–Esterified = Free **Comments:** Very common method; total cholesterol reaction overestimates concentration of esterified cholesterol; unstable color
2. Abell et al.; three-step method **Principle of analysis:** Cholesterol extracted with zeolite, esters chemically hydrolyzed (saponification), and total cholesterol measured by Liebermann–Burchard reaction **Comments:** Considered current reference method; laborious
3. Iron–salt–acid; two-step method **Principle of analysis:** Similar to reaction conditions of method 2, except Fe^{3+} ions are added to yield tetraenylic cation (Amax, 563 nm) **Comments:** Not frequently used; sevenfold more sensitive than L-B method; free and esterified cholesterol give same color; no need to hydrolyze esters
4. p-Toluene–sulfonic acid (p-TSA); three-step method **Principle of analysis:** Similar to method 3; p-TSA reacts with cholesterol derivative to form chromophere (Amax, 550 nm) **Comments:** Rarely used; free and esterified cholesterol give same color
5. Enzymatic reaction; one-step method **Principle of analysis**: a. Cholesterol–esters +Cholesterol esterase → Cholesterol + Fatty acids b.* Cholesterol + O_2 +Cholesterol oxidase → Cholest-4-en-3-one + H_2O_2 c. H_2O_2 + 4-Aminophenazone (or other dye) +Peroxidase → Oxidized dye (Amax, 500 nm) + H_2O **Comments:** Most common method; accurate and easily automated; future reference method
*Can monitor reaction by following O_2 consumption with oxygen electrode.

Table 2.3 Summary of molecularly imprinted polymer for cholesterol detection during 1995-2005

Polymer	F-C-T	Solvent	Rebinding medium	Imprinting efficiency	Rebinding mechanism	Ref.
1995						
Whitcombe et al. Bulk polymer, covalent	Cholesteryl 4-(vinyl) phenyl carbonate,EDMA, DVB	hexane	hexane	2.5	H-bonding	(13)
1997, 1998 Asanuma et al. Bulk, non covalent	CD, TDI,Chol CD,HMDI,Cho	DMSO	H_2O/THF	3.7 15	Hydrophobic binding to CD cavity	(116, 117)
1997						
Sreenivasan et al. Bulk, non covalent	HEMA,EDMA,Chol	MeOH	MeOH	24.5	H-bonding	(20)
1998						
Sreenivasan et al. Bulk, non covalent	CD-HEMA, EDMA, Chol	MeOH	MeOH	2.6	Hydrophobic	(118)
Sreenivasan et al. Membrane, non covalent	Polyurethan/ HEMA	DCM	MeOH	7.7	Hydrophobic ?	(119)
Sreenivasan et al. Bulk, non covalent	HEMA,NVP, EDMA, Chol	MeOH	MeOH	30.4 (HEMA) 21.8 (NVP)	Hydrophobic	(120)
Sellergren et al. Bulk, non covalent	Methacryloyl cholesterol, EDMA, Chol	EtOH,DCM	intestinal-mimicking solution	1.3	Hydrophobic/H-bonding	(21)
1999						
Hishiya et al. Bulk, non covalent	CD, TDI,Chol	DMSO	H2O/THF	2	Hydrophobic binding to CD cavity	(22)

Table 2.3 Summary of molecularly imprinted polymer for cholesterol detection during 1995-2005 (continued)

Polymer	F-C-T	Solvent	Rebinding medium	Imprinting efficiency	Rebinding mechanism	Ref.
1999 (continued)						
Piletsky et al. Film, Electrochemical sensor (based on ferro-feric redox reaction)	hexadecyl mercaptan (SAM), Chol	EtOH	electrolyte solution (chemical for the ferro-ferric redox reaction.)	Not mention	Hydrophobic	(121)
2000						
Flores et al. Bead (suspension polymerization), Semi-covalent	Styrene, EDMA,CVPC	dioctyl phthalate: *n*-decane	Hexane	2.46	H-bonding	(23)
Peres et al. Nanobead (core shell emulsion polymerization), Semicovalent	Styrene (core), EDMA,CVPC	sodium lauryl sulphate in deionized water	Isohexane	12.6	H-bonding	(24)
2001						
Zhong et al. Bulk, Covalent (Hydrophilic mip)	Cholesteryl acrylate and acryloyl-6-amino-6-deoxy-β or γ-CD, DAPA, Chol	THF/H_2O	2-propanol	5.6	Hydrophobic interaction	(122)
Sreenivasan et al. Bulk, non covalent	Acrylic acid, EDMA, Chol	DCM	DCM	13	Hydrogen bonding	
Kugimiya et al. Bulk, non covalent	2-(methacryloyloxy) ethyl phosphate, EDMA, Chol	Toluene/ chloroform	Hexane	2.5	Non- covalent	(25)

Table 2.3 Summary of molecularly imprinted polymer for cholesterol detection during 1995-2005 (continued)

Polymer	F-C-T	Solvent	Rebinding medium	Imprinting efficiency	Rebinding mechanism	Ref.
2001 (continued)						
Sreenivasan et al. Bulk, non covalent	Cu(II) acrylate monomer and EGDMA, Chol	DCM	DCM	19	Metal ion interaction	(123)
Peres et al. core- shell particle	Styrene: DVB (core), DVB, PS (surfactant) TS (template)	H_2O	propanolol: H_2O	2.5	Hydrophobic interaction	(124)
2002						
Hishiya (study mechanism of CD to form polymer)	CD, TDI, HMDI, Chol	DMSO	H_2O/THF	-	Hydrophobic binding to the CD cavity	(125)
Hwang et al., Bulk, covalent	cholesteryl (4-vinyl) phenyl carbonate, EDMA	hexane	glacial acetic acid	3.2	Hydrogen bonding	(126)
Hwang et al., Bulk, non-covalent	methacrylic acid or 4-vinylpyridine, EDMA,.Chol	Chloro form	glacial acetic acid	MAA: 3.0 VP: 2.9	Hydrogen bonding	(126)
2003						
Davidson et al Bulk, non-covalent	MAA, EDMA, Tweezer receptor, Chol	THF	THF	4.1	Hydrophobic interaction	(26)
Gong et al. Film polymer with electrochemical sensor	Poly(2-macapto-benzimidazole) (PMBI) films, Chol	Alkaline-ethanol	Alkaline- ethanol	Not mention	Not mention	(127)

Table 2.3 Summary of molecularly imprinted polymer for cholesterol detection during 1995-2005 (continued)

Polymer	F-C-T	Solvent	Rebinding medium	Imprinting efficiency	Rebinding mechanism	Ref.
2004						
Gore et al., Bulk, non-covalent	C1 (EDMA), C4 (monocholesteryl itaconate glycerol methacrylate;) , Chol	EtOH	intestinal mimicking solution	3.7	Hydrophobic interaction	(27)
2005						
Chou et al. Thick film Electrochemical sensor (based on ferro-feric redox reaction)	SAM,Chol	EtOH	electrolyte solution (chemical for the ferro-ferric redox reaction.)	Not mention	Hydrophobic interaction	(128)
Egawa et al. CD- microsphere, non-covalent	CD,TDI,Chol, PDMS (emulsion)	DMSO	H_2O/THF	1.65	Hydrophobic interaction	(129)
Wang et al. Bulk, Semi-covalent imprinting	EDMA, cholesteryl 2-hydroxyethyl methacrylate carbonate (CHOL-HEMA)	Hexane	Hexane	8.3	H-bonding	(28)
Spizzirri et al Hydrogel	MAA,EDMA,Chol	THF/ DMSO	THF/H2O	13.35	H-bonding	(130)

3.3 Reference and Definitive Methods

3.3.1 Reference methods

Reference techniques can be carried out with equipment available in many laboratories to give results that either statistically coincide with the definitive method or have a clearly defined bias. The procedures accepted as reference procedures are still based on the Liebermann–Burchard (L-B) reactions (Abell et al., (79) Schoenheimer–Sperry, (84) or Sperry-Webb (85) methods). The reference procedures are compared to definitive methods.

The Centers for Disease Control have proposed a modification of the Abell et al. procedure for use as a reference method for cholesterol (131).

3.3.2 Definitive Methods (Isotopic dilution–mass spectrometry)

Definitive techniques allow measurement of the concentration of a substance in a biological sample and give results accepted as the nearest attainable to true values. Isotopic dilution–mass spectrometry has been recommended as a definitive method for cholesterol determination, with a coefficient of variation (CV) no greater than 0.5% and a total uncertainty of no greater than 1% (132) . A candidate definitive method was also published by the Center for Analytical Chemistry, National Bureau of Standards (NBS) (133). This isotope dilution–mass spectrometric method was used to establish the accuracy of a candidate reference method (134) for total serum cholesterol. This method showed a CV for a single measurement of 0.36% and an absence of interferences. Schaffer et al (133). compared the Karolinska Institute and NBS isotope dilution–mass spectrometric methods for cholesterol; a 0.2% mean difference between the two methods was shown, and the Karolinska Institute standard was found to contain lathosterol (5-a-cholest-7-en-3-ol-3[b]). The NBS method appeared to be more precise, probably because of the more complex and time-consuming protocol for sample preparation and mass spectrometry.

4. Molecular Imprinting

4.1 General principle of molecular imprinting

The technique of molecular imprinting allows the formation of specific recognition sites in synthetic polymers through the use of templates or imprint molecules. These recognition sites mimic the binding sites of antibodies and other biological receptor molecules (135). Molecular imprinting processes are composed of the following three steps. First step is preparation of covalent or non-covalent adduct between a functional

monomer and template molecule. Second step is polymerization of monomer-template conjugate (adduct). Final step is removal of the template from polymer. Therefore, the space in the polymer originally occupied by the template molecule is left as a cavity. Under appropriate condition, these cavities satisfactorily remember the size, structure, and other physicochemical property of the template, and bind this molecule (or its analog) efficiently and selectively (136).

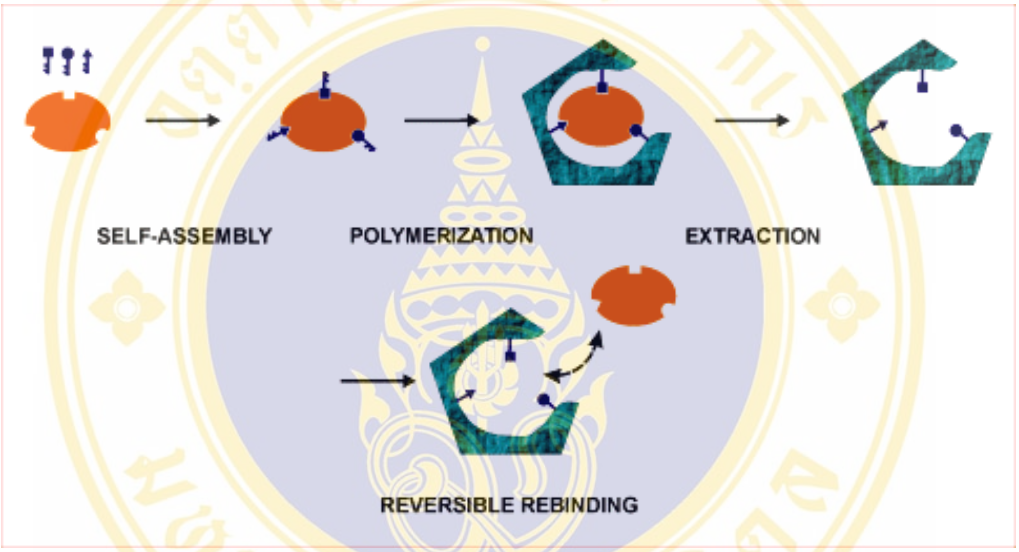

Figure 2.4 Schematic illustration of general molecular imprinting approach (137)

4.2 Molecular imprinting approach

4.2.1 Covalent imprinting

The covalent imprinting approach has firstly been established by Wulff and his coworker in 1977 (138). In general principle, prior to polymerization, functional monomer and template are bound to each other by covalent linkage. Then, this covalent conjugate is polymerized under the condition where the covalent linkage is intact. After polymerization, the covalent linkage is cleaved and the template is removed from the polymer matrix. Upon the template rebinding by the imprinting polymers, the same covalent linkage is formed. In case of Wulff and coworker, they synthesized covalent conjugate of *p*-vinylbenzeneboronic acid with 4-nitrophenyl-α-D-manopyranoside (the template), and copolymerized this conjugate with methacrylic acid and ethylene glycol dimethacrylate (cross-linking monomer). After polymerization, the boronic acid ester in the polymer was cleaved, and the 4-nitrophenyl-α-D-manopyranoside was removed. Therefore, the resultant polymers exhibit

rebinding characteristic for this template. In addition to covalent imprinting, Shea formed a ketal conjugate between the carbonyl group of a template and the 1,3-diol group in a functional monomer, and used this covalent conjugate for molecular imprinting (139).

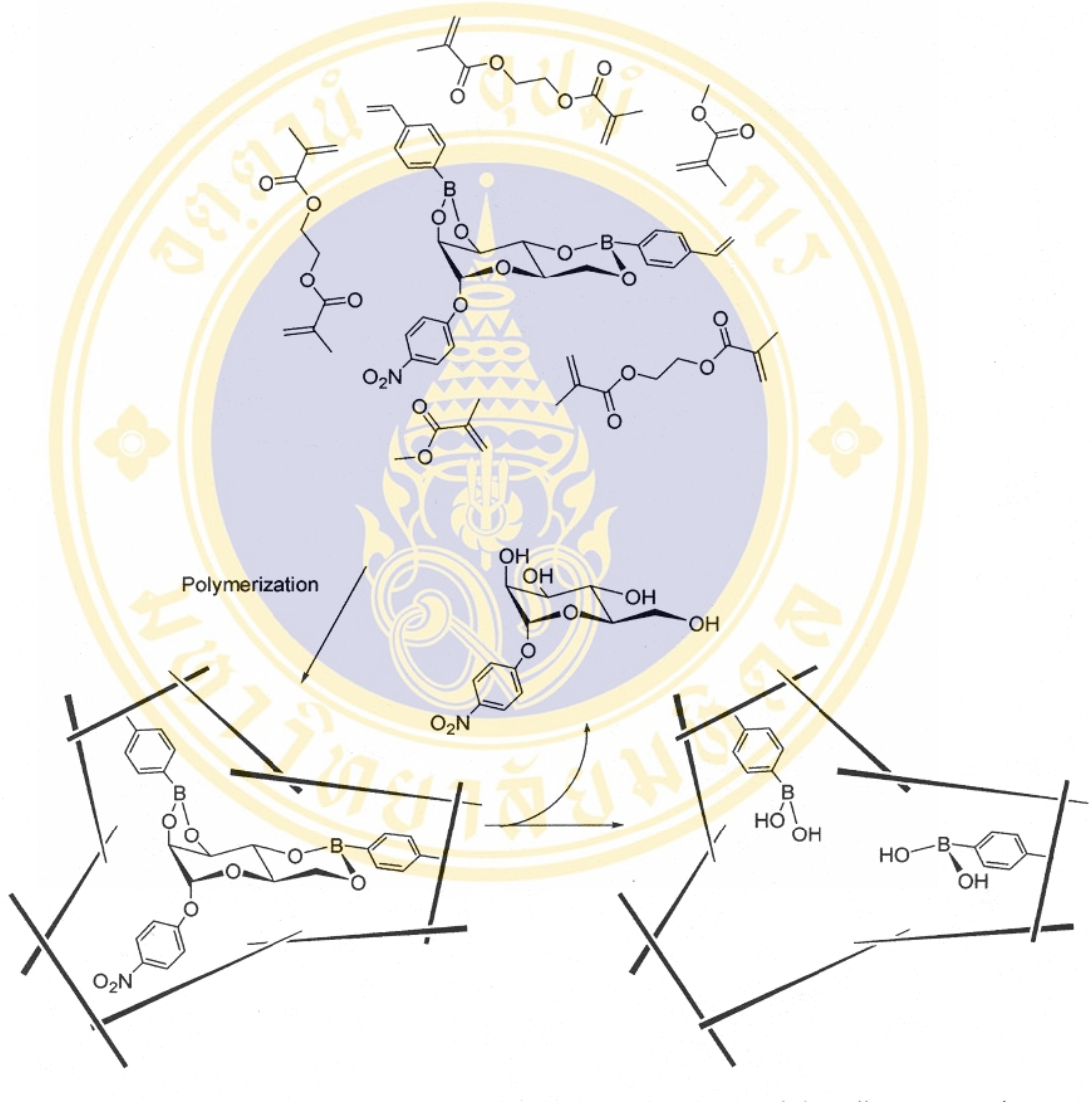

Figure 2.5 Covalent imprinting of mannopyranoside using its 4 vinylphenylboronic acid ester as a functional monomer (136, 138).

4.2.2 Non-covalent imprinting

The non covalent imprinting strategy (the self-assembly approach) was introduced by Mosbach and coworkers. They showed that covalent linkage between template and functional monomer are not necessarily required for molecular imprinting, and even non-covalent interaction between them work sufficiently (140, 141). This strategy provides

weak non-covalent intermolecular interactions, such as electrostatic interactions, hydrogen bonding, π– π bonding and hydrophobic interactions, between the template and the functional monomers serving to form molecular assemblies. Hence the selection of functional monomers which interact strongly with the template is crucial to generate high affinity binding sites (142). In the imprinting of methacrylic acid and theophylline (a drug), for instance, a non-covalent monomer-template adduct was form via hydrogen interaction. The same strategy was successful for the imprinting with various drugs, insecticides, and others (19, 143-145). Although, the strategy is so simple but the imprinting effects are so remarkable. Therefore, this method is satisfactorily applicable to a wide range of molecules and applied to use in many research areas.

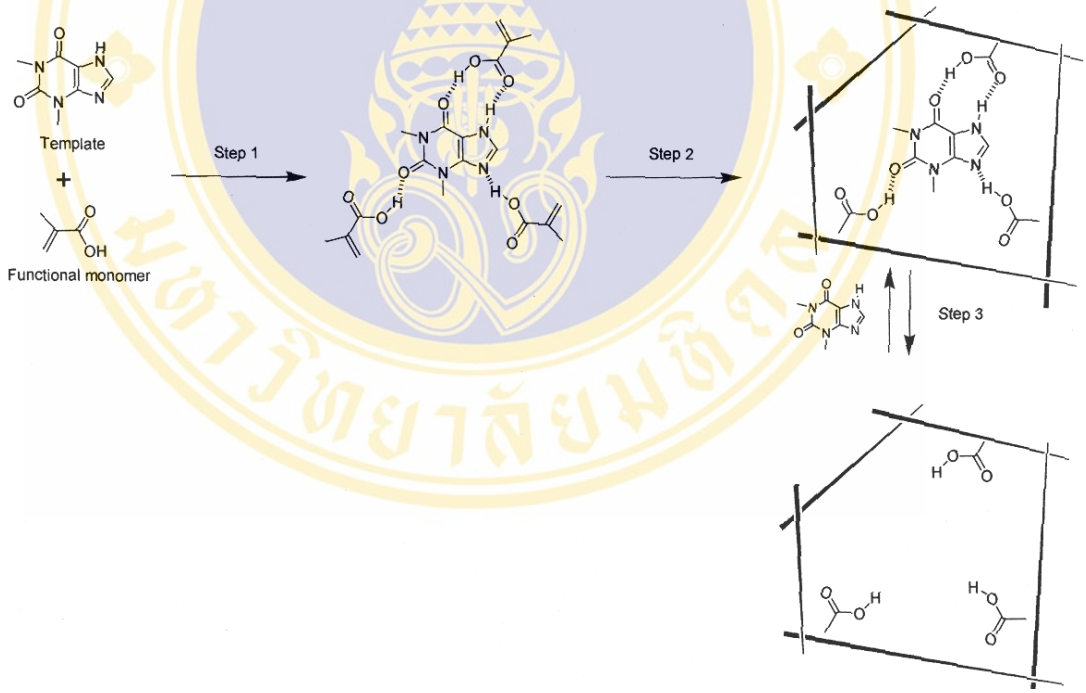

Figure 2.6 Non-covalent imprinting of theophylline using methacrylic acid as a functional monomer (136, 143)

4.2.3 Semi-covalent imprinting

It is generally believed that covalent imprinting gives better defined and more homogeneous binding sites than the non-covalent approach since the template-functional monomer interactions are far more stable and defined during the imprinting process than the template-functional monomer complex in the non-covalent approach. However, the

general applicability of the pre-organized approach is limited because it can be difficult to design suitable binding sites for the target molecule in which covalent bond formation and cleavage are readily reversible under mild conditions. In contrast, non-covalent imprinting is much more flexible in terms of the binding sites that can be exploited and therefore the range of templates can be targeted. Furthermore, the non-covalent approach is experimentally simpler to realize than covalent imprinting methods because the complexation step is achieved simply by mixing the template with the functional monomer(s) in a suitable solvent. No chemical derivatisation of the template is required, and template removal typically involves simply washing the polymer repeatedly with a suitable solvent or solvent mixture. A major drawback of non-covalent systems is the unavoidable heterogeneity of the binding sites obtained arising from the multitude of complexes formed between the template and the functional monomers which are apparently preserved to some extent during the polymerization. The non-covalent bonding is generally weak and thus an excess of functional monomer relative to the template is usually required to favor template-functional monomer complex formation and to maintain its integrity during the polymerization. As a result, a fraction of the functional monomers are randomly incorporated in the polymer matrix resulting in the formation of non selective binding sites (146, 147).

Therefore, a third approach was introduced by Whitcombe and coworkers in 1995, the semi-covalent approach or hybridization of covalent and non-covalent approach, which the template is covalently bound to a functional monomer during polymerization, as in the covalent approach, whereas only non-covalent interactions are exploited during the rebinding (13, 146). The fact that the template is covalently bound to the functional monomer at the outset, can in principle yield imprinted polymers with higher binding capacities since there is much better binding site integrity during polymerization. For instance, Whitcombe and coworkers used this approach to prepared molecularly imprinting polymer for cholesterol by bulk method. They prepared template-monomer conjugate, cholesteryl 4-vinyl carbonate and polymerized with either ethylene glycol dimethacrylate (EDMA) or divinylbenzene (DVB). After polymerization, template was removed by alkaline treatment and neutralized with acid. For binding, cholesterol was challenged for those polymers by hydrogen interaction.

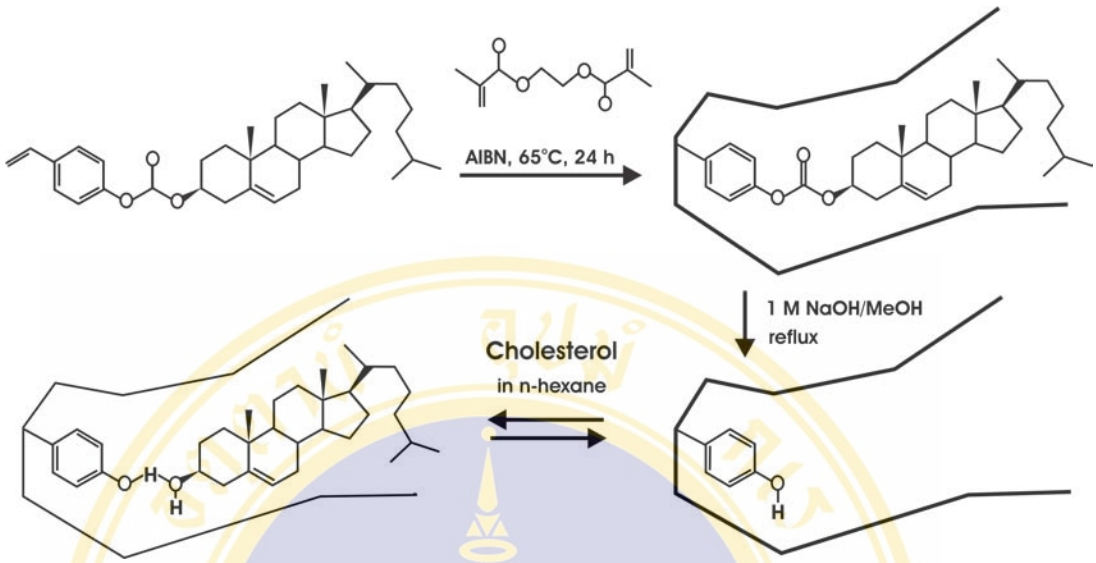

Figure 2.7 Semi-covalent imprinting of cholesterol (13)

4.3 Advantages and disadvantages of covalent and non-covalent imprinting (136)

4.3.1 covalent imprinting

Advantages:

1. Monomer-template conjugates are stable and stoichiometric, and thus the molecular imprinting processes (as well as the structure of guest-binding site in the polymer) are relatively clear cut.
2. A wide variety of polymerization condition (e.g. high temperature, high or low pH, and highly polar solvent) can be employed, since the conjugate are formed by covalent linkages and are sufficiently stable.

Disadvantages:

1. Synthesis of the monomer-template conjugate is often troublesome and less economical.
2. The number of reversible covalent linkages available is limited.
3. The imprinting effect is in some case diminished (cleavage of covalent linkages), which required rather severe condition.
4. Guest binding and guest releasing are slow, since they involve the formation and breakdown of covalent linkage.

4.3.2 noncovalent imprinting

Advantages:

1. Synthesis of covalent monomer-template conjugates is unnecessary.
2. Template is easily removed from the polymer under very mild conditions, since it is only bound by non-covalent interaction.
3. Guest binding and guest releasing, which take advantage of non-covalent interaction, are fast.

Disadvantages:

1. The imprinting process is less clear-cut (monomer template adduct is labile and not strictly stoichiometric).
2. The polymerization must be carefully chosen to maximize the formation of non-covalent adduct in the mixture.
3. The functional monomers exiting in large excess (in order to displace the equilibrium for adduct formation) often provide non specific binding site, diminishing the binding selectivity.

4.4 Polymerization method

4.4.1 Bulk polymerization

The first polymerization method employed to synthesize MIP was based on "bulk" polymerization (16, 148). This method is the most widely used by groups working on imprinting because of its simplicity and universality. It is used exclusively with organic solvents and consists basically of mixing all the components (template, monomer, solvent and initiator) and polymerizing them. The result is a polymeric block that needs to be crushed and ground to obtain particles of irregular shape and size between 20 and 50 μm. It has the disadvantage that a lot of the polymer produced (an estimated 70%) is wasted in the process of grinding. It may also produce areas of heterogeneity in the polymeric matrix resulting from the lack of control of the process during polymerization.

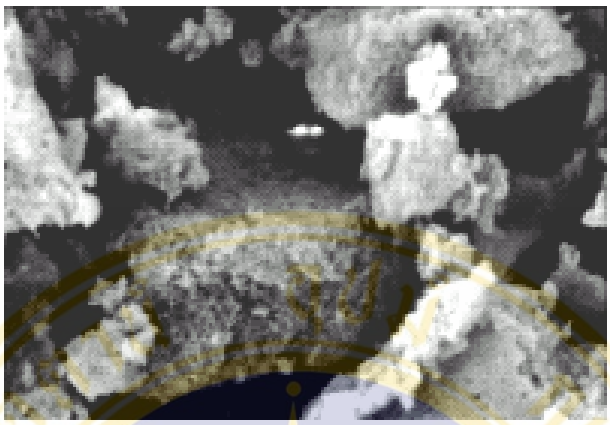

Figure 2.8 SEM of bulk polymerization (149)

4.4.2 Precipitation polymerization

Precipitation polymerization method was developed by Ye and coworkers (150). This method can provide monodisperse microspheres in the submicron scale (0.3–10 μm). The formation of highly crosslinked microspheres takes place in an excess amount of reaction medium, with the volume used generally being far greater than the volume of porogen used to prepare an imprinted polymer monolith via conventional methods. The mechanism for particle formation and growth in precipitation polymerization is based on the precipitation of the polymeric chains out of the solvent in the form of particles as they grow more and more insoluble in an organic continuous medium. In this case, particles are prevented from coalescence by the rigidity obtained from the cross-linking of the polymer, so there is no need of any extra stabilizer (151). These microspheres are easy to prepare, they have clean, stabilizer-free surfaces and therefore are devoid of nonspecific binding caused by strongly adsorbed stabilizers or surfactants. Importantly, neither polymer grinding nor sieving steps are necessary following precipitation polymerization, therefore the preparation of molecularly imprinted microspheres by this method is much less time-consuming. In conventional molecular imprinting protocols, the yield of imprinted polymer with the desired particle size range following successive grinding and sieving operations is usually less than 50%. In contrast, the present method allows polymer yields about 85% to be attained.

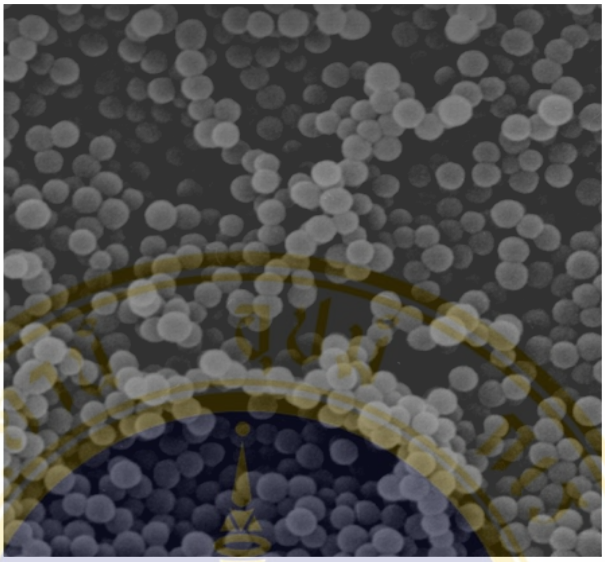

Figure 2.9 SEM of precipitation polymerization (150)

5. Nitroxide Mediated Living Free Radical Polymerization

Nitroxide **M**ediated **P**olymerization (NMP) has been introduced as one of highly valuable techniques for living free radical polymerization (LRP) in the field of polymer science. Up to now, this technique was growing up very fast because of many advantages over the conventional free radical polymerization such as constant rate of polymer synthesis, no need of catalyst addition, and narrow molecular weight distribution (152, 153). The difference between classical and living free radical polymerization lies in the occurrence of a reversible activation process for the latter. The growing polymer switches between a dormant (P-X) and an active state (P•). Chain extension with monomer (M) can only occur via the active state, which is the polymeric radical. Importantly, the equilibrium between the dormant and the active state lies far on the side of the dormant state (153). Hence, the concentration of free radicals is kept low during the entire polymerization. Therefore, side reactions such as dimerization and disproportionation of the polymeric radicals are suppressed and highly controlled polymerizations are obtained. A general picture of a living free radical polymerization is depicted in figure 2.10. In practically important systems, it usually holds that $[P\bullet]/ [P–X] < 10^{-5}$, meaning that a living chain spends most of its polymerization time in the dormant state (154).

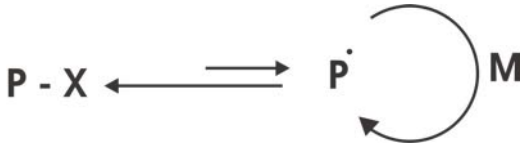

Figure 2.10 General process of living free radical polymerization based on reversible activation. (P-X= dormant polymer, P= polymer radical, M= monomer) (155)

The first report on a living free radical polymerization was published by Otsu in 1982 (156, 157). Although the control of the polymerization process was not ideal, those initial results paved the way to modern living free radical processes. During the past 10 years, the number of publications containing the term "nitroxide mediated polymerization" has shown exponential growth. This indicated the importance of this chemistry.

The general mechanism of NMP is shown in figure 2.11. The key to the success is a reversible thermal C-O bond cleavage of a polymeric alkoxyamine to generate the corresponding polymeric radical and a nitroxide. Monomer insertion with subsequent nitroxide trapping leads to chain-extended polymeric alkoxyamine. The whole process is controlled by the so called "Persistent Radical Effect" (PRE) (153, 158). The PRE is a general principle that explains the highly specific formation of the cross-coupling product (R1–R2) between two radicals R1 and R2 when one species is persistent (in NMP the nitroxide) and the other transient (in NMP the polymeric radical), and the two radicals are formed at equal rates (guaranteed in NMP by thermal C-O bond homolysis). The initial buildup in concentration of the persistent nitroxide, caused by the self termination of the transient polymeric radical, steers the reaction subsequently to follow a single pathway, namely the coupling of the nitroxide with the polymeric radical.

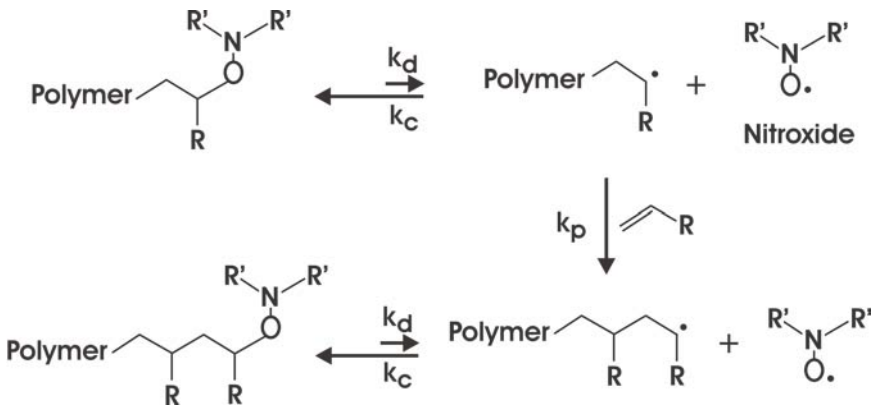

Figure 2.11 General mechanism of nitroxide mediated polymerization (155)

6. Green Fluorescent Protein

Green fluorescent protein, GFP, is a spontaneously fluorescent protein isolated from coelenterates, such as the Pacific jellyfish, *Aequoria victoria* or from the sea pansy, *Renilla renifermis* (159, 160). In *Aequorea victoria*, The green fluorescence came from the energy transfer of the blue chemiluminescence protein, aequorin, which was bind to calcium ion (161). Up to now, GFP is wildly used in various research and application fields because of its properties.

Figure 2.12 Structure of green fluorescent protein (162)

6.1 Properties of GFP

Green fluorescent protein is comprised of 238 amino acids. Its wild-type absorbance/ excitation peak is at 395 nm with a minor peak at 475 nm. (163, 164). The emission peak is at 508 nm. Interestingly, excitation at 395 nm leads to decrease over time of the 395 nm excitation peak and proportional increase in the 475 nm excitation band (165). This presumed photoisomerization effect is especially evident with irradiation of GFP by UV light. Analysis of a hexapeptide derived by proteolysis of purified GFP led to the prediction that the fluorophore originates from an internal Ser-Tyr-Gly sequence which is post-translationally modified to a 4-(*p*-hydroxybenzylidene)- imidazolidin-5-one structure (166). Studies of recombinant GFP expression in *E. coli* led to a proposed sequential mechanism

initiated by a rapid cyclization between Ser^{65} and Gly^{67} to form a imidazolin-5-one intermediate followed by a much slower (hours) rate-limiting oxygenation of the Tyr^{66} side chain by O_2 (167). Combinatorial mutagenesis suggests that the Gly^{67} is required for formation of the fluorophore (168). No co-factors or enzymatic components are required for this apparently auto-catalytic process. It is rather thermosensitive with the yield of fluorescently active to total GFP protein decreasing at temperatures greater than 30 C (169). However, once produced, GFP is quite thermostable. The mechanism of chromophore formation was illustrated in figure 2.13.

Physical and chemical studies of purified GFP have identified several important characteristics. It is very resistant to denaturation e.g. treatment with 6 M guanidine hydrochloride at 90 C or pH of 4.0 to 12.0. Partial to complete renaturation occurs within minutes following reversal of denaturing conditions by dialysis or neutralization (170). Circular dichroism predicts significant amounts of sheet structure that is subsequently lost on denaturation. Over a nondenaturing range of pH, increasing pH leads to a reduction in fluorescence by 395 nm excitation and an increased sensitivity to 475 nm excitation (170). Reduction of purified GFP by sodium dithionite results in a rapid loss of fluorescence that can be recovered in the presence of oxygen. While insensitive to sulfhydryl reagents such as 2-mercaptoethanol, treatment with the sulfhydral reagent dithiobisnitrobenzoic acid (DTNB) irreversibly eliminates fluorescence (171).

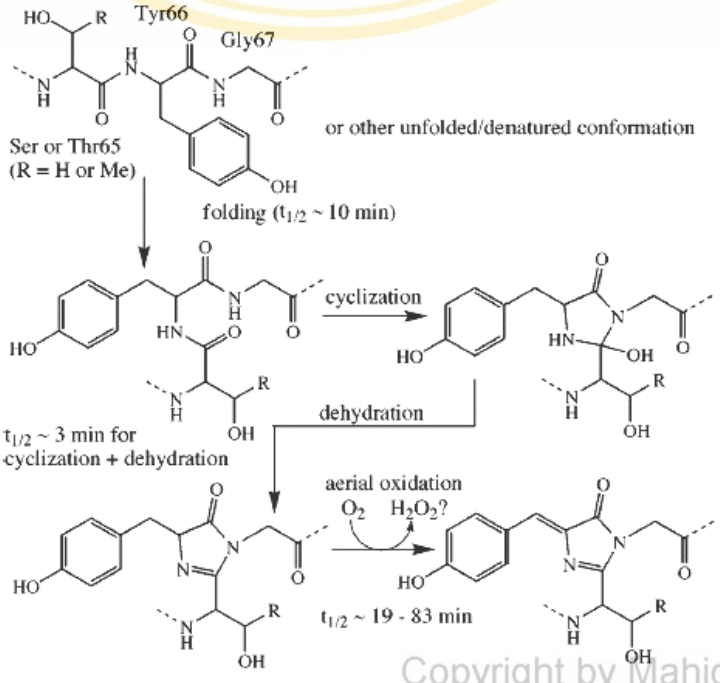

Figure 2.13 Mechanism of green fluorescent protein chromophore formation (172)

Due to the advantages and properties of green fluorescent protein, for instance ease of detection, no exogenous substrate are needed, no fixing or staining of samples, resistance to many critical conditions (e.g. high temperature, acid-base resistance, detergent), many researchers have successfully been used GFP for variety of applications such as reporter for monitoring gene expression (173, 174), fusion tag to monitor protein localization (175, 176). In addition, GFP can be used as a marker to study cell lineage during development (177) and metal determination (33, 178). Therefore, this molecule is very useful in the biological science in the future.

6.2 Applications of green fluorescent protein

Owing to the property of autofluorescence of green fluorescent protein, GFP has widely been used as a reporter molecule for monitoring gene expression, as fusion tags for monitor protein localization and protein-protein interactions (173-176, 179). All of these evidences were shown the potential of using GFP in many biological systems.

6.2.1 GFP as a reporter molecule

The GFP was applied as reporter molecule for gene expression, protein localization, protein-protein interaction (173-176, 179) and immunological detection system such as GFP fused to antibody (180), protein A (181) as well as protein G (182) because of its advantages. Firstly, it could be simply detected using either standard long-wave UV lamps or fluorescein isothiocyante (FITC) filter sets found in fluorescent microscope. Secondly, the substrate or cofactor would not be required. Third, it is a stable monomeric protein which would facilitate protein fusion and manipulation. Finally, the compact and stable nature of the folded GFP molecule makes it insensitive to the attached protein. In our lab, for instances, the GFP was used as a reporter by fusing to IGg binding domain (ZZ domain) from staphylococcal protein A and applied for *Leptospira* and antinuclear antibody detection (183).

6.2.2 Chimeric metal binding green fluorescent protein

The first intention of chimeric metal binding green fluorescent protein construction is for protein purification. The approach for GFP purification was done by attachment of the polyhistidine tail to the GFP via immobilized metal affinity chromatography (171, 184, 185). Moreover, the polyhistidine tagged GFPs were used for calibration of fluorescence resonance energy transfer in microscopy on nickle chelating beads (186). Furthermore, the

metal binding site was engineered on the GFP to study the metal-protein proximity and fluorescent quenching (187). In our lab, GFP was fused to the polyhistidine or cadmium binding sequence. These chimeric GFPs were used for metal determination on cellular and protein based system. In addition, metal toleration and accumulation have also been studied (33, 34, 178). However, the knowledge about the effect of metal binding protein to the GFP was still not explored.

CHAPTER 3
MOLECULARLY IMPRINTED POLYMER MICROSPHERES FOR CHOLESTEROL PREPARED BY PRECIPITATION POLYMERIZATION USING SACRIFICIAL COVALENT BOND

1. Abstract

Molecularly imprinted polymer microspheres were prepared by precipitation polymerization using a sacrificial covalent bond. In the present model cholesteryl (4-vinyl)phenyl carbonate was used as a template monomer. The imprinted microspheres were prepared using ethylene glycol dimethacrylate (EDMA) and divinylbenzene (DVB) as cross-linker. The base-labile carbonate ester bond was easily hydrolyzed to leave imprinted cavities in the resulting polymers. Radioligand binding analysis, elemental analysis and scanning electron microscopy were used to characterize the imprinted materials. Imprinted microspheres prepared from DVB cross-linker had larger and more defined spherical shape, and displayed better imprinting effect than EDMA-based microparticles. For comparison, imprinted bulk polymers were also prepared in the same reaction solvent as that used in precipitation polymerization. Elemental analysis results indicated that imprinted microspheres contained more template monomer units than bulk materials. The efficiency of template removal by hydrolysis treatment for microspheres was also higher than for bulk polymers. For DVB-based polymers, imprinted microspheres displayed higher specific cholesterol uptake than the corresponding bulk polymer.

2. Introduction

Molecular imprinting has attracted a broad research interest in recent years. The simplicity of creating tailored recognition sites in synthetic materials, as compared to complicated multi-step organic synthesis, is very attractive from an application's point of view, although certain limitations with molecularly imprinted polymers (MIPs) still need to be addressed, such as slow binding kinetics, aqueous compatibility and heterogeneity of binding site distribution. In general, two different approaches have been followed to prepare MIPs: non-covalent and covalent imprinting, depending on the molecular interactions utilized between the template and functional monomer during the free radical polymerization (14, 16, 188). Due to the easy access to a broad range of functional monomers from commercial sources, the non-covalent imprinting method has been used by most research groups, which resulted in a large number of non-covalent MIPs displaying favorable molecular recognition properties.

Previously we have demonstrated that non-covalent MIPs in microbead format can be easily prepared using precipitation polymerization (189, 190). In this study we intended to determine if the same synthetic methodology could be extended to the preparation of covalent MIP microspheres. In addition, the small particle size of microspheric MIPs should allow easy template removal using an appropriate chemical cleavage. Instead of using covalent interaction for MIPs to bind the target analyte, we select to follow the "semi-covalent" or "sacrificial bond" strategy introduced by Whitcombe et al (13), in which analyte binding was accomplished by non-covalent interaction inside the covalently imprinted cavities. We were also interested in investigating if the covalently imprinted polymers have a homogeneous binding site distribution as previously expected, or if binding site heterogeneity is rather an intrinsic character for MIPs prepared by free radical addition polymerization. For these purposes we had to study analyte binding covering a broad concentration range, in order to obtain a global binding isotherm. This was achieved using homologous radioligand binding experiments, where radioisotope-labeled and unlabeled analyte have the same chemical identity, and thus interact with imprinted sites with the same mechanism.

3. Experimental

3.1 Chemicals and methods

Methacrylic acid (MAA), ethylene glycol dimethacrylate (EDMA), and azobis-isobutyronitrile (AIBN) were purchased from Merck (Darmstadt, Germany) and used without purification. Divinylbenzene (technical, mixture of isomers, 80%) from Aldrich was passed through an aluminnium oxide column to remove the stabilizer, 4-tert-butylcatechol prior to use. 4-Acetoxystyrene was obtained from Aldrich and used as received. (*S*)-Propranolol hydrochloride was purchased from Fluka and converted into free base form before use. [1_,2_-^{3}H(N)]Cholesterol (specific activity 41.3 Ci mmol-1) was supplied by Sigma. [2,4,6,7-^{3}H(N)]Estradiol (specific activity 72.0 Ci/mmol) and (*S*)-[4-^{3}H]- propranolol (specific activity 15.0 Ci mmol-1) were purchased from NEN (Boston, MA, USA).Cholesteryl (4-vinyl)phenyl carbonate was synthesized according to a literature protocol (6). Solvents and other reagents were of analytical grade unless otherwise stated. Elemental analysis for oxygen content was carried out at MikroKemi AB, Uppsala, Sweden. Scanning electron microscopy (SEM) images were obtained with a JEOL JSM-840A microscope at the Department of Materials Chemistry, Chemical Center, Lund University.

3.2 Polymer synthesis

3.2.1 Molecularly imprinted polymers, unhydrolyzed (Chol-M1, Chol-M2, Ace-M2 and Chol-B2)

Imprinted polymer microspheres (Chol-M1, Chol-M2 and Ace-M2) were synthesized using the precipitation polymerization method described previously (4,5). Imprinted bulk polymer (Chol-B2) was synthesized from a concentrated monomer solution. Reagent feedings are detailed in Table 3.1. Briefly, the functional monomer, cross-linker and AIBN (17.5 mg, 0.106 mmol) were dissolved in a mixture of acetonitrile and toluene. The solution was gently flushed with argon for 5 min and sealed under argon. Polymerization was started at 60°C and continued for 24 h. After polymerization, the imprinted microspheres were collected by centrifugation. The imprinted bulk monolith was broken and fragmented with a mechanical mortar. The polymer particles were washed with methanol (2 × 20 mL), hexane (2 ×20 mL), and dried in vacuum.

3.2.2 Molecularly imprinted polymers, hydrolyzed (Chol-M1H, Chol-M2H, Ace-M2H and Chol-B2H)

Each of the imprinted polymers (Chol-M1, Chol-M2, Ace-M2 and Chol-B2) was suspended in 20 mL of 1 M NaOH solution in methanol and refluxed for 6 h. Upon returning to ambient temperature, the suspension was neutralized to pH 7 by adding 1 M HCl. Polymer particles were collected by centrifugation, washed with methanol (2 × 20 mL), hexane (2 × 20 mL), and dried in vacuum.

3.2.3 Non-imprinted polymers, hydrolyzed (M1H, M2H and B2H)

Non-imprinted polymers (M1H, M2H and B2H) were synthesized and hydrolyzed under the same conditions as that used to prepare polymers Chol-M1H, Chol-M2H and Chol-B2H, respectively, except that the functional monomer was omitted during the polymerization.

3.2.4 Radioligand binding analysis

Polymer particles were incubated in 1 mL of radioisotope labelled analyte solution (1.4 nM) at 20°C for 16 h. In competitive binding experiments, different unlabelled analyte was added in the same solution. A rocking table was used to provide gentle mixing. After the incubatuion, samples were centrifuged to separate the labelled analyte bound on the solid particles. Supernatant (200 mL) was taken and mixed with scintillation liquid Ecosint A (10 mL), and counted for 1 min using a Rackbeta 2119 liquid scintillation counter (LKB Wallac, Sollentuna, SE). The liquid counting results were used to calculate the percentage of radioligand that bound to polymer particles.

4. Results and discussion

4.1 Experimental design: investigation of covalently imprinted cavities with different molecular probes

Due to the high cross-linking density used for polymer preparation, complete removal of template from covalently imprinted polymers by hydrolytic cleavage is often difficult to achieve. The situation becomes even more complicated when a template is covalently linked to polymer matrix via multiple chemical bonds. In this study we selected to use the single carbonate sacrificial linkage first introduced by Whitcombe et al for preparation of

imprinted polymer microspheres (Figure 3.1a). After templateremoval, the free cavities were expected to bind cholesterol via non-covalent (hydrogen bond) interaction in non-polar organic solvent. Since highly specific molecular recognition (e.g. for chiral resolution of racemic mixtures) often requires multiple interaction points, we expected that the cholesterol-imprinted sites would show certain cross-recognition towards molecules that have similar size and functional group distribution.

To test the cross-recognition of imprinted sites, we decided to use radioisotope-labeled cholesterol, (*S*)-propranolol and 17β-estradiol (Figure 3.1a) to probe the imprinted binding sites. Imprinted but unhydrolyzed polymers, as well as non-imprinted but hydrolyzed polymers were used as two reference materials to estimate non-specific adsorption. In addition, a polymer containing a smaller binding site was prepared as another control (Figure 3.1b). This polymer, due to its limited cavity size, would not allow cholesterol to enter the specific sites, and the uptake of cholesterol can only be explained by nonspecific adsorption.

4.2 Effect of cross-linker on physical morphology of polymer particles

It is now generally accepted that the binding performance of MIPs can be largely influenced by the reaction solvent used during polymer preparation. We expected that MIP microspheres prepared using the "semi-covalent" approach under precipitation polymerization condition may have different binding performance, as compared to the bulk MIPs and MIP beads obtained previously (13, 23, 24). In the present work two different cross-linkers, EDMA and DVB were used to prepare molecularly imprinted microspheres in a large volume of a mixture of acetonitrile and toluene. The choice of acetonitrile as reaction solvent was based on previous findings that it resulted in regularly shaped microspheres when the two crosslinkers were employed. The use of toluene was due to that the template, cholesteryl (4-vinylphenyl) carbonate had poor solubility in pure acetonitrile. Polymer particles obtained from the precipitation polymerization had quite different morphologies when the two different cross-linkers were used. The EDMA-based MIP formed particle agglomerates that were composed of smaller nuclei (of diameter smaller than 0.4 μm) (Figure 3.2a). The DVB-based MIP existed as more defined microspheres, although with a rather large size distribution between 0.3 and 2.5 μm (Figure 3.2c). The less ideal particle morphology may be due to the use of the present solvent mixture, which deviated from the optimal composition used in previous precipitation polymerization reactions (189, 191). It should be mentioned that particle size distribution of imprinted

microspheres can be affected by many factors including template loading, the type of cross-linker used, and the composition of the imprinting solvent. For DVB-based polymers, appropriate agitation may also be required to assist narrowing particle size distribution.

The two imprinted polymers were subjected to the same hydrolysis treatment to remove the cholesterol template. It has been observed earlier that the treatment with NaOH in methanol, although under optimized condition, still caused the backbone of EDMA-based polymers to be partially hydrolyzed (23). The additional carboxyl groups generated by backbone hydrolysis may increase nonspecific cholesterol binding. For DVB-based polymers, treatment with NaOH in methanol can not change the cross-linked structure. Despite of the different behaviors of the EDMA and DVB polymers, scanning electron microscopy images (Figure 3.2b and 3.2d) indicated that the physical appearance of the polymers was not affected by the hydrolysis treatment.

4.3 Incorporation of templated sites and efficiency of hydrolytic cleavage for DVB-based microspheres

For the DVB-based microspheres, elemental analysis for oxygen content could be used to calculate the number of template units introduced into polymer matrix, as well as the hydrolysis-generated empty sites (Table 3.1). As an example, the calculation for polymer Chol-M2 and Chol-M2H is described in detail. For polymer Chol-M2, supposing the molar fraction of template monomer and cross-linker are x and y, respectively, the following equations are established:

$$x + y = 1 \quad (1)$$

$$532 \times 9.01\% \times x / (532 \times x + 130 \times y) = 3.3 / 100 \quad (2)$$

Where the following constants are used:
Molecular weight of cholesteryl (4-vinyl)phenyl carbonate: 532;
oxygen content of cholesteryl (4- vinylphenyl) carbonate: 9.01%;
molecular weight of divinylbenzene: 130;
oxygen content of polymer Chol-M1: 3.3%.
Solution of equation (1) and (2) gives:

$x = 0.12$
$y = 0.88$

Therefore, polymer Chol-M2 contains 12% (mol/mol) of template monomer unit. Now supposing the molar fraction of phenol and carbonate units in polymer Chol-M2H are x′ and y′, respectively, the following equations are established:

$$x' + y' = 0.12 \quad (3)$$

$$(120 \times 13.32\% \times x' + 532 \times 9.01\% \times y') / (120 \times x' + 532 \times y' + 0.88 \times 130) = 2.5 /100 \quad (4)$$

Where the following constants are used:
Molecular weight of cholesteryl (4-vinyl)phenyl carbonate: 532;
oxygen content of cholesteryl (4- vinylphenyl) carbonate: 9.01%;
molecular weight of 4-vinylphenol: 120;
oxygen content of 4- vinylphenol: 13.32%;
molecular weight of divinylbenzene: 130;
molar fraction of divinylbenzene: 0.88;
combined molar fraction of 4 vinylphenol and cholesteryl (4-vinylphenyl) carbonate: 0.12;
oxygen content of polymer Chol-M1H: 2.5%.
Solution of equation (3) and (4) gives:

$x' = 0.06$
$y' = 0.06$

Therefore, the efficiency of template removal, i.e. loss of cholesteryl carbonate, for polymer Chol- M2H is 50%. Based on the above value, the maximum number of binding sites in polymer Chol-M2H can be calculated as:

$$0.06 / (120 \times 0.06 + 532 \times 0.06 + 0.88 \times 130) = 3.9 \times 10^{-6} \text{ mol g}^{-1}$$

Using similar calculation, we obtained the amount of polymerized template and the level of template removal obtained by hydrolysis for other polymers, as listed in Table 3.1.

While microspheres Ace-M2 contained 5% (molar fraction) of acetoxy unit, which was identical to the feeding composition in the pre-polymerization solution, the molar fraction of cholesterol template in Chol-M2 and Chol-B2 were found to be 12% and 8%, respectively. The seemingly high reactivity of cholesteryl (4-vinylphenyl) carbonate may be explained by possible cholesterol-cholesterol interaction in acetonitrile: toluene mixture (192, 193). Formation of self-associated template clusters during imprinting reaction has

been discussed in several papers from other research groups (194-196). In fact, use of plausible cholesterol-cholesterol interaction for preparation of non-covalent MIPs in polar solvent has been reported (26, 27). In a dilute monomer solution used to synthesize Chol-M2, the cholesterol-cholesterol interaction may become more important in raising a local concentration of template monomer in vicinity of reactive radicals. As a result, the number of cholesterol units incorporated into a growing polymer chain can be increased even more.

The hydrolysis condition has been optimized by Whitcombe et al. for removing cholesterol template from EDMA-based bulk polymers (13). For the EDMA-based microparticles (Chol-M1 and Chol- M1H), we were not able to calculate the level of template incorporation or template removal by elemental analysis. However, because of the much reduced particle size, it is reasonable to assume that template removal from polymer Chol-M1H is more efficient than from bulk polymers, as well as than from the DVB-based polymer Chol-M2H (Table 3.1). In fact, it was more difficult to hydrolyze away cholesterol template from the present DVB-based bulk polymer (31%) than from the EDMA-based bulk polymer prepared by Whitcombe et al.(13)

4.4 Radioligand binding analysis

The two imprinted polymer microparticles prepared using EDMA and DVB as cross-linker were tested in hexane to bind cholesterol. Incubation with radioligand was continued for 16 h to ensure that binding equilibrium was reached for all samples. When EDMA was used as cross-linker, cholesterol uptake by Chol-M1H (67%) was only slightly higher than by the two control polymers, i.e. Chol-M1 (52%) and M1H (58%) (Table 3.1, last column). For the DVB-based polymer microspheres, Chol-M2H displayed cholesterol uptake more than two times higher (38%) than either Chol-M2 (13%) or M2H (12%). It is worth to mention that the above control polymers did not carry any free hydroxyl group, therefore uptake of cholesterol should be explained as a result of non-specific interaction with the polymer backbone. The high level of cholesterol uptake on EDMA-based polymers (Chol-M1, Chol- M1H and M1H) is presumably caused by hydrogen bond interaction between cholesterol and the ester functional groups on the polymer backbone. To verify that the specific cholesterol binding took place in template-generated cavities in polymer Chol-M2H, we synthesized another imprinted and hydrolyzed polymer Ace-M2H. Due to the smaller acetoxy templating moiety, Ace-M2H has reduced cavity size that does not allow cholesterol to form hydrogen bond interaction with the in-cavity hydroxyl groups (size exclusion). In fact, cholesterol uptake on Ace-M2H was almost equivalent to that obtained

on the other two control polymers (Chol-M2 and M2H, Table 3.1, last column).

The present DVB-based bulk polymer also displayed interesting binding performance: Chol-B2H bound two times more cholesterol (35%) than either Chol-B2 (14%) or B2H (16%). The improvement for DVB-based polymer is most probably caused by the new reaction solvent used in the present study. The poorer cholesterol recognition by the EDMA-based polymer Chol-M1H, as compared to previous results,6 may also be explained by the new solvent composition used for polymer synthesis. Although EDMA cross-linker in general gives better imprinting efficacy than DVB, this is true only if the crosslinker does not participate in molecular interaction with the template, either during the imprinting reaction or in re-binding experiment. When cross-linkers are involved in template binding, the situation may become different. For example, we found previously that replacing an acrylate-based cross-linker, trimethylolpropane trimethacrylate (TRIM) with DVB could greatly improve template recognition for propranolol-imprinted microspheres. In that case the improved binding selectivity was attributed to the additional solvophobic effect or π-π interaction between DVB and the template molecules, both during the imprinting reaction and in the binding experiments (190, 197). In the present system all the polymers were prepared in acetonitrile: toluene mixture, neither EDMA nor DVB could interact with the cholesterol template to enhance imprinting efficiency. On the contrary, when the binding experiments were carried out in hexane, the ester functional groups in EDMA-based polymers actually caused higher non-specific cholesterol absorption.

4.5 Binding isotherm measured by homologous competitive assay

Using tritium-labeled cholesterol, we carried out homologous competitive binding experiments: The labeled template was allowed to compete with increasing amount of unlabeled cholesterol to bind to a limited number of imprinted sites. As the labeled cholesterol has the same chemical structure as that of the unlabeled compound, it is reasonable to assume that they have the same binding characteristics when exposed to the same imprinted polymers (198, 199). Therefore, the fraction of bound labeled cholesterol should be equal to the fraction of bound cholesterol in total (Equation 5). This allowed us to establish binding isotherm for cholesterol in a broad concentration range.

[Chol*]bound / [Chol*]total = ([Chol*]bound + [Chol]bound) / ([Chol*]total+ [Chol]total) (5)

Where [Chol*] is the concentration of labeled cholesterol, [Chol] the concentration of un-labeled cholesterol.

When DVB was used as cross-linker, the amount of cholesterol bound to imprinted and hydrolyzed microspheres (Chol-M2H) was much higher than to the two control polymers (imprinted microspheres before hydrolysis (Chol-M2), and non-imprinted microspheres after hydrolysis (M2H)) (Table 3.1). The in-cavity binding was mainly mediated by hydrogen bond interaction, because replacement of hexane with a polar solvent (acetonitrile:toluene = 2:1, v/v) drastically reduced cholesterol uptake to below 5% (data not shown).

Despite of the favorable imprinting effect, the binding isotherm observed in Figure 3.3a indicated a heterogeneous site distribution for the present covalent imprinting system. This somewhat surprising result can be more clearly demonstrated by presenting the binding data in a Scatchard polt (Figure 3.3b), which shows the apparent two types of binding sites with very different affinities for cholesterol. The number of high affinity sites was however very limited. A simple linear curve fit in the high affinity range ([Bound] = 40 pM - 350 nM) was used to get an approximate apparent dissociation constant (*K*D) of (5.2 ± 0.3) × 10-6 M with a corresponding site population (*B*max) of 85 ± 5 nmol g-1. Similarly, for the low affinity sites ([Bound] = 350 nM - 2.5 mM), the parameters were calculated to be *K*D = (1.9 ± 0.1) × 10-2 M and *B*max = 258 ± 13 µmol g-1.While the high affinity sites accounted for less than 0.02% of the hydrolysis-generated cavities (390 µmol g-1, calculated from oxygen content value), the portion of low affinity binding sites were approximately 66%. Based on the present result, we suggest that the covalent molecular imprinting technique does not necessarily generate homogeneous binding sites. This is true at least for the present DVB-based microspheres that are prepared in acetonitrile: toluene mixture. Several factors during the imprinting reaction, for example the relative reactivity of functional monomer and cross-linker, and the non-ideal packing of polymer backbone at gelation point, may hamper the formation of identically defined, three dimensional binding sites in cross-linked polymer matrix. In the present system, an additional impact might come from the possible cholesterol-cholesterol interaction that led to formation of local template clusters during the cross-linking reaction.

4.6 Cross-reactivity of cholesterol-imprinted microspheres

Due to the fact that only a single functional group (phenol) was introduced into each binding site, we expected that cholesterol-imprinted polymer microspheres could exhibit certain cross-reactivity towards molecules that have size and hydrogen bond capability similar to cholesterol. The imprinted microspheres were therefore challenged with the same concentration of radioisotope labelled 17β- estradiol and (*S*)-propranolol in hexane. Although total binding of these compounds by the imprinted microspheres was much higher than that of cholesterol, the specific part, as reflected by the difference between hydrolyzed and unhydrolyzed polymers, was almost identical (approximately 20%, Figure 3.4). More interestingly, the majority of (*S*)-propranolol bound to polymer Chol-M2H was within the imprinted cavities (Figure 3.4).

To further confirm that propranolol uptake by cholesterol-imprinted polymer was caused by incavity hydrogen bond interaction, we attempted to saturate the limited number of binding sites with increasing amount of (*S*)-propranolol. This was simply achieved using the same homologous competition experiment as used for measuring cholesterol binding. A saturation curve for propranolol binding was obtained (Figure 3.5a). Using the same binding data, the Scatchard plot (Figure 3.5b) indicated that only one type of binding site could be probed by propranolol molecule.

The binding curve for propranolol shown in Figure 3.5a could be fitted with a Langmuir isotherm using Equation 6:

$$B = B\max \cdot F / (K\mathrm{D} + F) \qquad (6)$$

This gives propranolol the following apparent dissociation constant and site population: KD = (6.2 ± 0.4) × 10-4 M, and Bmax = (66.4 ± 0.9) μmol g-1. Thus the number of binding sites for (*S*)-propranolol only accounted for 17% of the hydrolysis-generated cavities in polymer Chol-M2H. These cholesterolimprinted binding sites were however homogeneous and displayed higher affinity for (*S*)-propranolol.

If (*S*)-propranolol binding was mediated by hydrogen bond interaction with the phenol groups located within the imprinted cavity, it should be possible to displace the bound propranolol molecules with a large excess of cholesterol. This was tested by incubating 5 mg of Chol-M2H with labeled (*S*)-propranolol (1.4 nM) and unlabeled cholesterol (14 mM) until equilibrium. The added cholesterol could displace up to 34% of (*S*)-propranolol in hexane, indicating that the competing molecules were binding to the same cavities. When smaller compounds (isopropanol and 3-methylindole) were tested in the competition experiment, they were not able to show the same competing effect as that obtained with

cholesterol. Therefore, the cross-recognition of cholesterol-imprinted sites had certain selectivity: part of the imprinted cavities could take up compounds that have molecular size and functionality similar to the original template. The high affinity of Chol-M2H for (*S*)-propranolol may be attributed to a favorable hydrogen bond interaction between the in-cavity phenol and the amino group of (*S*)-propranolol, rather than the weaker phenol-alcohol interaction (Figure 3.1a).

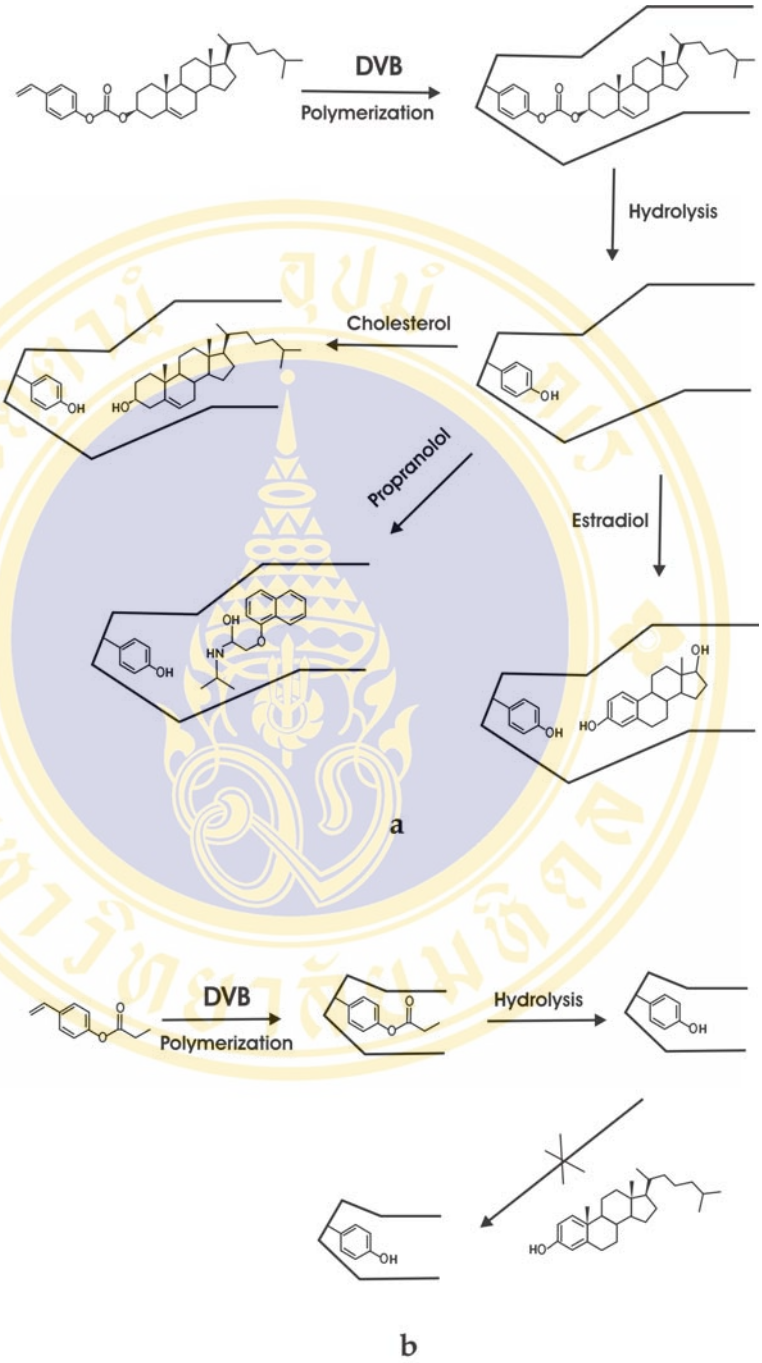

Figure 3.1. Schematic representation of the sacrificial approach used in the present study.
(a) Cholesterolimprinted cavities bind the template and related molecules.
(b) Smaller cavities can not take up large cholesterol molecule.

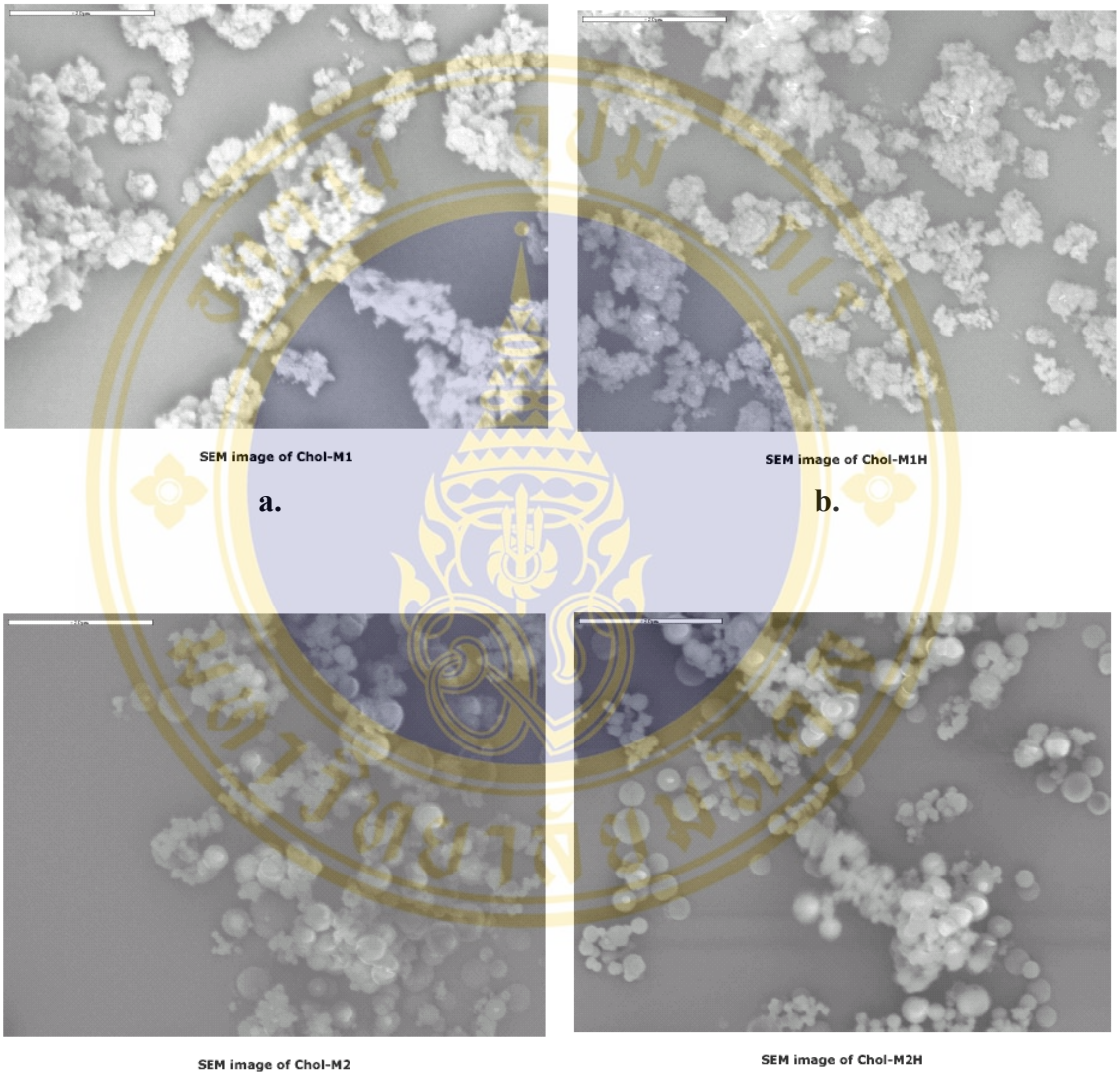

Figure 3.2. SEM image of Chol-M1 (a), Chol-M1H (b), Chol-M2 (c) and Chol-M2H (d). The scale bar represents 20 μm.

a.

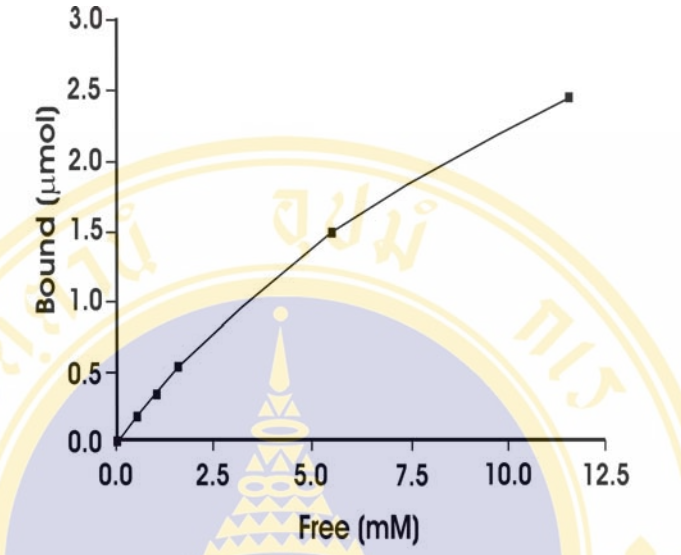

Binding isotherm for cholesterol on 25 mg of polymer Chol-M2H.

b.

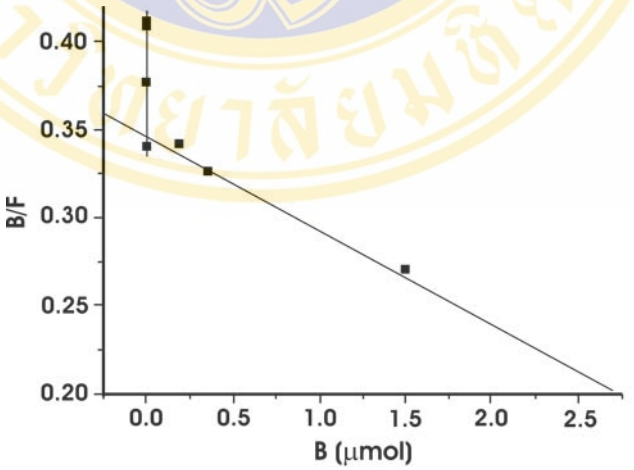

Scatchard plot for cholesterol binding to polymer Chol-M2H.

Figure 3.3. (A) Binding isotherm for cholesterol on 25 mg of polymer Chol-M2H. (B) Scatchard plot for cholesterol binding to polymer

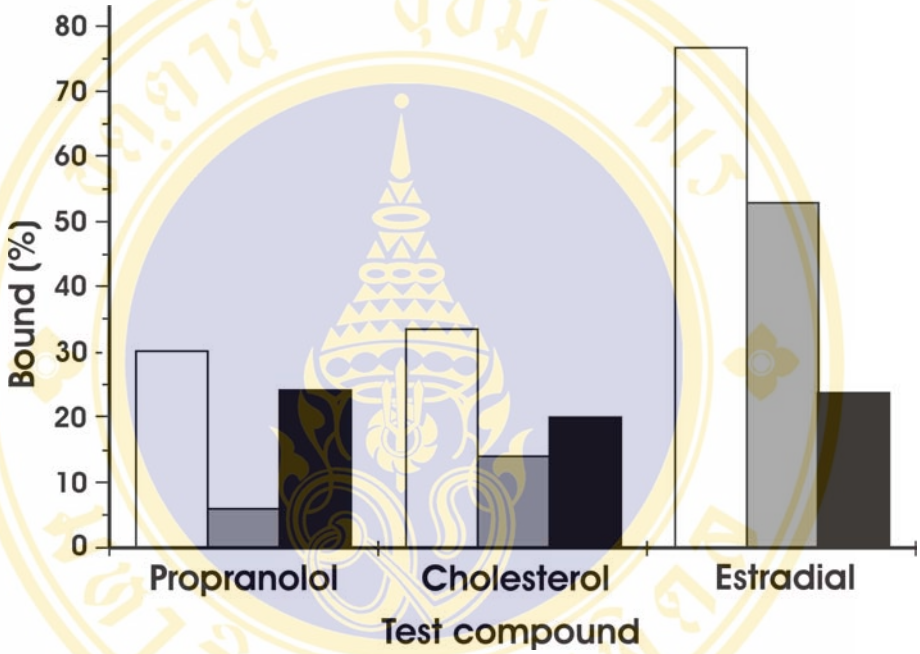

Figure 3.4. Uptake of different test compounds by polymer Chol-M2H (empty column) and Chol-M2 (grey column). The black column indicates the difference of analyte binding to the two polymers. For propranolol and estradiol, 5 mg polymer was used. For cholesterol, 25 mg polymer was used.

a.

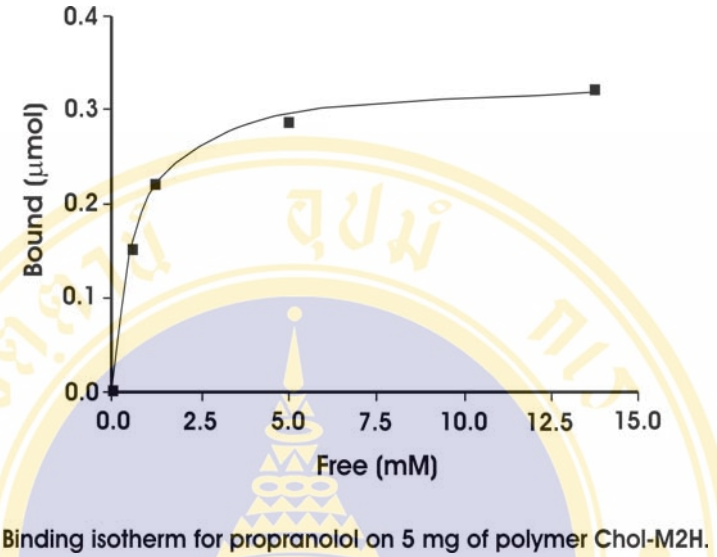

b.

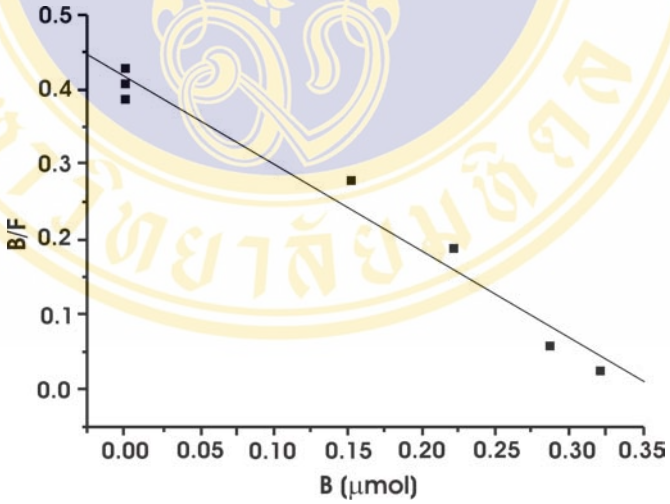

Figure 3.5. (a) Binding isotherm for propranolol on 5 mg of polymer Chol-M2H. (b) Scatchard plot for propranolol binding to polymer Chol-M2H.

Table 3.1 Preparation and characterization of molecularly imprinted polymers

Polymer	Template monomer		Crosslinker		Solvent[a] (mL)	O content[b] (wt %)	Polymerized template (mol %)[c]	Template removal (mol %)[c]	Cholesterol uptake[d] (%)
	Chol (mmol)	Ace (mmol)	DVB (mmol)	EDMA (mmol)					
Chol-M1	0.29	0	0	5.51	60	n.d.	n.d.	n.d.	52
Chol-M1H	0.29	0	0	5.51	60	n.d.	n.d.	n.d.	67
M1H	0	0	0	5.80	60	n.d.	0	0	58
Chol-M2	0.29	0	5.51	0	60	3.3	12	0	13
Chol-M2H	0.29	0	5.51	0	60	2.5	12	50	38
M2H	0	0	5.80	0	60	0	0	0	12
Ace-M2	0	0.29	5.51	0	60	1.2	5	0	n.d.
Ace-M2H	0	0.29	5.51	0	60	0.9	5	43	12
Chol-B2	0.29	0	5.51	0	0.88	2.3	8	0	14
Chol-B2H	0.29	0	5.51	0	0.88	1.9	8	31	35
B2H	0	0	5.80	0	0.88	0	0	0	16

Chol, cholesteryl(4-vinylphenyl) carbonate; Ace, 4-acetoxystyrene; n.d., not determined.
[a] Acetonitrile: toluene (2:1, v/v).
[b] Results from elemental analysis.
[c] Calculated from O content.
[d] Cholesterol binding to 25 mg polymer in 1 mL of hexane. Initial cholesterol concentration was 1.4 nM.

CHAPTER 4
MOLECULARLY IMPRINTED POLYMERS FOR CHOLESTEROL USING NITROXIDE-MEDIATED LIVING RADICAL POLYMERIZATION

1. Abstract

The use of molecularly imprinted polymers (MIPs) in chemical and bioanalytical applications has gained increased interest in recent years. Compared to their biological receptor counterparts, MIPs are easy to prepare, have long shelf stability and can be used under different harsh conditions. The majority of MIPs currently used are produced by traditional free radical polymerization. One drawback with the traditional radical polymerization is the difficulty of controlling the chemical process that forms the final imprinted cavities. We have been interested in applying controlled (living) free radical polymerizations for preparation of MIPs. An additional benefit of the living reaction system is that surface modification of MIPs following the imprinting reaction can be made straight forward, which is beneficial for MIPs that are to be used in solvents different from the imprinting porogen. As an example, we used nitroxide-mediated polymerization (NMP) to prepare cholesterol imprinted bulk polymers. A sacrificial covalent bond was employed to maintain imprinting fidelity at elevated temperature. Selective cholesterol uptake with imprinted polymers prepared under different conditions was studied in hexane. The imprinted hydrolyzed MIP prepared by NMP displayed higher selective cholesterol binding than that prepared by a traditional radical polymerization.

2. Introduction

Molecular imprinting is a powerful method for preparation of synthetic receptors for a given target guest molecule. This synthetic approach typically involves polymerization of functional and cross-linking monomers in the presence of a molecular template, which controls the distribution of functional groups in the resulting three-dimensional polymer network. After polymerization and template removal, specific binding sites are left in the polymer material, which can be used to afford effective separation, chemical sensing or selective catalysis. The broad use of the traditional free radical polymerization for preparation of molecularly imprinted polymers (MIPs) can be attributed to its good functional group tolerance to a large variety of template molecules. In essence, the free radicals generated during the addition polymerization do not interfere with the intermolecular interactions critical for the non-covalent imprinting system. Despite of optimization efforts made in the selection of functional monomers and improvement in the physical shape and morphology of MIPs, target binding provided by MIPs is often associated with a relatively low affinity, broad site heterogeneity and slow kinetics. Perhaps part of the poor performance of MIPs can be explained from a molecular level: the polymerization chemistry itself, which largely influences the local structure of the cross-linked polymer network has not been thoroughly investigated. The traditional radical polymerization process has been difficult to control in view of chain propagation and termination. This situation is drastically different from the synthesis of small organic receptors by stepwise reactions, where each reaction step is precisely controlled to furnish a desired intermediate. By gaining better control over the polymerization reaction, it is expected that improved molecular recognition with MIPs can be achieved.

Recently, Zimmerman and co-workers used metal-catalyzed ring-closing metathesis polymerization to prepare monomolecularly imprinted dendrimers, in which a porphyrin binding site was formed by cross-linking of the peripheral vinyl groups (200). Steinke and co-workers used ring-opening metathesis polymerization to prepare bulk polymers that displayed chiral-selective binding for L- and D-menthol (201). The use of the special catalysts in these studies required that a covalent imprinting – non-covalent binding strategy to be adopted.

Research on living radical polymerization systems has gained great advancement during the past years. By living radical polymerization the problematic chain termination encountered in traditional addition polymerization can be minimized. This can result in a more constant rate for polymer chain growth, and a narrow molecular weight distribution for non cross-linked linear polymers. Living radical polymerization has so far been mainly used to synthesize non-cross-linked polymers with different terminal functional groups. Application of living radical polymerization in cross-linked systems was less exploited. Among the most feasible living radical polymerization methods, only atom-transfer radical polymerization (ATRP) (202) has recently been used to prepare MIPs in a non-covalent imprinting system (203). The other living radical polymerization methods, i.e. reversible association fragmentation polymerization (RAFT) (204) and nitroxide-mediated polymerization (NMP) (205) have not been used for MIP preparation.

The present work aimed at studying nitroxide-mediated polymerization for preparation of molecularly imprinted polymers. We were particularly interested in NMP because it does not require any additional catalyst or chain transfer reagent: a single NMP initiator is sufficient to achieve reaction control. In addition, NMP can also simplify surface modification for MIPs to bring in better compatibility with differnt solvent systems. For more, NMP can be potentially used in both covalent and non-covalent imprinting systems, given that new low temperature NMP initiators are being developed (206). In the present study we used a nitroxide reagent that requires a relatively high activation temperature (125°C). To maintain stable functional monomer – template complexation under this reaction condition, we selected to adopt the sacrificial spacer method to keep a cholesterol template covalently bound to a monomer during its polymerization (13). After polymerization and template removal by hydrolytic cleavage, the resulting MIP contained specific binding sites that could take up cholesterol via non-covalent hydrogen bond interaction in a non-polar solvent. The binding performance of MIP prepared with NMP was compared to that prepared with a traditional radical polymerization. The equilibrium binding results indicated that the cholesterol-imprinted polymer prepared by NMP was superior to the polymer prepared by the traditional radical polymerization.

3. Materials and methods

3.1 Materials

Divinylbenzene (DVB, technical, mixture of isomers, 80%), 4-tert-butylstyrene (TBS, 93%), 2,2,6,6-tetramethyl-1-piperidinyloxy (TEMPO, 99%), 2,2'-azoisobutyronitrile (AIBN, 98%), benzoyl peroxide (BPO, 75%), 4-acetoxystyrene (96%), cholesteryl chloroformate (98%) and m-xylene (anhydrous, 99+%) were purchased from Aldrich. TBS was purified by vacuum distillation. AIBN and BPO were purified by re-crystallization from methanol. Prior to use, DVB was passed through an aluminnium oxide column to remove the stabilizer, 4-tert-butylcatechol. [1α,2α-^{3}H(N)]Cholesterol (specific activity 41.3 Ci mmol^{-1}) was supplied by Sigma. Scintillation liquid Ecoscint A was from National Diagnostics (Atlanta, GA, USA). The NMP initiator, 3-(4-tert-butylphenyl)-1,1-dimethyl-3-(2,2,6,6-tetramethyl piperidinooxy)propyl cyanide (**1**), was synthesized using a literature method (Abrol, et al., 1997). Cholesteryl (4-vinyl)phenyl carbonate was synthesized following the published protocol (Whitcombe et al., 1995). Other solvents and reagents were of analytical grade unless otherwise stated. Elemental analysis for oxygen content was performed by MikroKemi AB, Uppsala, Sweden.

3.2 Polymers preparation

Cholesterol-imprinted polymers (MIP) and non-imprinted polymers (NIP) were prepared using either the NMP reagent **1** or BPO as initiator (Table 4.1). The monomers and initiator were dissolved in 0.88 mL of m-xylene, the solution was purged with a gentle flow of Ar for 5 min. Thereafter, the reaction mixture was heated in an oil bath to 125°C and kept for 48 h. After polymerization, the polymer monolith was crushed into small particles, washed with methanol, hexane, and dried in a vacuum chamber. To remove the covalently linked cholesterol, half of the imprinted polymers were refluxed in 20 mL of 1 M NaOH for 48 h. After neutralization with 1 M HCl, polymer particles were collected by centrifugation, washed with methanol, hexane, and dried in a vacuum chamber. For comparison, the non-imprinted polymers were subjected to the same hydrolysis treatment.

3.3 Equillibrium binding analysis

Polymer particles were incubated in 1 mL of [1α,2α-^{3}H(N)]cholesterol solution in hexane (1.4 nM), with and without addition of non-labeled cholesterol, at 20°C for 16 h. A rocking table was used to provide gentle mixing. After the incubation, samples were centrifuged to sediment polymer particles. A fraction of the supernatant (200 μL) was taken and mixed with scintillation liquid Ecosint A (10 mL), and counted for 1 min in a Rackbeta 2119 liquid scintillation counter (LKB Wallac, Sollentuna, SE). The liquid counting results were used to calculate the percentage of [1α,2α-^{3}H(N)]cholesterol that bound to the polymers.

4. Results and discussion

4.1 Polymerization systems for preparation of cholesterol imprinted polymers

In the present study we prepared cholesterol-imprinted polymers using a template-monomer conjugate containing the sacrificial carbonate spacer. The template-monomer conjugate was originally designed to prepare imprinted polyacrylate type polymers, which showed highly selective cholesterol binding in a non-polar organic solvent (13). With the present nitroxide-mediated reaction system, a relatively high temperature was required to activate the TEMPO-capped dormant radicals (Figure 4.1). The polymer chain growth and cross-linking can be easily stopped or re-initiated by simply changing reaction temperature. The polymerization using NMP reagent **1** turned out to be much slower compared to that using BPO as initiator. The NMP system did not reach gelation point after 16 h reaction, whereas the BPO-involved mixture changed into amorphous solid within 20 min at 125°C. The slow polymerization rate for the NMP system can be explained by the reversible association of the TEMPO with the growing chain radicals. We expected this to allow the growing polymer chain to adopt a microscopic structure different from that obtained with the traditional BPO initiator. The NMP reaction process involves reversible capping of the chain radicals by the TEMPO moiety to prevent early termination. The NMP of the imprinting system is under certain level of thermodynamic control.

In the BPO initiated system, chain propagation stopped within a very short time due to termination reaction, which was in turn caused by the high free radical concentration at the beginning. In a sense the polymer network was formed without allowing any self-optimizing opportunity, and the imprinting process was predominantly under a kinetic control. In deed, the cross-linked polymers prepared using the two initiators had rather different surface area, i.e. the BPO initiated polymer had surface area about 20% higher than the NMP polymer (Table 4.1).

The cholesterol template was removed by hydrolytic treatment after polymerization. The use of DVB cross-linker allowed us to use a rather harsh condition to gain maximum template cleavage. We noticed that the hydrolysis treatment caused surface area of the two imprinted polymers to increase by about 30% (Table 4.1). Comparison of oxygen content before and after the hydrolysis gave a rough measure of the efficiency of template removal. The hydrolysis treatment caused oxygen content for MIP(NMP) to decrease by 64%, and MIP(BPO) by only 33% (Table 4.1). This indicated that removal of the cholesterol template from MIP(NMP) was much more easily achieved, even though MIP(BPO) had larger surface area. The different accessibility of the imprinted sites in MIP(NMP) and MIP(BPO) may be caused by the different reaction mechanisms involved in the polymerization.

4.2 Eqilibrium binding analysis

The imprinted unhydrolyzed polymers were used as control samples to measure non-specific cholesterol adsorption outside the cavities. The two imprinted hydrolyzed polymers (MIP(NMP)-H and MIP(BPO)-H) bound much more cholesterol than the corresponding imprinted un-hydrolyzed polymers (MIP(NMP) and MIP(BPO)) from a dilute solution in hexane (Figure 4.2). The difference in cholesterol binding before and after hydrolysis indicated that, the imprinted sites had much higher cholesterol affinity, as a result of the combination of hydrogen bond interaction and the complementary fit of cholesterol in the cavities. The change in surface area caused by the hydrolysis treatment may affect cholesterol binding in hexane as well. To compensate for this effect, two purely poly(DVB) polymers prepared by NMP and BPO initiator were subjected to the same hydrolysis condition and used as additional controls. Figure 4.2 shows that the non-specific cholesterol binding on these polymers was slightly higher than on MIP(NMP) and MIP(BPO). However, cholesterol binding in the specific cavities of the two imprinted hydrolyzed polymers was still predominant.

It is more interesting to compare the specific cholesterol binding on the two imprinted hydrolyzed polymers. Thus, MIP(NMP)-H displayed much higher cholesterol affinity than MIP(BPO)-H, even though its surface area was 15% lower than MIB(BPO)-H. This clearly indicated that the increased cholesterol binding by MIP(NMP)-H was only caused by the different imprinting process, rather than any non-specific effect such as the altered surface area. If the specific cholesterol binding is simply defined as the difference in cholesterol adsorption by the imprinted polymers after and before the hydrolysis treatment, the NMP-based imprinting is clearly superior to the BPO-based system. The specific cholesterol binding on MIP(NMP)-H (21%) was almost 60% higher than that on MIP(BPO)-H (13%). At the very low cholesterol concentration tested, the difference in cholesterol uptake may only be accounted by the difference in binding affinity. As MIP(NMP)-H showed largely increased cholesterol affinity, the nitroxide-mediated imprinting seemed to generate better binding sites than with the traditional free radical initiator.

4.3 Cholesterol binding isotherm

The use of radioisotope-labeled cholesterol allowed us to study cholesterol binding on the imprinted hydrolyzed polymers in a broad concentration range. Therefore, a fixed amount of MIP(NMP)-H and MIP(BPO)-H were titrated in hexane with increasing amount of cholesterol in the presence of 1.4 nM [^{3}H]cholesterol. As the tritrium-labeled cholesterol has the same chemical structure as that of the unlabeled compound, it is reasonable to assume that they have the same binding characteristics when exposed to the same imprinted polymers. Therefore, the fraction of bound labeled cholesterol was equal to the fraction of bound cholesterol in total:

$$[Chol^*]_{bound} / [Chol^*]_{total} = ([Chol^*]_{bound} + [Chol]_{bound}) / ([Chol^*]_{total} + [Chol]_{total})$$

Where [Chol*] is the concentration of labeled cholesterol, [Chol] the concentration of un-labeled cholesterol. This allowed us to establish binding isotherm for cholesterol in a broad concentration range using simple liquid scintillation counting (207). The equilibrium binding isotherms obtained were shown in Figure 4.3. Clearly, both the two polymers contained heterogeneous binding sites. No saturation was observed within the workable cholesterol concentration range. The two polymers also displayed quite different binding isotherms (Figure 4.3). When the same binding data were converted into Scatchard plots (Figure 4.4), the presence of two apparently different types of binding sites in the two polymers is easy to appreciate. Applying simple linear curve fit, the approximate binding

parameters for MIP(NMP)-H and MIP(BPO)-H could be calculated as listed in Table 4.1. Although the two imprinted hydrolyzed polymers had similar number of high affinity sites (B_{max}) (corresponding to [Bound] = 20 pM – 300 nM), the cholesterol affinity of MIP(NMP)-H corresponding to these sites was almost two folds of MIP(BPO)-H. The high affinity K_D and B_{max} values for the present MIP(NMP)-H were similar to that obtained from previous cholesterol-imprinted microspheres synthesized at a lower temperature (207).

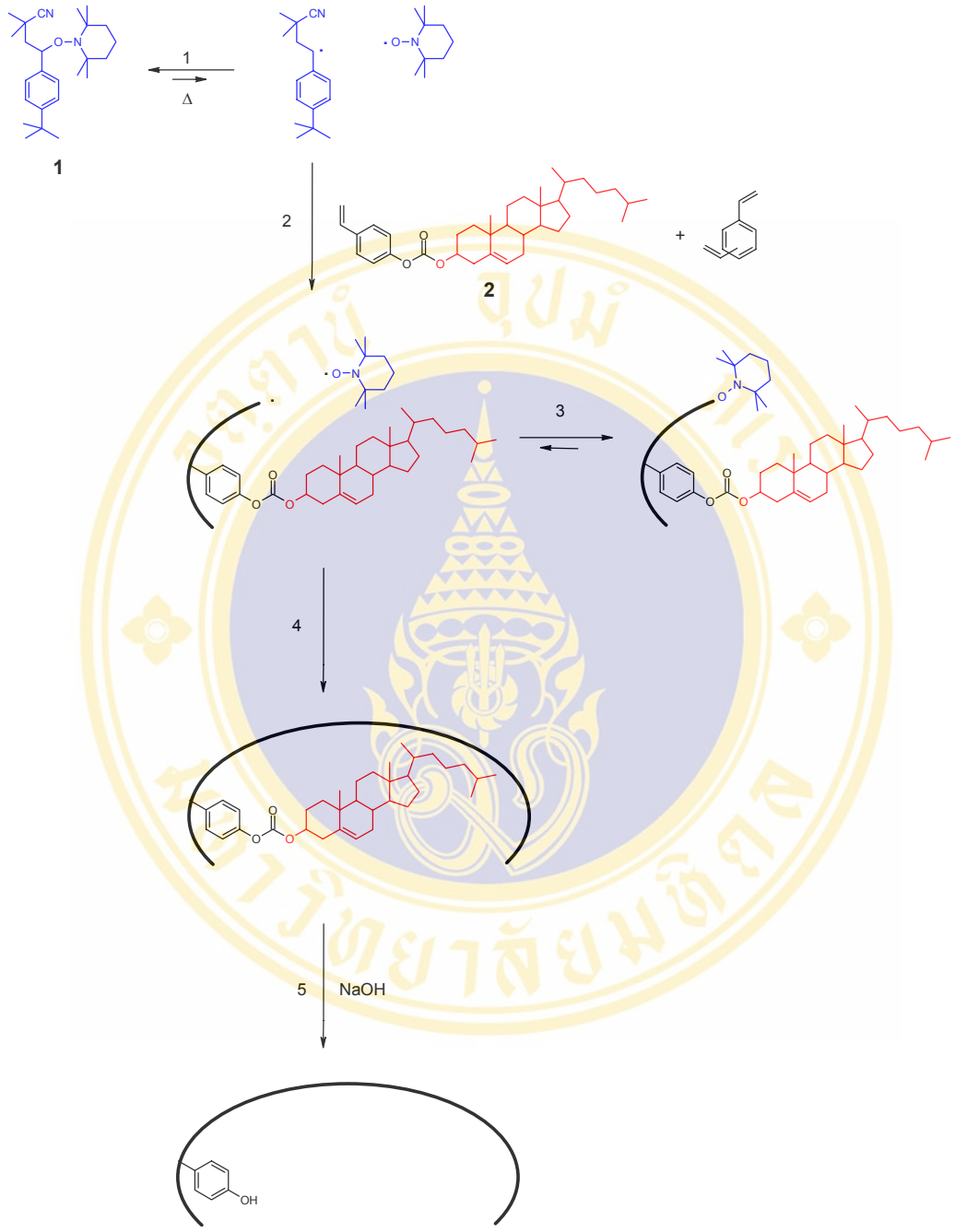

Figure 4.1 Preparation of cholesterol-imprinted polymer using nitroxide-mediated polymerization. The transient free radicals generated from **1** (Step 1) initiate chain polymerization of **2** and DVB (Step 2). The majority of the growing chain radicals are stabilized by their reversible association with TEMPO (Step 3), so that permanent chain termination is avoided. This living polymerization finally leads to the formation of imprinted sites in the cross-linked polymer network (Step 4), which after hydrolysis (Step 5) afford specific cholesterol binding cavities.

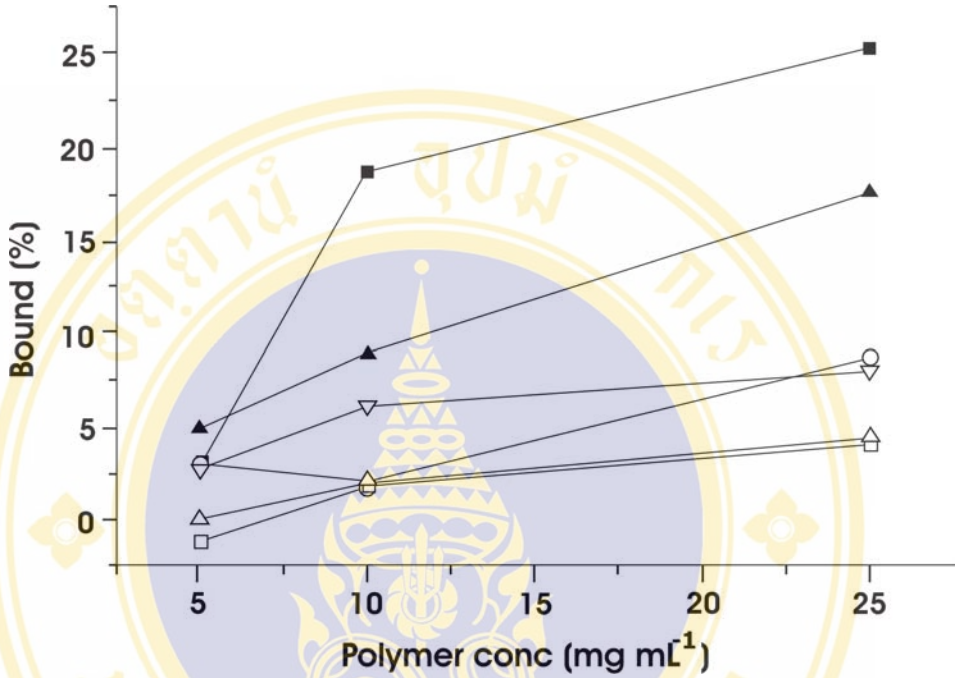

Figure 4.2 Uptake of [^{3}H]cholesterol by MIP(NMP)-H (■), MIP(NMP) (❑), NIP(NMP)-H (◇), MIP(BPO)-H (▲), MIP(BPO) (△) and NIP(BPO)-H (▽) in hexane. The initial concentration of cholesterol was 1.4 nM.

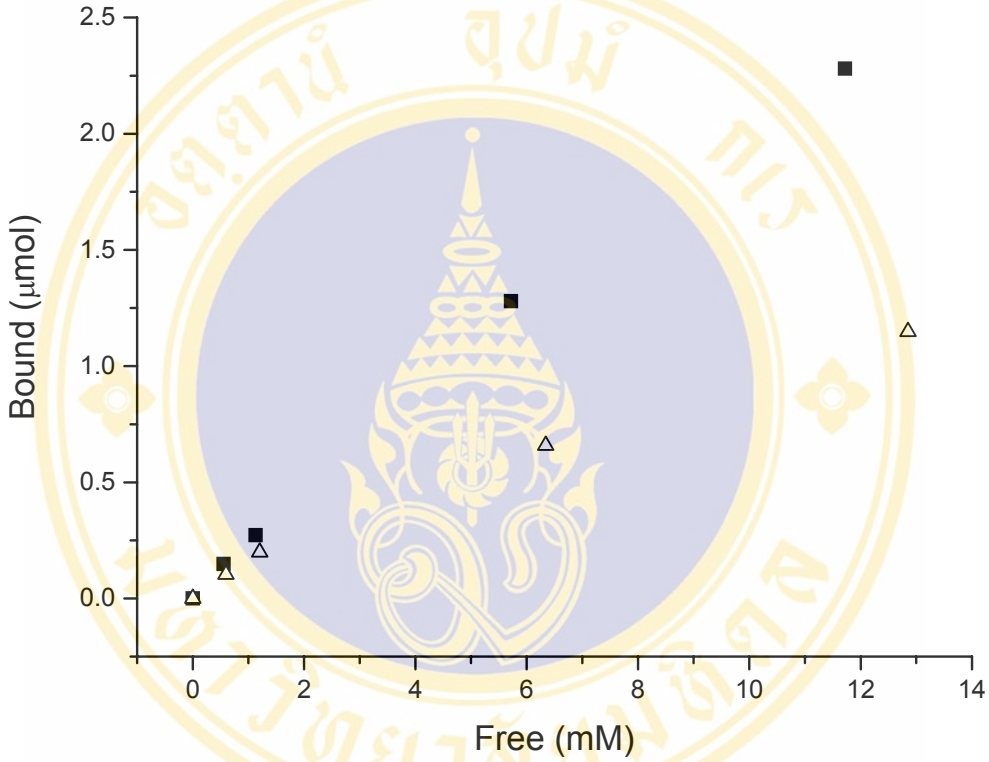

Figure 4.3 Cholesterol binding isotherms for MIP(NMP)-H (■) and MIP(BPO)-H (Δ). The polymers (25 mg) were titrated in hexane with increasing amount of cholesterol in the presence of 1.4 nM [3H]cholesterol.

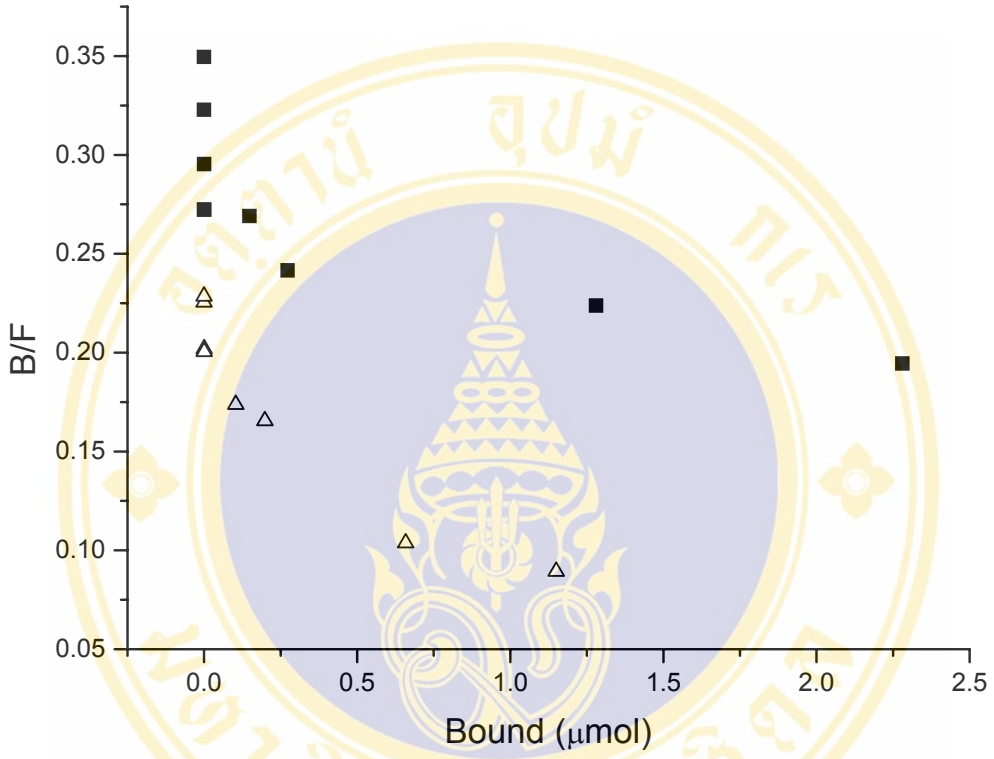

Figure 4.4 Scatchard plots for cholesterol binding on MIP(NMP)-H (■) and MIP(BPO)-H (Δ).

Table 4.1 Preparation and characterization of molecularly imprinted polymers

Polymer	Initiator	Monomer (mmol)		Hydrolysis treatment	BET surface area (m^2g^{-1})	O content (%)	High affinity site		Low affinity site	
		2	DVB				K_D (μM)	B_{max} (nmol g-1)	K_D (mM)	B_{max} (μmol g-1)
MIP(NMP)	**1**	0.29	5.51	No	470	1.1				
MIP(NMP)-H	**1**	0.29	5.51	Yes	621	0.4	4.5±1.2[a]	61±15	31±5.4	33±5.6
NIP(NMP)-H	**1**	0	5.81	Yes	705	n.d.[b]				
MIP(BPO)	BPO	0.29	5.51	No	571	1.2				
MIP(BPO)-H	BPO	0.29	5.51	Yes	730	0.8	8.1±2.5	73±22	12±2.6	84±18
NIP(BPO)-H	BPO	0	5.81	Yes	789	n.d.				

[a] Standard error of the linear regression.
[b] n.d.: not determined.

CHAPTER 5
LIPID-MEMBRANE AFFINITY OF CHIMERIC METAL-BINDING GREEN FLUORESCENT PROTEIN

1. Abstract

The Green Fluorescent Protein (GFP) is a useful marker to trace the expression of cellular proteins. However, little is known about changes in protein interaction properties after fusion to GFP. In this study, we present evidence for a binding affinity of chimeric cadmium-binding green fluorescent proteins to lipid membrane. This affinity has been observed in both cellular membranes and artificial lipid monolayers and bilayers. At the cellular level, the presence of Cd-binding peptide promoted the association of the chimeric GFP onto the lipid membrane, which declined the fluorescence emission of the engineered cells. Binding affinity to lipid membranes was further investigated using artificial lipid bilayers and monolayers. Small amounts of the chimeric GFP were found to incorporate into the lipid vesicles due to the high surface pressure of bilayer lipids. At low interfacial pressure of the lipid monolayer, incorporation of the chimeric Cd-binding GFP onto the lipid monolayer was revealed. From the measured lipid isotherms, we conclude that Cd-binding GFP mediates an increase in membrane fluidity and an expansion of the surface area of the lipid film. This evidence was strongly supported by epifluorescence microscopy, showing that the chimeric Cd-binding GFP preferentially binds to fluid-phase areas and defect parts of the lipid monolayer. All these findings demonstrate the hydrophobicity of the GFP constructs is mainly influenced by the fusion partner. Thus, the example of a metal-binding unit used here shines new light on the biophysical properties of GFP constructs.

2. Introduction

Green fluorescent protein (GFP) is an autoilluminating protein isolated from the jellyfish, *Aequorea victoria*. It is a relatively small monomeric protein composed of 238 amino acids with molecular mass of 29 kDa (163, 164, 208). It has a major excitation peak at 395 nm and a minor peak at 470 nm with a single emission peak at 509 nm(174). The GFP expression is species-independent and requires no substrates or cofactors for the fluorescence formation. The fluorescence is generated by an internal chromophore via spontaneous posttranslational oxidation of residues Ser^{65}, Tyr^{66}, and Gly^{67} within a hexapeptide at position 64–69 (166). The chromophore is amazingly resistant to a wide variety of hazardous conditions including high temperature, extreme pH, and proteases (209). Even under drastic acidic/basic conditions or highly potent denaturants, e.g. 6 M guanidine hydrochloride or 8 M urea, GFP regains its natural fluorescence after removal of the drastic condition (170, 209). In the present study, we used a GFP variant (GFPuv), which was optimized for UV excitation and emitting 18 times more fluorescence intensity than wild-type GFP. This variant GFP can also easily be detected by irradiation with standard long-wave UV or blue light (210).

Due to the autofluorescent property of GFP, much attention has been focused on applying the GFP as a fusion partner to monitor gene expression and protein localization in both prokaryotic and eukaryotic cells (173-176, 184, 211). In addition, GFP has also been used for investigation of protein-protein interactions (179). Because of the variety of applications of GFP, the fluorescence properties of this molecule have been improved and the physical and chemical effects on fluorescence emission have been extensively explored (171, 209, 212-215). However, more knowledge at the molecular level, particularly on binding to other biomolecules, needs to be discovered to allow the design of molecular fluorescent proteins for a variety of applications.

We have constructed a series of chimeric genes encoding chimeric GFP carrying a variety of metal-binding peptides including the chimeric GFPs having hexapolyhistidine or Cd-binding peptide. Such engineered chimeric GFPs have been applied as a potential tool for metal determination both at the purified protein and at the cellular level (33, 34, 178). The Cd-binding peptide (His-Ser-Gln-Lys-Val-Phe) is composed of hydrophobic amino acids flanked by basic amino acids in tandem repetition (29). In this study we used these

Cd-binding peptides as tools to study the association of chimeric green fluorescent proteins to lipid membranes. Evidences of chimeric proteins binding to cellular as well as artificial lipid membrane are presented. Our present findings, using one class of fusion peptides presently under consideration for metal sensing, may also apply to other chimeric GFP-proteins.

3. Materials and methods

3.1 Bacterial strain and plasmids

Escherichia coli (*E. coli*) strain TG1 (lac-pro), Sup E, thil, hsd D5/F' tra D36, pro A^+ B^+, lacI, lacZ, M15; (ung^+, dut^+) was used as host. Plasmids pHis6GFPuv (33) and pCdBP_4GFPuv (178) were used for construction.

3.2 Lipids, chemicals and biological reagents

1,2-Dipalmitoyl-sn-glycero-3-phosphocholine (DPPC), 1,2-dipalmitoyl-sn-glycero-3-phosphoserine (DPPS), l,2-dipalmitoyl-sn-glycero-3-(phospho-rac-(1-glycerol)) (DPPG), 1,2-dipalmitoyl-sn-glycero-3-phosphate (DPPA), 1,2-dioleoyl-sn-glycero-3-phosphocholine (DOPC), and 1,2-dioleoyl-sn-glycero-3-(phospho-L-serine) (DOPS) were purchased from Avanti Polar Lipids (Alabaster, AL) and were used without further purification. Solvents were high performance liquid chromatography grade and purchased from Merck (Darmstadt, Germany). Water was first purified through a millipore water purification system Milli-Q RO 10 Plus (Millipore GmbH, Eschborn, Germany) and then finally with the millipore ultrapure water system Milli-Q Plus 185 (18.2 MΩ cm^{-1}). For all experiments, a PBS (50 mM Na_2HPO_4, 0.3 M NaCl, pH 7.4) was used, if not stated otherwise. Lipid stock solutions were made by dissolving powdered lipid in chloroform or chloroform/methanol at appropriate molar ratio (1:1 or 1:3).

Restriction endonucleases, T4 DNA ligase and molecular weight marker (λ/*Hind*III) were obtained from New England Biolabs. Chelating Sepharose Fast Flow gel was purchased from Pharmacia Biotech, Sweden.

3.3 Chimeric gene construction

Cloning procedures were performed as described by Maniatis et al (216). To construct a chimeric green fluorescent protein having a combination of hexahistidine and four Cd-binding regions as the metal-binding site, the gene encoding Cd-binding regions fusing to GFP was cleaved out from the pCdBP4GFPuv, then ligated into the *Sac*I site of the pHis6GFPuv. The ligation product was subsequently transformed into *E. coli*. Transformants were selected and the inframe-fusing of chimeric gene was checked via restriction endonuclease analysis. The chimeric gene was subsequently expressed in *E. coli* strain TG1. Gene expression was readily monitored by following the cell fluorescence.

3.4 Protein preparation and purification

Both native and chimeric green fluorescent proteins were harvested from cultures of *E. coli* TG1 carrying constructed plasmids. Briefly, the culture was spun at 10,000 × *g* for 5 min and the cell pellet was resuspended in 50 mM sodium phosphate buffer, pH 7.4, containing 0.3 M NaCl. Cells were disrupted by sonic disintegration (sonicator ultrasonic processor model XL, Heat System Incorporation, USA) at output 6 for 20 s (six times) with resting of 40 s in between and debris was removed by centrifugation (10,000 × *g*, 5 min). The supernatant was attained as crude constructed protein preparation.

In the cases of $CdBP_4GFP$ and His6CdBP4GFP chimeric proteins, the majority of the constructed protein was associated with the debris fraction. Therefore, the pellet of cell debris of the centrifugation was collected. The chimeric proteins were released by resuspending in phosphate buffer containing 6 M guanidine hydrochloride. The sample was clarified by spinning at 10,000 × *g* for 5 min at 4°C prior to further purification by the IMAC-Zn affinity chromatography as previously described (33).

3.5 Fluorescence measurements

Fluorescence was assayed by irradiation of either the purified GFPs or the engineered cells at 395 nm and subsequent emission of photons at 509 nm was recorded via fluorescence multi-well plate readers (BIOTEK, USA and BMG Labtechnologies, FRG).

3.6 Determination of binding capacity of chimeric metal-binding GFPs to multilamella vesicles (mlvs)

Binding capacity of chimeric His6CdBP4GFP to liposomes was determined as compared to the chimeric His6GFP. Briefly, multilamella vesicles (MLVs) of pure DPPC/DOPC or lipid mixtures (DPPC:DPPS/DPPG/DPPA; 4:1) were prepared. Aliquots of lipids in a small glass tube were evaporated to dryness under a stream of nitrogen and then under high vacuum. PBS was added and the lipid was dispersed above the phase-transition temperature of each lipid by vortexing for 30 s (3–4 times). The MLVs (100 μg) were incubated with the chimeric GFPs (10 μg) at room temperature for an hour followed by centrifugation at 10,000 × *g* at 4°C for 15 min. The pellets were then washed with the buffer to remove unbound protein. The supernatants were collected and the remaining proteins were precipitated using 20% trichloroacetic acid (TCA). Finally, both fractions were analyzed on SDS-PAGE.

3.7 Film-balance measurements

Measurements were performed on a Wilhelmy film balance (Riegler and Kirstein, Mainz, Germany) with an operation area of 40 cm^2 and a bulk volume of 24 ml PBS at a temperature of 20°C. The position and scanning speed of the film-balance barrier, as well as the recording of area–pressure isotherms, were computer controlled. Monolayers were composed of either DPPC or DOPC. Prior to each experiment, the trough and barrier were cleaned with mucasol™ and dichloromethane followed by rinsing with deionized water. Phospholipid films were spread from a chloroform solution with a microsyringe at the air/liquid interface. After an equilibration time of 10 min, the film was compressed with a constant compression rate (5.81 cm^2/min) until the final surface pressure reached 10 mN/m. The interface was allowed to equilibrate for a minimum of 30 min to maintain constant pressure. The subphase was gently and continuously stirred by a magnetic bar. The chimeric GFP dissolved in PBS was then injected into the subphase underneath the monolayer via an inlet port in the trough. Changes of the lateral pressure after injection were measured at constant surface area and recorded for a minimum of 60 min. In addition, the isotherms before and after protein injection were determined.

3.8 Epifluorescence measurements

Fluorescence of the lipid monolayer (DPPC) doped with either His6CdBP4GFP or His6GFP was excited and visualized via an epifluorescence microscope (Olympus STM5-MJS, Hamburg, Germany). The Langmuir trough equipped with a computer-controlled movable barrier and a Wilhelmy system for measurement of the surface tension was placed on a specially designed stage (Riegler and Kirstein, Mainz, Germany) for the microscope. With the help of the remote-controlled stage, the trough could be moved independently in the three directions of the axes (*x*,*y*,*z*) of a Cartesian coordinate system where the *x* and *y* axes were oriented perpendicular to the optical axis of the objective lens. For excitation, a high-pressure mercury lamp with a power of 50 Watt was used. Discrimination of excitation light and emitted light of the green fluorescent protein was achieved by cut-off filters. To perform the experiment, drops of the lipid stock solution were formed on the end of a Hamilton syringe and carefully spread to the air-liquid interface. The solvent was allowed to evaporate for at least 10 min. After evaporation, the interface was compressed until the surface pressure reached 5 mN/m. Then, the chimeric GFP was injected into the subphase without disturbance of the lipid monolayer and the interface was further compressed to 10 and 35 mN/m, respectively. In parallel, the fluorescence at each pressure was detected using a SIT-camera (Hamamatsu, Hamamatsu, Japan).

4. Results

4.1 Construction and expression of chimeric gene encoding chimeric metal-binding green fluorescent proteins

A series of chimeric genes encoding chimeric metal-binding green fluorescent proteins (chimeric GFPs) have successfully been constructed. These included chimeric genes of His6GFP encoding a hexapolyhistidine and green fluorescent protein (33); CdBP4GFP encoding a peptide with four cadmium-binding regions and the green fluorescent protein (178) and His6CdBP4GFP encoding a hexapolyhistidine tail, a peptide with four cadmium-binding regions and the green fluorescent protein (Fig. 5.1). Those proteins were primarily constructed to build up biosensor devices. Herein, however, they are used as tools to investigate the membrane-binding properties, which are important to know not only for this but also for other GFP-constructs used in biotechnology.

Engineered cells (*E. coli*) expressing all chimeric GFPs possessed fluorescence activity (Fig. 5.2 *A*). However, fluorescence intensity at the cellular level varied and this was determined by spectrofluorometry. The cells expressing chimeric His6GFP were approximately 3-fold higher in fluorescence activity (8,239 FU/10^7 cells) compared to cells expressing native GFP (2,454 FU/10^7 cells). The fluorescence of cells expressing CdBP4GFP was 1.6-fold (1,530 FU/10^7 cells) lower than those of cells with the native green fluorescent protein. The cells expressing His6CdBP4GFP provided the same fluorescence intensity level as CdBP4GFP (1,589 FU/10^7 cells).

Engineered cells expressing chimeric genes were fractionated. As shown in Fig. 5.2 *B*, the native GFP was expressed and found in the cytosol, while the chimeric CdBP4GFP was found to be almost all associated with membranes, thus remaining in the debris fraction after centrifugation. The presence at the membranes and not in inclusion bodies has been proven by fluorescence microscopy. The chimeric His6GFP remained exclusively in the cytosol. Engineering of a hexahistidine into the four cadmium-binding sequences of the chimeric protein did not affect the hydrophobic association of CdBP4GFP to the membrane. Therefore, almost all of the His6CdBP4GFP was found in the cell debris after disruption of the cells by sonic disintegration and centrifugation (Fig. 5.2. *B*).

Association of chimeric GFP to the cell compartment might subsequently affect the fluorescence at the cellular level. Therefore, fluorescence intensity of each purified chimeric GFP was further determined. The chimeric CdBP4GFP and the His6CdBP4GFP were extracted using guanidine hydrochloride. The chimeric proteins possessing dual characteristics of both metal binding and fluorescence emission were purified to homogeneity via immobilized metal affinity chromatography (IMAC) loaded with zinc ions. The integrity of recombinant protein was analyzed on SDS-PAGE. The increase in molecular weight of chimeric His6CdBP4GFP as compared to the original chimeric proteins (His6GFP and $CdBP_4GFP$) is obvious (Fig. 5.3 *A*). The fluorescence intensity (FU/μg) decreased in the order of His6GFP (3,210 FU/μg) > CdBP4GFP (2,583 FU/μg) > His6CdBP4GFP (1,889 FU/μg) > native GFP (1,191 FU/μg), as represented in Fig. 5.3 *B*.

4.2 Interaction of chimeric green fluorescent proteins with artificial membrane

4.2.1 Binding of Chimeric GFPs to Multilamellar Vesicles

To test whether the chimeric GFP consisting of the Cd-binding regions possessed an affinity for lipid membranes, the chimeric His6CdBP4GFP was incubated with multilamellar vesicles of either saturated or nonsaturated phospholipids with different head groups (e.g., DPPC, DPPS, DPPG, DPPA, DOPC or DOPS). Lipid-bound chimeric protein was then precipitated and subsequently analyzed on SDS-PAGE. This lipid-protein complex yields two bands in the SDS-gel with the molecular masses corresponding to the lipid and the chimeric His6CdBP4GFP as represented in Fig. 5.4 *A*. For comparison, the His6GFP was applied as control and exhibited similar results. The other saturated lipids (DPPS, DPPG and DPPA) exhibited the same binding activity. Binding of only minor amounts (5–10%) as compared to the remaining protein in the supernatant of either His6CdBP4GFP or His6GFP to the vesicles was observed (*data not shown*). However, the chimeric His6CdBP4GFP seemed to have more affinity for the liposomes than the His6GFP, especially in the case of DOPC vesicles (Fig. 5.4 *B*). These findings give clear evidence for a preferential binding of the His6CdBP4GFP to fluid-phase lipids.

4.2.2 Effect of chimeric GFPs on the isotherm and interfacialPressure of phospholipid monolayers

To test the binding capacity of the chimeric His6CdBP4GFP to lipid layers at a given interfacial pressure, which is about 30–35 mN/m in the liposome, we investigated the lipid-protein interaction on monolayers at the air/water interface. Figure 5.5 demonstrates the obtained isotherms of DOPC monolayers before and after injection of chimeric GFPs and the corresponding changes of lateral pressure. Injection of chimeric His6CdBP4GFP underneath a DOPC monolayer at 10 mN/m caused an increase in fluidity and expansion of the surface area of lipid molecule (Fig. 5.5*A*). An increase in fluidity and surface expansion was also observed upon addition of His6GFP, but much less pronounced (Fig. 5.5 *B*). At high pressure (40 mN/m), the surface area per lipid molecule before and after protein injection was the same in both cases. This clearly indicates that the chimeric GFP is squeezed out from the lipid monolayer under compression without loss of lipid molecules.

Addition of His6CdBP4GFP to DOPC-monolayers at 10 mN/m caused a dramatic increase in the interfacial pressure up to 6.5 mN/m within one hour; a much slower and less pronounced increase of lateral pressure by approximately 4 mN/m was observed in the case of His6GFP (Fig.5.5 *C*).

The effect of chimeric GFPs on the monolayer isotherms was also investigated in saturated phospholipids, e.g., DPPC. As shown in Fig. 5.6 *A–B*, the surface pressure/area isotherm of DPPC exhibited the typical phase transition at approximately 5 mN/m from the liquid expanded (*le*) to the liquid condensed (*lc*) phase. In the presence of the chimeric His6CdBP4GFP, the isotherm was shifted to a higher area per lipid molecule at low surface pressure, which clearly demonstrates that the incorporation of the chimeric protein caused an expansion of the lipid monolayer. Upon compression, the area per molecule became identical to that of a pure DPPC monolayer at high surface pressure (Fig. 5.6 *A*). Again, an increase in fluidity in the phospholipid phase-transition region was observed upon injection of His6GFP (Fig. 5.6 *B*). However, the fluidization effect was much less compared to the His6CdBP4GFP. A similar pattern upon high compression was revealed.

For a better understanding of the interaction between the His6CdBP4GFP and the lipid monolayer, we injected the chimeric His6CdBP4GFP underneath the DPPC monolayer at constant area and at the initial surface pressure of 10 mN/m. This pressure was chosen to represent the situation at the *le–lc*-transition region (10 mN/m). The increase of surface pressure with time caused by the injection of His6CdBP4GFP was more pronounced than that of the His6GFP (Fig. 5.6 *C*). It is noteworthy that injection of the His6CdBP4GFP caused a two-step (biphasic) increase of the lateral pressure. In the first step, the pressure rapidly increased by about 2 mN/m within 5 min, followed by a gradual increase until saturation is reached within 30–45 min. In contrast, the presence of His6GFP caused the change of pressure with a slower rate only and the second step of incorporation was not observed.

To investigate the interaction with a rigidified membrane the chimeric His6CdBP4GFP was injected under the DPPC monolayer precompressed to 25 mN/m, which is above the plateau region. We found that the chimeric protein at this pressure did not affect the physical state of the monolayers (*data not shown*). This infers that the chimeric His6CdBP4GFP is unable to incorporate into the high-pressure lipid layers—an evidence that is also supported by the low binding of His6CdBP4GFP to the liposome.

4.2.3 Epifluorescence measurements of interaction between chimeric GFPs and lipid monolayers

Since binding of the chimeric His6CdBP4GFP was restricted to fluid-phase lipids, we applied epifluorescence measurements to DPPC monolayers in the *le–lc* phase-transition region where rigid and fluid domains coexist. Epifluorescence of DPPC monolayers in the presence of His6CdBP4GFP after compression to 10 or 35 mN/m were determined and compared to the effect of His6GFP. As shown in Fig. 5.7 *A*, the His6CdBP4GFP was able to bind to the extended areas of fluid phase (arrow *b*), but binding was much more pronounced to the narrow defect parts (rim) of the rigid domains (arrow *c*). At high compression (35 mN/m), the fluorescence emission of chimeric protein became more condensed. This indicates the enrichment of proteins in the fluid phase (Fig. 5.7 *B*). In the case of His6GFP, only low fluorescence intensity was detected in the DPPC monolayers. A faint fluorescence of fluid phase is observable between the rigid domains (Fig. 5.7 *C*, arrow *a*) and at the defect part up to 10 mN/m (Fig.5.7 *C*, arrow *c*) but at a very low intensity compared to the fluorescence pattern obtained with His6CdBP4GFP. When the pressure was increased to 20 or 35 mN/m, no fluorescence could be observed.

5. Discussion

Chimeric GFPs are widely used to tag proteins, but have not yet been systematically investigated with respect to changes in their interaction properties with other cellular compounds. We have used a set of metal-binding chimeric peptides and investigated their interaction with membrane. Modification of GFP even at the extra-chromophore region of the molecule may affect the fluorescence emission intensity, which depends on the nature of the partner peptide and arrangement of the chimeric molecule. From our findings, the presence of the Cd-binding peptide was proven to cause changes in fluorescence emission activity of engineered cells with the difference in fluorescence intensity of engineered cells in the order of His6GFP >>> native GFP > CdBP4GFP > His6CdBP4GFP (Fig. 5.2 *A*). At the protein level, the fluorescence intensity decreased in the order His6GFP > CdBP4GFP > His6CdBP4GFP > native GFP (Fig. 5.3 *B*).

The peptide fused to the GFP subsequently affects the localization of the modified GFP molecule intracellularly. We found that the chimeric Cd-binding green fluorescent proteins (CdBP4GFP and His6CdBP4GFP) remained in the cell debris after disintegration of the cell structure. Localization of the chimeric CdBPGFPs in membrane debris as compared to the other cellular compartments could be detected by the autofluorescence property (Fig. 5.2 *B*). This observation was also reported by others. Cha et al. reported the expression and purification of human interleukin-2 (hIL-2) in insect cells and *E. coli* (211, 217, 218). Fusion of hIL-2 to the GFP caused a localization of the fusion protein in the pellet after cell lysis. Expression of the native GFPuv yielded over 70% of the protein in the soluble fraction. Expression of a fusion protein with hIL-2 exhibited only 13–30% soluble protein. Interestingly, insoluble GFPuv was typically non-fluorescent, so it might be that the fusion protein was soluble but embedded in the membranous material. Similarly, when the hIL-2-GFP was expressed in *E. coli*, the GFP fluorescence was found to be significantly reduced and almost all of the fusion protein was retained in the cell pellet.

Recovery of the chimeric CdBP4GFP and His6CdBP4GFP from the cell debris required 6 M guanidine hydrochloride to solubilize. Neither addition of mild detergent (e.g. Triton X-100) nor changes of ionic strength of the buffer solution caused any expelling effect (*unpublished data*). This again indicates the strong interaction between the chimeric CdBPGFPs with the membrane debris. The possible explanation for this strong interaction might be due to the composition of the Cd-binding peptide. The chimeric CdBP4GFP and His6CdBP4GFP possess tandem repeats of a His-Ser-Gln-Lys-Val-Phe sequence, which contains hydrophobic and hydrophilic amino acids and which are able to bind Cd^{2+}. Such a peptide may undergo conformational arrangements to transfer the chimeric GFP into a more lipid-soluble form, thus causing membrane association. This was strongly supported by the earlier evidence for a decrease of lactate dehydrogenase activity in the cytosol as compared to the total protein of the cell with increasing number of tandem sequences of the Cd-binding peptide to the chimeric LDH (34). Similar effects of amino acid composition on the binding properties of the GFP to lipid membranes has also been observed when the protein was fused to natural membrane-bound peptides. For example, the effect on caveolae, the vesicular invaginations of the plasma membrane, has been studied using GFP-caveolin constructs. A short membrane-attachment sequence (KYWFYR) within the caveolin-1 has been fused to the GFP. These six residues, which consisted of the central

aromatic and flanking basic residues, were required for membrane attachment. This sequence was sufficient to anchor the soluble cytoplasmic GFP to membranes. Removal of this sequence prevented membrane attachment in cells. In addition, the lack of the two basic amino acids (lysine and arginine) prevented the adequate localization of GFP in the membrane pellet. These results suggested the need for electrostatic interactions mediated by the flanking basic residues in addition to the hydrophobic interaction caused by the aromatic residues for membrane association (219).

To further investigate membrane-binding properties of the chimeric green fluorescent proteins, here the binding of the chimeric His6CdBP4GFP to artificial lipid membrane was determined as compared to that of the His6GFP. First focussing on the interaction of chimeric His6CdBP4GFP with lipid vesicles, we observed the binding of a small amount of the His6CdBP4GFP to the lipid (Fig. 5.4). This might be due to the high surface pressure of lipid bilayer of about 30 mN/m. When the His6CdBP4GFP was injected underneath the lipid monolayer compressed to a variable low initial pressure, a considerable increase of the interfacial pressure was observed. Furthermore, an increase in fluidity corresponding to an expansion of the surface lipid layer was shown (Figs. 5.5 and 5.6). At high pressure, the His6CdBP4GFP could not incorporate into the lipid monolayers. This evidence strongly supports our finding of the low binding of protein to lipid vesicles.

Second, the effect of lipid fluidity upon protein binding was also investigated. The chimeric His6CdBP4GFP seemed to have more affinity for unsaturated phospholipids than for saturated lipids (Figs. 5.4-5.6). This was supported by the fact that the His6CdBP4GFP preferentially binds to fluid phase and to the defect parts of lipid domains, as determined by fluorescence microscopy (Fig. 5.7). The chimeric His6CdBP4GFP exhibited strong fluorescence upon incorporation to the liquid phase of a DPPC-monolayer, while very low intensity could be observed in the case of His6GFP. A possible explanation might be non-specific adsorption of His6GFP to the lipid, which caused unfolding of the protein accompanied by loss of fluorescence within a few seconds. This result was also reported by Dorn et al., namely, that the fluorescence of GFP coupled to hexahistidine vanished within 20 min, whereas the lateral pressure was not decreased (220). Third, the interaction of His6CdBP4GFP with DPPC-monolayers exhibited biphasic kinetics, including a rapid initial phase and a slower second phase (Fig. 5.6 *C*). In contrast, the His6GFP induced only

the first phase, however, with a slower rate of pressure increase compared to the His6CdBP4GFP. The lack of the second phase indicated that the pressure increase within this phase might be due at least partially to the specific insertion of the Cd-binding peptide into the monolayer. In contrast to the second-phase interaction, the first phase was due to non-specific interactions between an integral part of GFP and the monolayers, as evidenced by the fact that the His6GFP was capable of inducing this rapid phase to a lesser extent than the His6CdBP4GFP (Fig. 5.6*C*). However, the effect of various concentrations of these chimeric GFPs on changes of lateral pressure need to be further investigated. Determination of binding constants between these chimeric GFPs and lipid molecules has to be envisaged. Fourth, we demonstrated that the chimeric His6CdBP4GFP was bound peripherally to the lipid monolayers. Upon injection of the chimeric protein underneath the lipid monolayer, the isotherm was shifted to higher area per lipid molecule at low surface pressure. Upon compression to high pressure, the area per molecule became identical to that of a pure DPPC-monolayer (Figs. 5.5 and 5.6). This indicates that the chimeric GFP is squeezed out of the lipid monolayer, in agreement with our fluorescence microscopy data. At high pressure (35 mN/m), the fluorescence became more condensed, caused by the reduction of the fluid-domain area. At 50 mN/m, very low fluorescence intensity could be observed due to the rigid packing of the lipid monolayer (*data not shown*). All these findings indicate the higher binding affinity of the His6CdBP4GFP to fluid phase domains within lipid monolayers as compared to His6GFP.

Two aspects seem to be relevant for discussion with respect to the use of GFP-constructs in general. First, changes of hydrophobicity of a protein upon insertion of the fusion partner and consequent interaction at the cellular level have to be considered. Second, the effects of the fusion partner on the lipid-binding properties of the construct opens up more useful applications in cell biology and biotechnology. For example, the GFP tagged with a cysteine-rich domain from protein kinase C (Cys1-GFP) was constructed and applied as fluorescence indicator for diacylglycerol signaling in mammalian cells. The cysteine-rich domain provided affinity not only for zinc ions but also for lipid membrane in the presence of diacylglycerol or phorbol ester. Therefore, transient translocation of cytosolic Cys1-GFP to the plasma membrane was observed upon stimulation of G proteins or tyrosine kinase-coupled receptors (221-223). Moreover, the insulin receptor substrate

(IRS) protein and the pleckstrin homology domains (PH) were fused to the GFP and applied as reporters for subcellular localization. These chimeric proteins were found to be localized exclusively in the cytoplasm. Stimulation with insulin caused a translocation of the chimeric protein to the plasma membrane within 3–5 min (30, 223). Moreover, Obrdlik et al. (224) constructed and expressed a chimeric protein between β-subunit of G-protein and GFP in transgenic plants. They demonstrated that G_{β} was located at the membrane surface and attached to membranes via hydrophobic interactions. Mutation in the β-domain caused severe decrease of the membrane association.

Beyond those useful applications, we have previously applied all these chimeric GFPs and engineered cells as a potential tool for metal determination (33, 34, 178). Therefore, this study opens up the possibility to attach the chimeric metal-binding GFPs onto membrane surfaces while they may then be applied for development of a fluorescent membrane-based metal sensor or a biofunctionalized membrane in the future, e.g., as a supporting layer on a glass fiber (225-229).

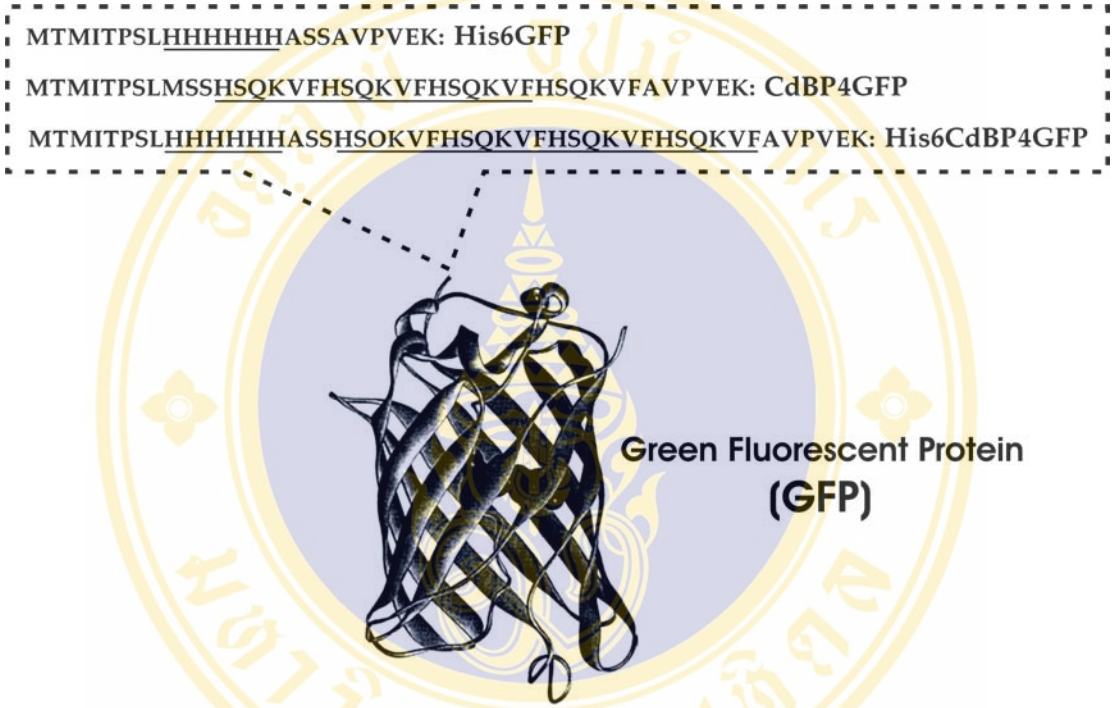

Figure 5.1 Schematic representation of chimeric green fluorescent protein carrying hexahistidine (*His6GFP*), peptide with four Cd-binding regions (*CdBP4GFP*) or peptide with hexahistidine-four-Cd binding regions (*His6CdBP4GFP*).

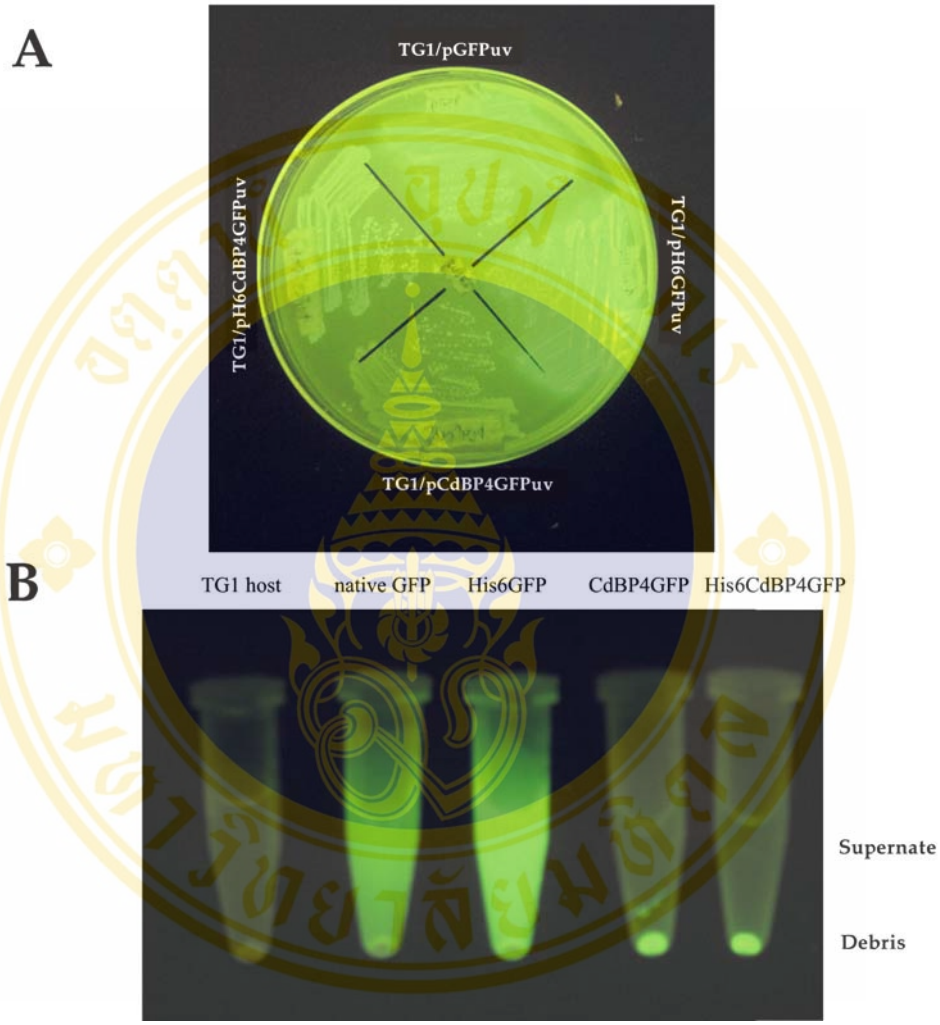

Figure 5.2 (*A*) Fluorescent emission of engineered cell expressing native GFP, His6GFP, CdBP4GFP and His6CdBP4GFP. (*B*) Localization of chimeric proteins in various compartments of sonicated cells expressing native GFP, His6GFP, CdBP4GFP and His6CdBP4GFP.

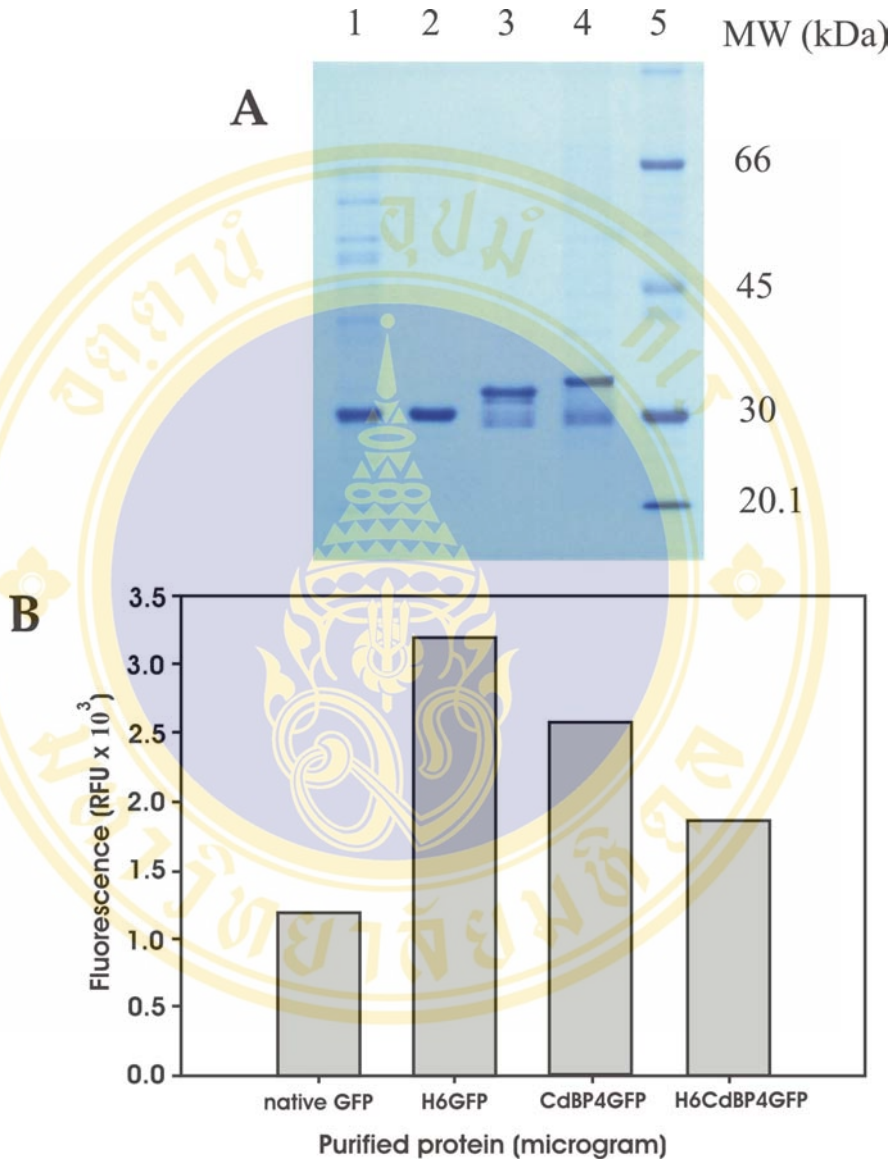

Figure 5.3 (*A*) SDS-PAGE of chimeric metal-binding green fluorescent proteins. Lane *1*, native GFP; lane *2*, His6GFP; lane *3*, $CdBP_4GFP$; lane *4*, $His6CdBP_4GFP$; and lane 5, standard protein markers. (*B*) Specific fluorescence activity (RFU/μg) of purified chimeric GFPs.

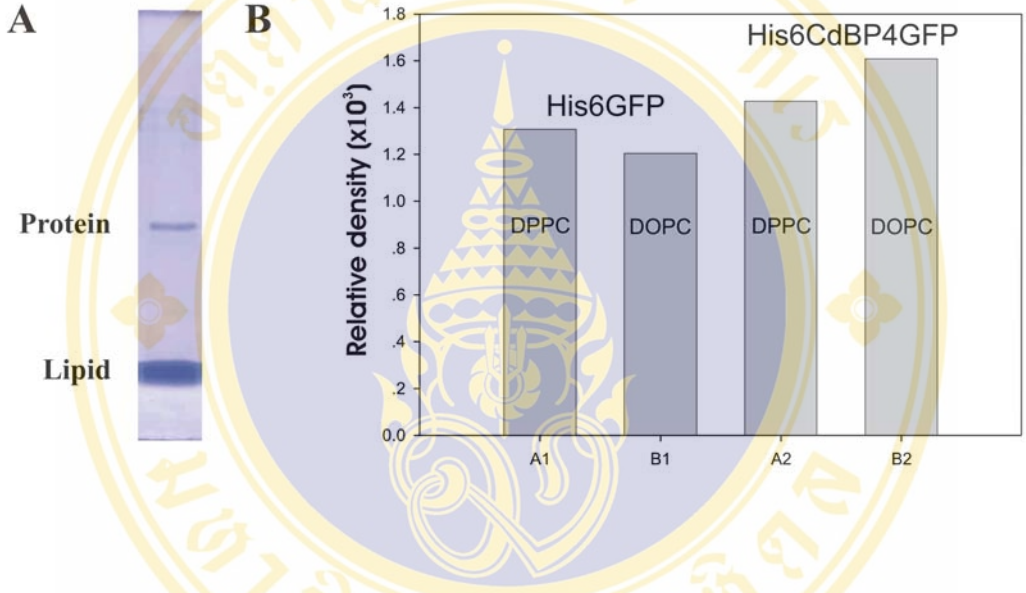

Figure 5.4 (*A*) Analysis of lipid-binding capability of chimeric GFP on SDS-PAGE. (*B*) Amount of chimeric His6GFP (*1*) or His6CdBP4GFP (*2*) bound to DPPC (*A*) or DOPC (*B*), as determined by densitometry using Quantity One version 4.2(Bio-Rad^{TM}).

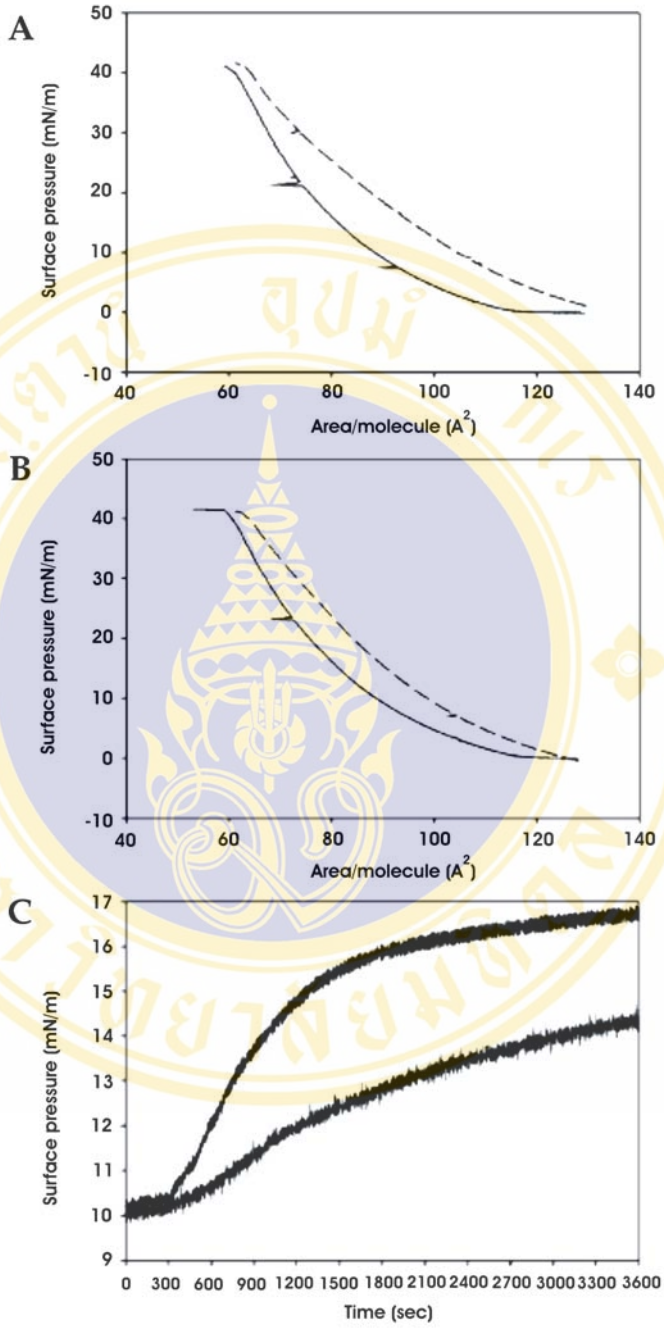

Figure 5.5 (*A, B*) Isotherms of DOPC monolayer before (*solid line*) and after (*dashed line*) addition of His6CdBP4GFP (*A*) or His6GFP (*B*). (*C*) Changes of lateral pressure upon injection of 18 nM His6CdBP4GFP or His6GFP underneath the DOPC monolayer.

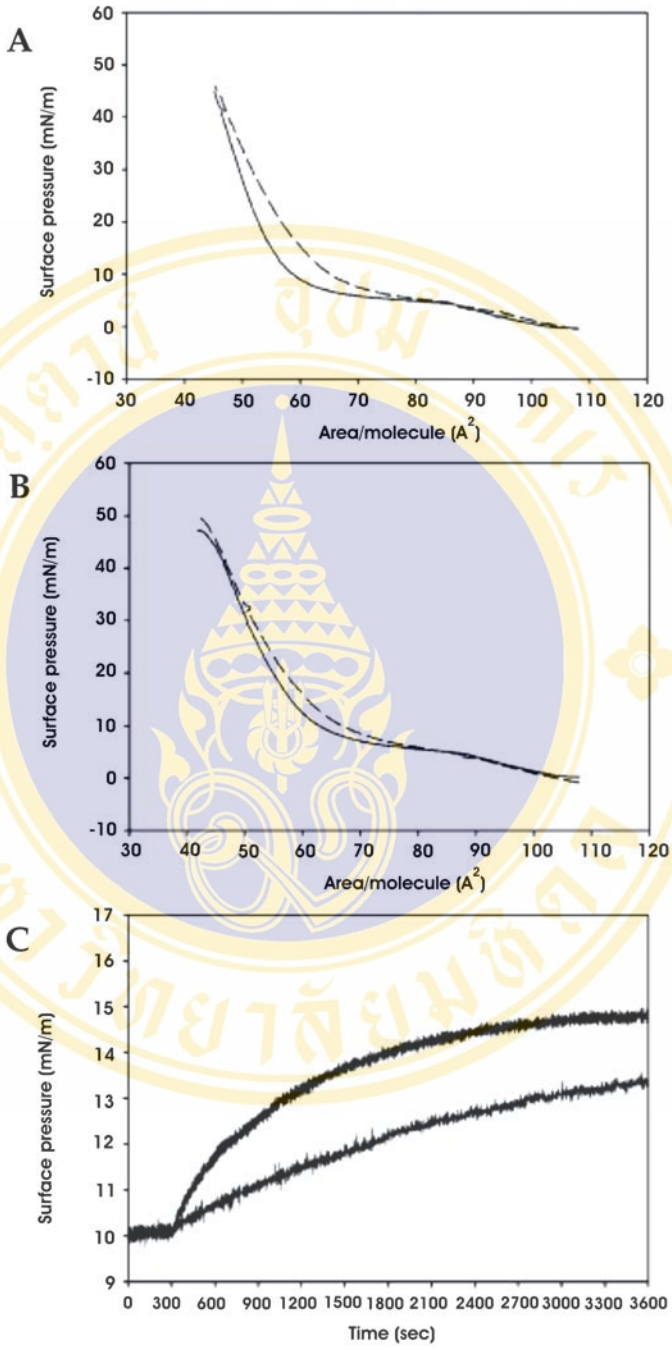

Figure 5.6 (*A, B*) Isotherms of DPPC monolayer before (*solid line*) and after (*dashed line*) addition of His6CdBP4GFP (*A*) or His6GFP (*B*). (*C*) Changes of lateral pressure upon injection of 12 nM His6CdBP4GFP or His6GFP underneath the DPPC monolayer.

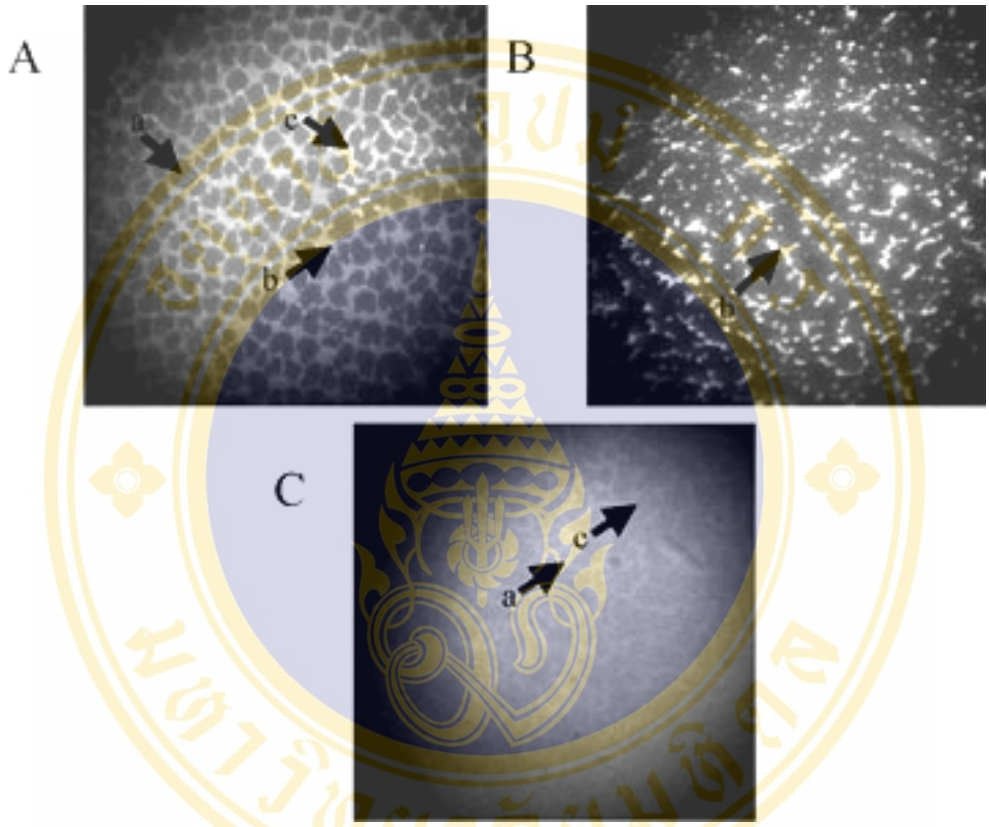

Figure 5.7 Epifluorescence of DPPC monolayer in the presence of His6CdBP4GFP (*A, B*) or His6GFP (*C*) after compression at 10 mN/m (*A, C*) or 35 mN/m (*B*) (Subphase: 50 mM Na_2HPO_4, 0.3 M NaCl, pH 7.4 at 20°C). Arrows *a*,*b* and *c* indicate solid domain, liquid domain, and defect part of solid domain, respectively.

CHAPTER 6
CO-EXPRESSION OF ZINC-BINDING MOTIF AND GFP AS A CELLULAR INDICATOR OF METAL IONS MOBILITY

1. Abstract

A significant role of zinc-binding motifs on metal mobility in *E. coli* was explored using a chimeric metal-binding green fluorescent protein (GFP) as an intracellular zinc indicator. Investigation was initiated by co-transformation and co-expression of two chimeric genes encoding the chimeric GFP carrying hexahistidine (His6GFP) and the zinc-binding motif fused to outer membrane protein A (OmpA) in *E. coli* strain TG1. The presence of these two genes was confirmed by restriction endonucleases analysis. Co-expression of the two recombinant proteins exhibited cellular fluorescence activity and enhanced metal-binding capability of the engineered cells. Incorporation of the zinc-binding motif onto the membrane resulted in 60 folds more binding capability to zinc ions than those of the control cells. The high affinity to metal ions of the bacterial surface influenced influx of metal ions to the cells, which could readily be detected via a declining of fluorescent intensity of GFP. Meanwhile, balancing of metal homeostasis due to the presence of cytoplasmic chimeric His6GFP enhanced the fluorescent emission. This infers the role of intracellular chelating effect to the metal in taking of cell. These findings provide the first evidence of real-time monitoring of intracellular mobility of zinc by autofluorescent proteins.

2. Introduction

Zinc is an essential trace element required for the normal growth and viability of organisms (274, 275). This metal ion plays critical roles in many cellular processes including cofactor of enzymes, nuclear factor and hormone. A large number of enzymes and proteins contain zinc as a structural or catalytic cofactor such as alkaline phosphatase, RNA polymerase, superoxide dismutase and zinc finger proteins. In some eukaryotes, level of intracellular zinc triggers various important cell events. Depleting of zinc ions from the cell leads to cell death and apoptosis meanwhile deficiency of zinc ions in human can cause anemia, loss of appetite, defective of immune function, loss of epithelium integrity and growth retardation (276, 277). Although zinc is not redox active under physiological conditions, excess of zinc ions can cause toxic to cells. Zinc toxicity may mediate via binding to other cation binding sites which subsequently alter the appropriate function of proteins and cofactors. The intracellular level of zinc ions is needed to be regulated to maintain viability and cell function. Precise regulatory systems have been evolved in many organisms to control the uptake, distribution, storage, and detoxification of zinc ions [for recent review see (278). Several families of integral membrane proteins play role to transport zinc ions across the membranes into and out of the cells. In *Escherichia coli*, zinc homeostasis is accomplished largely through the transcriptional control of zinc uptake (Zur) and efflux (ZntR) transporters (167, 279). In mammalian cells, the transmembrane transporters (e.g. ZIP and ZnT families) are involved in the regulatory processes. However, little is known on the molecular mechanism and location of intracellular zinc storage. Recent studies revealed that no persistent cytoplasmic pool (zinc quota) of free zinc exists in *E. coli* under steady-state growth conditions (280). In eukaryotic cells, labile zinc level has been stimulated at the low-nanomolar range (281). Monitoring of intracellular zinc level usually requires the fluorescent zinc-specific probes e.g. zinquin, zinpyr-1 and TSQ (210, 228, 282, 283). Increasing of the intracellular labile zinc upon up taking from the extracellular medium can be visualized by the fluorescent intensity of cells. Depletion of intracellular pools by metal chelators e.g. TPEN (membrane-permeable) and CaEDTA (membrane-impermeable) reveals a rapid decrease of fluorescence. However, limitation has been on the high background of fluorescence, photobleaching and cell toxicity.

Herein, we therefore explore a feasibility of using metal-binding green fluorescent proteins together with the expression of the zinc-binding motif as tools to study the metal mobility of the cells. The co-expression of the chimeric genes encoding the zinc-binding motif fused to outer membrane protein (OmpA) (210) and the chimeric GFPs (221) was performed in *E. coli* strain TG1. With an advantage of autofluoresce of the GFP, depletion of zinc ions and metal homeostasis has been monitored in real time.

3. Materials and Methods

3.1 Bacterial strains and plasmids

Escherichia coli (*E. coli*) strain TG1 [(lac-pro), Sup E, thi1, hsd D5/F' tra D36, pro A^+B^+, lacI, lacZ, M15; (ung^+, dut^+)] was used as host. Plasmids pGFPuv (Clontech Laboratories, USA), pHis6GFPuv (221) and pEVZn (210) were used for co-transformation and co-expression.

3.2 Enzymes and chemical

Restriction endonucleases and molecular weight marker (λ/*Hin*dIII) were obtained from New England Biolabs. Chelating Sepharose Fast Flow gel was purchased from Pharmacia Biotech, Sweden. All other chemicals were of analytical grade and commercially available.

3.3 Co-transformation of chimeric genes

Transformation of chimeric genes into *E. coli* was performed according to the standard procedure. A plasmid pEVZn, which has previously been proven to express polyhistidine on the cell surface, was firstly transformed into *E. coli* strain TG1. These cells were grown and treated with 50 mM $CaCl_2$ to become the competent cells. The plasmid of either pGFPuv or pHis6GFPuv was then co-transformed into the cells. Cells were subsequently spread onto LB agar containing 100 mg ampicillin/l. Transformants those possessed greenish fluorescence (observed under UV transiluminator) were picked and subcultured onto the LB media for isolation. Plasmids were extracted from the cells by Miniprep standard protocol as described by Maniatis. Successfulness of co-transformation was verified via restriction endonucleases analysis.

3.4 Verification of co-expression of two recombinant proteins

Cells carrying these two plasmids were grown in liquid LB medium containing 100 mg ampicillin/l at 35C with shaking for overnight. Cultures were pelleted by centrifugation then washed twice and resuspended in phosphate buffered saline (PBS; 50 mM Na_2HPO_4, 0.3 M NaCl, pH 7.4). Cell suspension was loaded onto the Immobilized Metal Affinity Chromatography (IMAC) charged with zinc ions. Unbound cells were removed by washing with phosphate buffer. Binding of cells to the gel was detected by determination of fluorescence emission under UV translumination and fluorescence microscope. Bound cells were eluted with 500 µl phosphate buffer containing 20 mM EDTA. Eluate was collected and subjected to microplate fluorescence reader for fluorescence measurement (excitation at 395 nm and emission at 508 nm).

3.5 Effect of zinc ions on fluorescence emission of engineered cells

Cells carrying pEVZn co-transformed with either pGFPuv or pHis6GFPuv were cultivated to allow co-expression between zinc-binding motif on the cell surface and native GFP or His6GFP in the cytoplasm. Cultures were harvested, washed, and resuspended in 5 mM HEPES buffer, 0.85 % (w/v) NaCl, pH 7.1. Cell suspensions were adjusted to 0.5 OD measured at 600 nm. Aliquots of 50 µl cell suspension were further incubated with various concentrations (50 nM-50 mM) of $ZnSO_4$ in 96-well microtiter plates. Effect of zinc ions on fluorescent emission of engineered cells was investigated. The fluorescence intensity was measured at 5, 15, 30, 45, 60, 120, 180, and 240 min using the microplate fluorescence reader.

4. Results and Discussion

On this, we report the first evidence using of the chimeric GFP as an intracellular zinc indicator in *E. coli.* Expression of the zinc-binding motif on the surface membrane clearly indicated that limitation of zinc uptake into the cell decreased the fluorescent intensity of the GFP. Meanwhile, the presence of cytoplasmic metal-binding region (His6GFP) plays an active role for metal homeostasis.

4.1 Co-expression of chimeric GFP and zinc binding motif

Co-transformation of the two chimeric genes encoding zinc-binding motif fused to outer membrane protein A (OmpA) (210) and chimeric green fluorescent protein carrying hexapolyhistidine (His6GFP) (221) in *E. coli* strain TG1 was performed. The presence of these two chimeric genes was verified via restriction endonucleases analysis. With respect to the presence of a unique *Eco*RI site on each plasmid (pEVZn and pHis6GFPuv), the extracted plasmid was cleaved by *Eco*RI and subsequently analyzed on an agarose gel electrophoresis. As shown in figure 1, two corresponding bands (3.9 and 3.3 Kb) were observed as compared to the pEVZn and the pHis6GFPuv, respectively (lane 2, 4 and 7).

To further confirm the co-expression of these two recombinant proteins, cells those exhibited green fluorescence were grown and expression of the zinc-binding motif on the cell surface was investigated via binding to the immobilized metal affinity chromatography (IMAC) charged with zinc ions. Binding of engineered cells (TG1/pEVZn + pHis6GFPuv) on the IMAC gel was determined by using UV transiluminator as compared to cells expressing His6GFP intracellularly. As shown in figure 2, the engineered cells exhibited not only a strong fluorescence as comparable to the control cell (upper panel) but these cells also provided the metal-binding capability (lower panel). Immobilized cells were further visualized via a fluorescence microscope as represented in figure 3. All these findings inferred not only the success of co-expression but also exploring a feasibility of applying this approach as a tool for verification of metal-binding avidity of the engineered cells. Similar investigations have also been reported by using phase contrast microscopy, electron transmission and fluorescence micrograph or confocal laser scanning microscope (209, 284, 285).

To further calculate the metal-binding capability of the engineered cells, a linear correlation between fluorescence intensity and amount of by-standing cells on the IMAC gel was determined. Figure 4 showed such the correlation of cells expressing His6GFP intracellularly (figure 4A) or co-expression of His6GFP and zinc-binding motif (figure 4B). Both cases demonstrated the linear correspondence with a correlation coefficient very close to 1. In addition, the engineered cells exhibited a bit higher fluorescence emission per se than the cell expressing His6GFP. From these data, calculation could easily be taken by dividing of the fluorescence intensity of cells eluted from the gel by the amount of gel. The amounts of engineered cells and cells

expressing intracellular His6GFP immobilized onto the gel were 0.98×10^8 cfu/ml and 0.0173×10^8 cfu/ml, respectively. This finding suggested that the metal-binding capability of engineered cell was approximately 60-folds higher than that of the control cell. The strong binding affinity is mainly attributable to the presence of zinc-binding motif consisting of several histidine residues throughout the bacterial surface membrane. These basidic amino acids provide more affinity to zinc ions than the polar head group of the membranous material or the peptidoglycan layer of control cells (286)

4.2 Location of metal-binding regions on fluorescence responses

To investigate whether location of zinc-binding motif affected intracellular metal mobility, the alteration in fluorescent intensity of engineered cells was monitored. For this purpose, co-transformation between pEVZn and pGFPuv was performed in a similar manner and applied for comparison. All the cells were incubated with various concentrations (50 nM-50 mM) of $ZnSO_4$ and the fluorescence responses were measured. As shown in figure 5A, a gradually reduction of fluorescent emission of cells expressing zinc-binding motif on the cell surface and native GFP (TG1/pEVZn + pGFPuv) according to time was observed in the absence of zinc ions. Low concentration of zinc ions (50 nM) had no significant effect on the fluorescent intensity while contrarily metal at higher concentrations (50 μM – 50 mM) enhanced the fluorescence of the cells. In case of cells expressing zinc-binding motif on the cell surface together with intracellular His6GFP, the declining of fluorescent emission in the absence of metal ions was not observed (Figure 5B). More importantly, when various concentrations of zinc ions (50 nM – 50 mM) were applied the enhancement effect on the fluorescent intensity was revealed as concentration dependent. A plausible explanation to the discrepancy observation was the competitive binding to metal ions between the zinc-binding motif on the cell surface and intracellular metal-binding region. In case of the native GFP, availability of zinc ions passing through the cellular membrane is limited by binding of the zinc-binding motif on the cell surface. Since we have previously reported that zinc ions enhanced the fluorescent emission of GFP *in vivo* (20).

Therefore, depletion of zinc resulted in a reduction of the fluorescent intensity of native GFP. Supportive evidence is that fluorescence emission of native GFP expressed in the TG1 host without expression of the zinc-binding motif on the cell surface is up to 8-10 folds higher than that of the cell carrying pEVZn and pGFPuv (data not shown). Furthermore, an alteration on colony morphology of the engineered cells is detected upon metal deprivation. This is in a good agreement with the reduction of cell viability in the presence of zinc chelator (TPEN) (282).

It is worth to state that there was no significant difference in fluorescent emission between cells expressing His6GFP and cells co-expressing zinc-binding motif in the absence of metal ions (figure 4). The enhancement effect of zinc ions on the fluorescence emission has readily been observed even at very low amount of metal applied to the cells (figure 5B). Explanation is that the presence of intracellular polyhistidine may act as a high affinity-binding domain capable of efficiently capturing metals from the environment, which may increase the uptake and in turn modulate the function of metal ions for the cells. Supportive evidences can be taken into accounts i) *E. coli* strain TG1 expressing His6GFP intracellularly provided more metal accumulation than the others (287), ii) the hexahistidine provided a high affinity toward divalent cations as has been demonstrated by the association to chelating membrane lipid (288, 289) and IMAC-Zn^{2+} binding (221), iii) the relative mobility of zinc ions across the cell membrane in a similar fashion was observed upon addition of a membrane-impermeable chelator e.g. CaEDTA (228) and iv) the histidine residue plays a major role in many zinc-transport systems (175, 213, 290, 291).

All these findings suggest not only the significant role of zinc-binding motif on the metal regulation at the cellular level but also supporting a high feasibility to apply the chimeric GFPs as an intracellular metal indicator in the future (292, 293). For circumstances, linear response between zinc concentrations and fluorescent intensity of the engineered cells was investigated (figure 6). Cells co-expressing the zinc-binding motif and His6GFP provided a linear response ranging from 0.5 μM - 5 mM with the correlation coefficient greater than 0.9 (figure 6B). However, little is known on the enhancement of the fluorescent emission upon addition of zinc or cadmium ions to the cells expressing chimeric GFPs.

Further work is required to understand whether the hexapolyhistidine exert their action by mediating direct transfer of the metal ions into the chromophore region as in case of the intra or intermolecular mechanism of copper transfer from the N-terminal histidine rich region to the active site of Cu/Zn SOD (294) or by increasing the local concentration of the metal around the chromophore of the GFP.

Figure 6.1 Restriction endonucleases analysis. Lane 1 pEVZn uncut, lane 2 pEVZn/*Eco*RI, lane 3 pHis6GFPuv uncut, lane 4 pHis6GFPuv/*Eco*RI, lane 5 λ/*Hin*dIII, lane 6 Co-transformation (pEVZn + pHis6GFPuv) uncut, lane7 Co-transformation (pEVZn + pHis6GFPuv)/*Eco*RI.

Figure 6.2 Determination of metal-binding capability of engineered cells via fluorescent analysis. Upper panel suspension of cells expressing His6GFP intracellularly (TG1/pHis6GFPuv) and cells co-expressing zinc-binding motif on the cell surface and His6GFP in the cytoplasm (TG1/pEVZn + pHis6GFPuv). Lower panel metal-binding capability of engineered cells immobilized onto the IMAC gel charged with zinc ions.

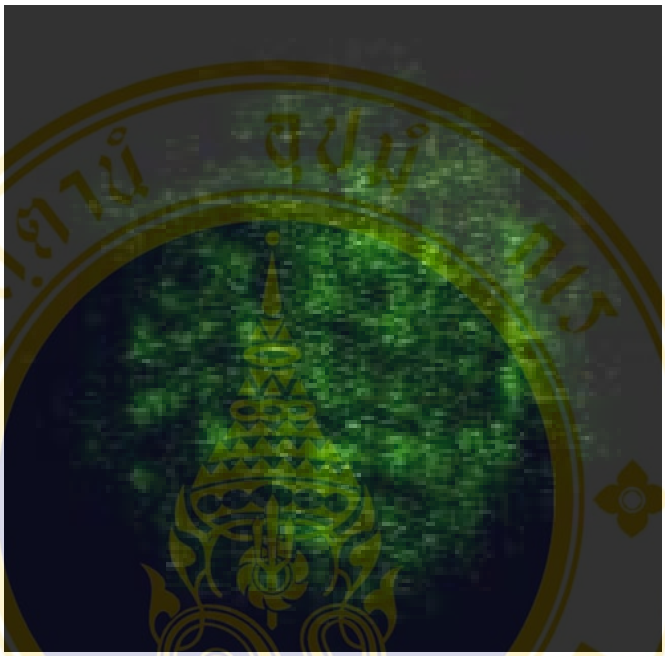

Figure 6.3 Metal-binding capability of engineered cells co-expressing zinc-binding motif on the cell surface and His6GFP intracellularly to the immobilized zinc ions on the IMAC gel determined by fluorescence microscope (400 X magnification).

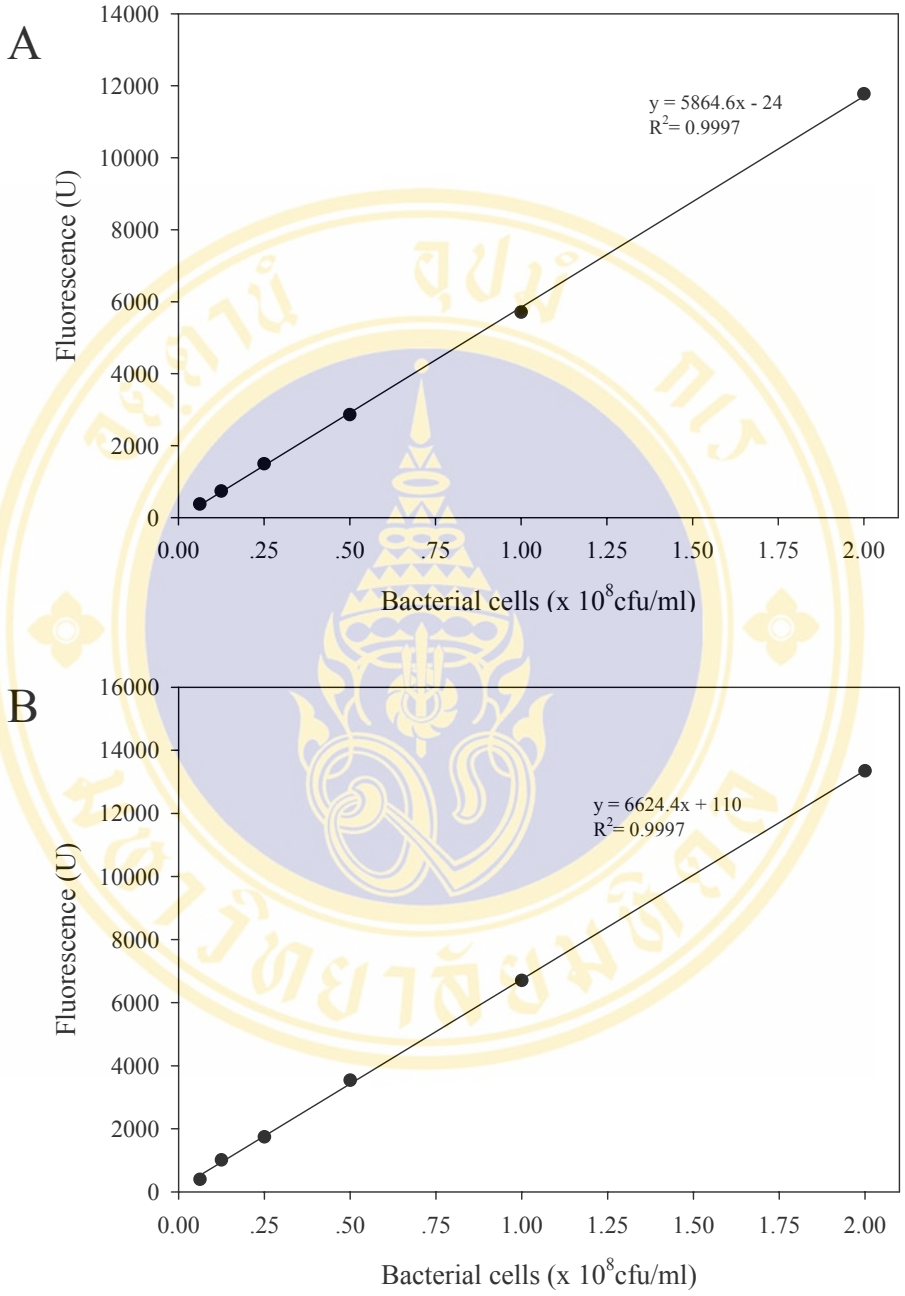

Figure 6.4 Linear correlation between fluorescent intensity and amount of cells expressing His6GFP intracellularly (TG1/pHis6GFPuv) (A) and engineered cells co-expressing zinc-binding motif on the cell surface and His6GFP in the cytoplasm (TG1/pEVZn + pHis6GFPuv) (B).

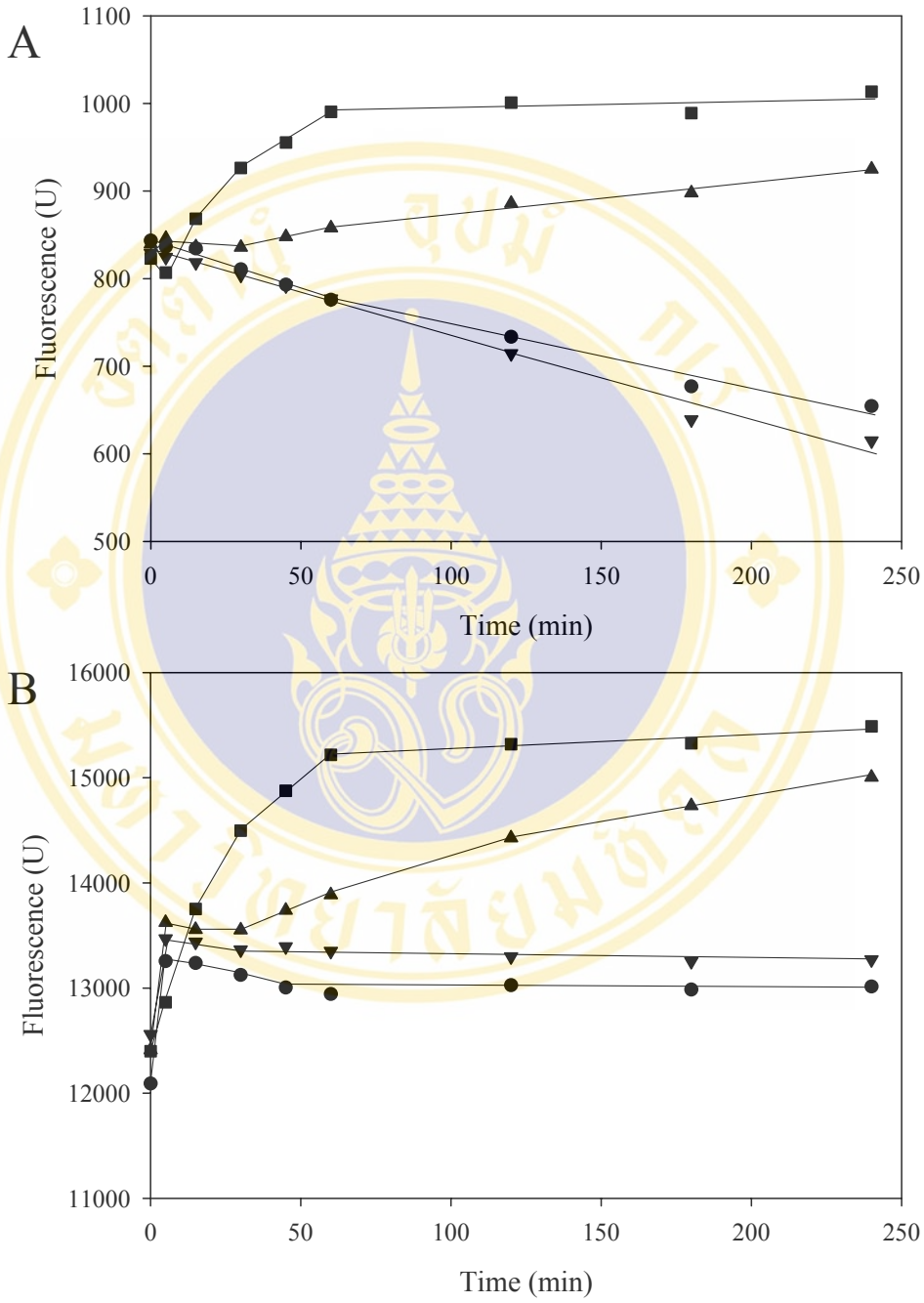

Figure 6.5 Effect of various concentrations of zinc ions on fluorescence level of *E. coli* co-expressing zinc-binding motif on the cell surface and native GFP (A) or His6GFP (B) in the cytoplasm. *Values represented means ($n \geq 2$). [Symbols:● (no metal); ▼ (50 nM); ▲ (50 μM); ■ (50 mM)

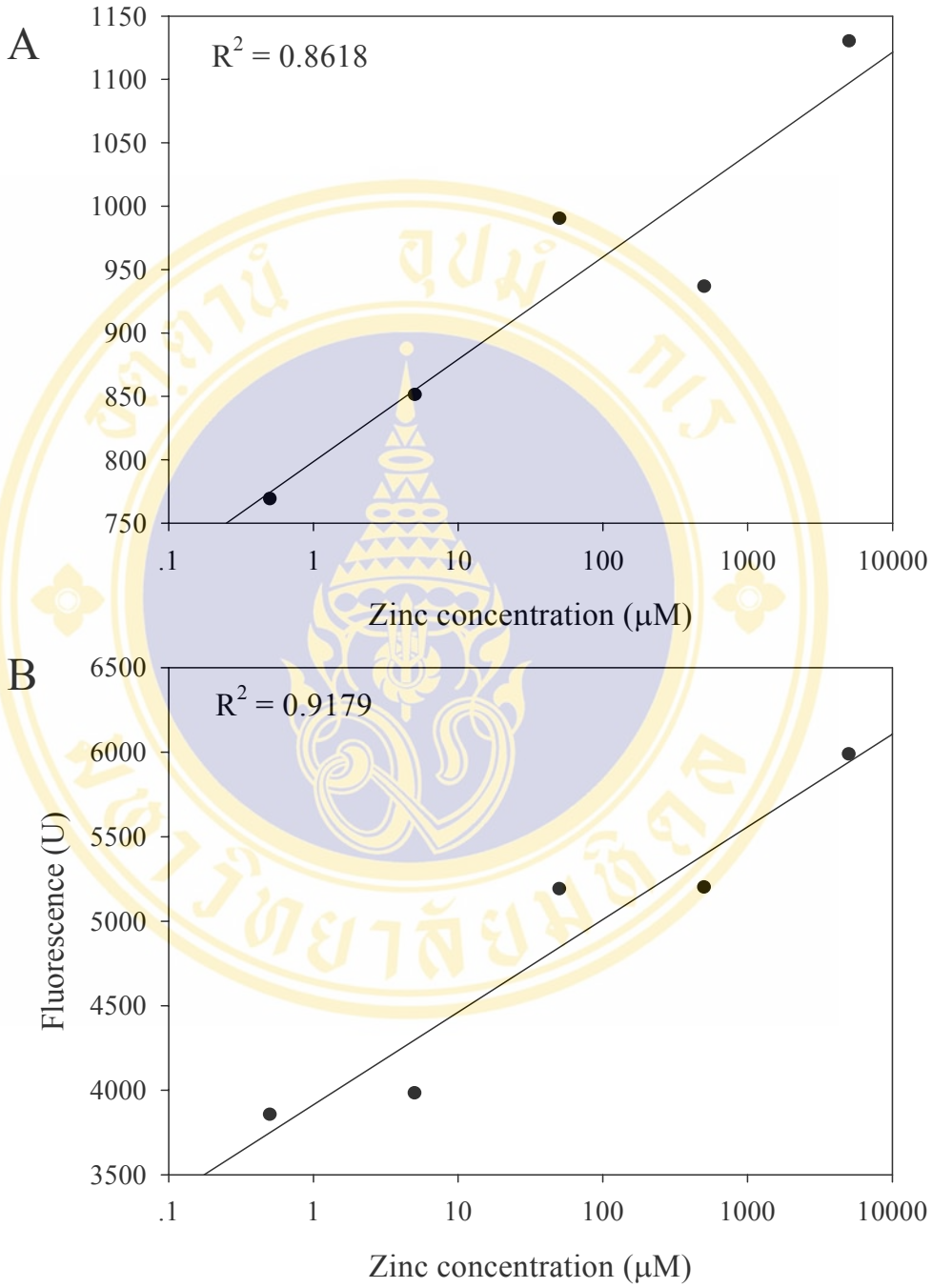

Figure 6.6 Linear correlation between zinc concentration and fluorescence level of *E. coli* co-expressing zinc-binding motif on the cell surface and native GFP (A) or His6GFP (B) in the cytoplasm.

CHAPTER 7
CONCLUSION AND FUTURE PERSPECTIVES

Although the method for cholesterol determination has been developed and widely performed about 100 years, the common principle for cholesterol determination is based upon chemical and enzymatic detection system. However, there are some drawbacks for both methods. The chemical method is an indirect assay. Samples have to be treated with solvent or corrosive reagent before measurement. This method is also sensitive to interference such as bilirubin. The enzymatic method is a direct method and is frequently used for cholesterol determination due to its specific catalytic reaction. While it provides some disadvantages, on the multiple assay step, involvement of carcinogenic or toxic substances and short half-life of enzymes.

In this thesis, construction of MIPs as tools for alternative method for cholesterol determination has been demonstrated. The improvement of property and structure of cholesterol imprinting polymer have been performed by combination of semi-covalent imprinting strategy with nitroxide mediated radical polymerization or precipitation polymerization. Those are the first major part of the thesis (chapter 3 and 4) while the second major part (chapter 5 and 6) involved the studies of chimeric metal binding GFP. From the epifluorescence microscopy and isotherm measurement, it has been demonstrated that the hydrophobicity of the chimeric GFP is mainly influenced by the fusion partner, the cadmium binding motif. Meanwhile, studies at the cellular level indicate role playing of H6-GFP particularly on the limited intaking of zinc ion at the expression of zinc binding motif on the cell surface of *E. coli* cell.

For cholesterol imprinted polymers, the microsphere polymers have successfully been prepared by precipitation polymerization using semicovalent imprinting approach. The cholesterol imprinted microsphere polymer prepared by divinyl benzene (DVB) as cross linker had large and more define spherical shape and displayed better imprinting effect than those prepared by ethylene glycol dimethacrylate (EDMA). The diameter of DVB and EDMA based cholesterol microsphere polymer were 0.4 and 0.3-2.5 μm respectively, where as the imprinting effect of DVB based microspheres polymer was almost 3 times higher than EDMA based microspheres polymer. Compared to cholesterol DVB based

imprinted bulk polymers prepared with the same condition, imprinted microsphere displayed slightly higher specific cholesterol uptake than imprinted bulk polymer. In addition, because of the small particle size, template removals by hydrolysis are easier with imprinted polymer microspheres. However, cholesterol binding isotherm of DVB based microspheres polymer indicated a heterogeneous binding site for the present covalent imprinting system. Two types of binding site with very different affinities for cholesterol have been demonstrated. The number of high affinity sites was very limited, the maximum binding site and dissociation constant were 85± 5 nmol g^{-1} and 5.2±0.3 x 10^{-6} M respectively. High affinity sites account for less than 0.02% of hydrolysis generated cavity, the portion of low affinity binding site were approximately 66%. This result suggested that the covalent molecular imprinting technique does not necessarily generate homogeneous binding site for our model. Interestingly, the cholesterol imprinted microsphere polymers could exhibit certain cross reactivity toward molecules that have size and hydrogen bond capability similar to cholesterol, such as S-propanolol and 17β– estradiol because of the fact that only single functional group was introduced into each binding site. Even though total binding capability of these compounds by imprinted microspheres was much higher than that of cholesterol, the specific part was almost the same (20%). Moreover, the S-propanolol bound to cholesterol DVB based microsphere polymers was within the imprinted cavity. The binding isotherm of S-propanolol by cholesterol imprinted microspheres shown the homogeneous binding site for propanolol molecule and account for 17 % of the hydrolysis-generated cavity.

In addition, nitroxide mediated polymerization (NMP) has firstly been applied and reported for construction in field of molecularly imprinted polymer. In this thesis, the cholesterol imprinted bulk polymers have successfully been prepared by this method. The binding capability of the MIP(NMP)-H (hydrolyzed form) to cholesterol was about 6 and 3 fold higher than that those of the unhydrolyzed form [MIP(NMP)-UH] and the control polymers [NIP(NMP)-H]. When compared to cholesterol imprinted bulk polymer prepared by traditional radical polymerization using benzyl peroxide (BPO), MIP (BPO)-H, the specific cholesterol binding to the MIP(NMP)-H (21%) was almost 60% higher than that shown by MIP(BPO)-H (13%). These indicated that nitroxide mediated imprinting seem to generate better binding site than the traditional free radical initiator. However, cholesterol binding isotherm of both imprinted polymers demonstrates that both polymers contain heterogeneous binding site: high and low affinity site for cholesterol. Although the number of high affinity site (Bmax) of MIP(NMP)-H and MIP(BPO)-H were 61±15 and 73±22

nmol g^{-1} respectively, the cholesterol affinity of MIP (NMP)-H corresponding to these site was almost two fold higher than that of MIP(BPO)-H. In addition, template removal from cholesterol imprinted polymer prepared by nitroxide was much more efficient than using BPO as radical generator. Even though the reverse reaction of nitroxide initiator provides the advantage over the traditional initiator, the temperature use in the reaction is very high and not appropriate for non-covalent imprinting. Hence, the development of new NMP initiator that allows low temperature polymerization need to be explored in the future.

Furthermore, the chimeric H6CdBP4GFP has successfully been constructed and used for studying the effect of cadmium binding peptide that changes the property of chimeric GFP resulting in change of the localization of chimeric green fluorescent protein. This study also compared to H6GFP and CdBP4GFP that have already been constructed by Prachayasittikul et al 2000 and 2001 (33, 178). All of chimeric proteins have intensively been explored not only in cellular membrane but also in artificial lipid membrane. At cellular level, the chimeric GFP carrying cadmium binding protein promoted the association of chimeric GFP to lipid membrane. Declining of fluorescence of chimeric GFP might be due to the cadmium binding protein that associates with the cellular membrane of engineered cell. The fluorescence of cells expressing chimeric H6GFP was approximately 3 fold higher than cell expressing native GFP fluorescence of cell expressing cadmium binding proteins, Cd4BPGFP, H6Cd4BPGFP were about 1.6 fold lower than that of native GFP. On the other hand, the fluorescence of chimeric protein decreased in order of H6GFP > Cd4BPGFP > H6Cd4GFP > native GFP respectively. Binding affinity to lipid membrane of chimeric GFP was further investigated by using artificial lipid bilayers and monolayers. Small amounts of the chimeric H6Cd4BPGFP were found to incorporate to liposome because of high surface pressure of lipid bilayer. For binding to monolayer, the H6Cd4BPGFP were incorporated into lipid monolayer at low interfacial pressure and caused an increase in fluidity and expansion of the surface area of lipid molecule higher than H6GFP. In contrast, this effect was not observed in both of H6Cd4GFP and H6GFP at high surface pressure. The surface area per lipid molecule before and after protein injection was similar. This phenomenon indicates that the chimeric GFP is squeezed out from the monolayer under the compression without loss of lipid molecules. This evidence of chimeric GFP binding to the lipid monolayer was strongly supported by epifluorescent microscopy, showing that the chimeric cadmium binding GFP preferentially binds to fluid phase area and defect parts of the lipid monolayers. All these findings demonstrate that the hydrophobicity of the GFP constructs is mainly influenced by the fusion partner. Therefore,

the demonstration of metal binding protein used here reveals the biophysical property of GFP constructs and understanding of mechanism of lipid and protein interaction In addition, one class of metal binding, cadmium binding protein, presents here may also apply to other chimeric proteins.

All these findings in this thesis suggest that cholesterol imprinted polymer prepared by not only semicovalent imprinting along with precipitation polymerization but also semicovalent imprinting combine with nitroxide mediated polymerization can be a promising approach for construction of effective cholesterol imprinted polymers. The incorporation of cholesterol imprinted polymer onto the sensor devices, such as quartz crystal microbalance (QCM), can support to feasibility of using imprinting polymer for cholesterol determination in the future. In addition, the study of lipid membrane affinity of metal binding GFP show the mechanism of lipid protein affinity and provides the opportunity to use this property of chimeric GFP for set up the fluorescent membrane based metal sensor or bifunctionalized membrane in the future.

REFERENCES

1. Levine GN, Keaney JF, Vita JA. Cholesterol reduction in cardiovascular disease. N Eng J Med 1995; 332: 512-521.
2. Natio HK: Nutrition and heart disease. New York, Spectrum Publication, Inc, 1982.
3. Goodman DS. New guidline for lowering blood cholesterol. Clin Lab Med 1989; 9: 17-28.
4. Grundy SM. Nation Cholesterol Education Program. Second report of the expert panel on detection, evaluation and treatment of high blood cholesterol in adults. Circulation 1994; 89: 1329-1445.
5. Ascaso JF, et al. Significance of high density lipoprotein-cholesterol in cardiovascular risk prevention: recommendations of the HDL forum. Am J Cardiovasc Drugs 2004; 4: 299-314.
6. Hang TC, Chen CO, Verna W, Alan R. A stable reagent for the Libermann-Burchard reaction. Anal Chem 1961; 33: 1045-1047.
7. Zlatkis A, Zak B, Boyle A. A new method for direct determination of cholesterol. J Lab Clin Med 1953; 41: 486-492.
8. Witte D, Barett D, Wycoff D. Evaluation of an enzymatic procedure for determination of serum cholesterol with the Abbott ABA-100. Clin Chem 1974; 20: 1282-1286.
9. Murata M, Ide T. Determination of cholesterol in subnanomolar quantity in biological fluids by high performance liquid chromatography. J Chromatogr: Biomed App 1992; 579: 329-333.
10. Blomhoff J. Serum cholesterol determination by gas-liquid chromatography. Clin Chim Acta 1973; 43: 257-265.
11. Situmorang M, Alexander P, Hibbert D. Flow injection potentiometry for enzymatic assay of cholesterol with a tungsten electrode sensor. Talanta 1999; 49: 639-649.
12. Costanza M, Wolff H, James R, Morabia A. In a quasi-simultaneous assessment, imprecise cholesterol monitoring and screening tests were improved. J Clin Epidemio 2005; 58: 841-848.

13. Whitcombe M, Rodriguez M, Villa P, Vulfson E. A new method for the introduction of recognition site functionality into polymers prepared by molecular imprinting: synthesis and characterization of polymeric receptors for cholesterol. J Am Chem Soc 1995; 117: 7105-7111.
14. Shea KJ. Molecular imprinting of synthetic network polymers: the de novo synthesis of macromolecular binding and catalytic sites. Trends Polym Sci 1994; 2: 166-173.
15. Mayes AG, Mosbach K. Molecularly imprinted polymers: useful materials for analytical chemistry? Trends Anal Chem 1997; 16: 321-332.
16. Wulff G. Molecular imprinting in crosslinked materials with the aid of molecular templates - a way towards artificial antibodies. Angew Chem Int Edit 1995; 34: 1812-1832.
17. Sellergren B. Noncovalent molecular imprinting: antibody-like molecular recognition in polymeric network materials. Trends Anal Chem 1997; 16: 310-320.
18. Tan SZ, Li GX, Li ZQ. Study and application of the molecular imprinting technique. Yingyong Huagong 2004; 33: 4-6.
19. Kandimalla VB, Ju H. Molecular imprinting: a dynamic technique for diverse applications in analytical chemistry. Anal Bioanal Chem 2004; 380: 587-605.
20. Sreenivasan K. Imparting cholesterol recognition sites in radiation polymerised poly(2-hydroxyethyl methacrylate) by molecular imprinting. Pol Int 1997; 42: 169-172.
21. Sellergren B, Wieschemeyer J, Boos K, Seidel D. Imprinted polymers for selective adsorption of cholesterol from gastrointestinal fluids. Chem Mater 1998; 10 4037-4046.
22. Hishiya T, Shibata M, Kakazu M, Asanuma H, Komiyama M. Molecularly imprinted cyclodextrins as selective receptors for steroids. Macromol 1999; 32: 2265-2269.
23. Flores A, Cunliffe D, Whitcombe MJ, Vulfson EN. Imprinted polymers prepared by aqueous suspension polymerization. J Appl Polym Sci 2000; 77: 1841-1850.
24. Perez N, Whitcombe MJ, Vulfson ENJ. Molecularly imprinted nanoparticles prepared by core-shell emulsion polymerization. Appl Polym Sci 2000; 77: 1851-1859.
25. Kugimiya A, Kuwada Y, Takeuchi T. Preparation of sterol-imprinted polymers with the use of 2-(methacryloyloxy)ethyl phosphate. J Chromatogr A 2001; 938 131-135.

26. Davidson L, Blencowe A, Drew MGB, Freebairn KW, Hayes W. Synthesis and evaluation of a solid supported molecular tweezer type receptor for cholesterol. J Mater Chem 2003; 13: 758-766.
27. Gore MA, Karmalkar RN, Kulkarni MG. Enhanced capacities and selectivities for cholesterol in aqueous media by molecular imprinting: role of novel cross-linkers. J Chromatogr B 2004; 804: 211-221.
28. Wang S, Xu J, Tong Y, Wang L, He C. Cholesterol-imprinted polymer receptor prepared by a hybrid imprinting method. Polym Int 2005; 54: 1268-1274.
29. Prachayasittikul V, Isarankura Na Ayudhya C, Bulow L. Lighting E. coli cells as biological sensors for Cd2+. Biotechnol Lett 2001; 23: 1285-1291.
30. Isarankura Na Ayudhya C, Prachayasittikul V, Galla H. Binding of chimeric metal-binding green fluorescent protein to lipid monolayer. Eur Biophys J 2004; 33: 522-534.
31. Prachayasittikul V, Sarah Ljung, Isarankura Na Ayudhya C, Bulow L. NAD(H) recycling activity of an engineered bifunctional enzyme galactose dehydrogenase/lactase dehydrogenase. Int J Biol Sci 2006; 2: 10-16.
32. Helen Carlsson, Prachayasittikul V, Bulow L. Zinc ion bound to chimeric His4/lactase dehydrogenase facilitate decarboxylation of oxaloacetate. Prot Eng 1993; 6: 907-911.
33. Prachayasittikul V, Isarankura Na Ayudhya C, Mejare M, Bulow L. Construction of a chimeric histidine6-green fluorescent protein: role of metal on fluorescent characteristic. Thammasat Int J Sc Tech 2000; 5: 61-68.
34. Prachayasittikul V, Isarankura Na Ayudhya C, Tantimongcolwat T, Galla HJ. Nanoscale oreintation and lateral organization of chimeric metal-binding green fluorescent protein on lipid membrane determined by epifluorescence and atomic force microscopy. Biochem Biophys Res Commun 2005; 326: 298-306.
35. http://www.nhlbi.nih.gov/health/dci/Diseases/Cad/CAD_WhatIs.html.
36. Ross R. The pathogenesis of atherosclerosis--an update. N Engl J Med 1986; 314: 488−500
37. Ross R: The pathogenesis of atherosclerosis, ed 3. Philadelphia, Saunders, 1988.
38. Ross R. The pathogenesis of atherosclerosis: a perspective for the 1990s. Nature 1993; 362: 801-809.

39. Libby P. Atherosclerosis: The new view. Sci Am 2002; 286: 46-55.
40. Cushing S, et al. Minimally modified low density lipoprotein induces monocyte chemotactic protein 1 in human endothelial cells and smooth muscle cells. Proc Natl Acad Sci USA 1990; 87: 5134-5138.
41. Rajavashisth TB, et al. Induction of endothelial cell expression of granulocyte and macrophage colony-stimulating factors by modified low-density lipoproteins. Nature 1990; 344: 254-257.
42. Dong Z, Wagner D. Leukocyte-endothelium adhesion molecules in atherosclerosis. J Lab Clin Med 1998; 132: 369-375.
43. Collins R, et al. P-Selectin or intercellular adhesion molecule (ICAM)-1 deficiency substantially protects against atherosclerosis in apolipoprotein E-deficient mice. J Exp Med 2000; 191: 189-194.
44. Qiao JH, et al. Role of macrophage colony-stimulating factor in atherosclerosis: studies of osteopetrotic mice. Am J Pathol 1997; 150: 1687-1699.
45. Gerhard GT, et al. Premenopausal black women are uniquely at risk for coronary heart disease compared to white women. Prev Cardiol 2000; 3: 105-117.
46. Schonbeck U, Sukhova GK, Shimizu K, Mach F, Libby P. Inhibition of CD40 signaling limits evolution of established atherosclerosis in mice. Proc Natl Acad Sci USA 2000; 97: 7458 - 7463.
47. Libby P, Aikawa M, Schönbeck U. Cholesterol and atherosclerosis. Biochim Biophys Acta 2000; 1529: 299-309.
48. http://www.texheartsurgeons.com/Images/CADheart.gif.
49. Gotto Jr AM, Farmer J: Risk factors for coronary heart desease, ed 3. Philadelphia, Saunders, 1988.
50. Grundy S. Role of low density lipoproteins in atherogenesis and development of coronary heart disease. Clin Chem 1995; 41: 139-146.
51. Roheim P, Asztalos B. Clinical significance of lipoprotein size and risk for coronary atherosclerosis. Clin Chem 1995; 41: 147-152.
52. Malinow M. Plasma homocyst(e)ine and arterial occlusive diseases: a mini-review. Clin Chem 1995; 41: 173-176.
53. Srinivasan S, Berenson G. Serum apolipoproteins A-I and B as markers of coronary artery disease risk in early life: the Bogalusa Heart Study. Clin Chem 1995; 41: 159-164.

54. Wilson P. Relation of high-density lipoprotein subfractions and apolipoprotein E isoforms to coronary disease. Clin Chem 1995; 41: 165-169.
55. Zilversmit D. Atherogenic nature of triglycerides, postprandial lipidemia, and triglyceride-rich remnant lipoproteins. Clin Chem 1995; 41: 153-158.
56. Kaplan LA, Pesce AJ, Kazmierczak SC: Clinical chemistry: theory, analysis, correlation, ed 4. St. Louis, Mosby company, 2003.
57. Gibbon G, Mitopoulos K, Myant N: Biochemistry of cholesterol. Amsterdam, Elsevier Biomedical Press, 1982.
58. Kritchevsky D: Cholesterol. New York, John Wiley and Son Inc, 1958.
59. Cleeman JI, Lenfant C.The National Cholesterol Education Program: progress and prospects. JAMA. 1998;280(24):2099-104.
60. Voet D, Voet G: Biochemistry. New York, John Wiley and Son Inc, 1990.
61. Stein E, Mayer G: Lipids , lipoprotein and apolipoprotein. Philadelphia, W.B. Saunders Company, 1994.
62. David L, Michael M: Lehninger principles of biochemistry. New York, Worth Publishers, 2000.
63. Voet D, Voet G, CE. P: Fundamentals of biochemistry. New York, John Wiley and Sons Inc, 1999.
64. Natio H: Cholesterol. St. Louis, The C.V. Mosby Company, 1989.
65. Lindop G, Dargie H: Cardiovascular system. London, ES BS with Edward Arnole, 1994.
66. Dryer R: LIPIDS. Philadelphia, W.B. Saunders Company, 1970.
67. Lehninger A: Principles of biochemistry. New York, Worth Publishers Inc, 1982.
68. Chang T: Mammalian HMG-CoA reductase and its regulation. New York, Academic Press, 1983.
69. Duncan I, Culbreth P, Burtis C. Determination of free, total, and esterified cholesterol by high performance liquid chromatography. J Chromatogr A 1979; 162: 281-292.
70. Goldstein J, Brown M. The low density lipoprotein pathway and its relation to atherosclerosis. Annu Rev Biochem 1977; 46: 897-930.
71. Glomset J. The plasma lecitin: cholesterol acyltransferase reaction. J Lipid Res 1968; 9: 155-167.

72. Walmsley R, White G: A guide to diagnostic clinical chemistry. Oxford, Blackwell Scientific Publication, 1996.

73. http://www.ovc.uoguelph.ca/BioMed/Courses/Public/Pharmacology/pharmsite/98-409/Blood/Images/cholesterol_metab.gif.

74. Fielding C, Fielding P: Metabolism of cholesterol and lipoprotein. California, The Benjamin/ Cummings Publishing Company Inc, 1985.

75. Huang T, Wefler V, Raferty A. A simplified spectrophotometric method for determination of total and esterified cholesterol with tomatine. Anal Chem 1963; 35: 1757-1758.

76. Pearson S, Stern S, Mcgavak T. A rapid method for the determination of total cholesterol in serum. Anal Chem 1953; 25: 813-814.

77. Allian C, Poon L, Chan C, Richmode W, Fu P. Enzymatic determination of total cholesterol in serum. Clin Chem 1974; 20: 470-475.

78. Pesce M, Bodourian S. Enzymatic rate method measuring cholesterol in serum. Clin Chem 1976; 22: 2042-2045.

79. Abell L, Lavy B, Brodie B, Kendall F. Simplified method for the estimation of cholestrol in serum and demonstration of its specificity. J Biol Chem 1952; 195: 357-366.

80. Zak B, Ressler N. Methodology in determination of cholesterol. Am J Clin Pathol 1955; 25: 433-443.

81. Carr J, Drekter I. Simplified rapid for the extraction and determination of cholesterol without sponification. Clin Chem 1956; 2: 353-368.

82. Bloor W. The determination of small amounts of lipid in blood plasma. J Biol Chem 1928; 77: 53-73.

83. Chiamori N, Henry R. Study of ferric chloride method for the determination of total cholesterol and cholesterol esters. Am J Clin Pathol 1959; 31: 305-309.

84. Schoenheimer R, Sperry W. A micromethod for determination of free and combined cholesterol. J Biol Chem 1934; 106: 745-760.

85. Sperry W, Webb M. A revision of the Schoenheimer and Sperry for cholesterol determination. J Biol Chem 1950; 87: 97-106.

86. Natio H, David J: Laboratory consideration: determination of cholesterol, triglyceride,phospholipid, and other lipids in blood and tissue. New York, Alan R Liss Inc, 1984.

87. Liebermann C. Ueber das Oxychinoterpen. Dtsch Chem Geselsch 1885; 18: 1803-1809.
88. Burchare H. Beitrage zur Kenntnis DES. Chelesterins Chem Zentralbl 1890; 61: 25-27.
89. Copeland B. Serum cholesterol methodology: 100 years of development. Ann Chem Lab Sci 1990; 20: 1-11.
90. Richmond W. Analytical reviews in clinical biochemistry: the quantitative analysis of cholesterol. Anal Clin Biochem 1992; 29: 577-597.
91. Levine J, Zak B. Automated determination of serum total cholesterol. Clin Chem Acta 1964; 10: 381-384.
92. Block W, Jarett K, Levine J. An improved automated determination of serum total cholesterol with a single reagent. Clin Chem 1966; 12: 681-689.
93. Jordan W, Knoblock E. A micromethod for total cholesterol eliminating the effect of high bilirubin level. Clin Chem 1969; 15: 807-808.
94. Solow E, Freeman L. A fluorometric ferric chloride method for determinating cholesterol in cerebrospinal fluid and serum. Clin Chem 1970; 16: 472-476.
95. Robertson G, Cramp D. An evaluation of cholesterol determination in serum and serum lipoprotein fractions by a semiautomated fluorimetric method. J Clin Pathol 1970; 23: 243-245.
96. Richmond W. Preparation of properties of cholesterol oxidase from *Norcadia sp.* and its application to the enzymatic assay of total cholesterol in serum. Clin Chem 1973; 19: 1350-1356.
97. Borner K, Klose S. Enzymatische Bestimmung des Gesamtcholesterins mit dem Greiner Selective Analyzer (GSA-11). J Clin Chem Biochem 1977; 15: 121-130.
98. Tarbutton P, Guther C. Enzymatic determination of total cholesterol in serum. Clin Chem 1974; 20: 1282-1286.
99. Rautela G, Liedtke R. Automated enzymatic measurement of total cholesterol in serum. Clin Chem 1978; 24: 121-131.
100. Huang H, Kuan S, Guilbault G. Amperomertric determination of total cholesterol in serum with use of immobilized cholesterol ester hydrolase and cholesterol oxidase. Clin Chem 1977; 23: 671-676.
101. Huang H, Kuan JW, Guilbault G. Fluorometric enzymatic determination of total cholesterol in serum. Clin Chem 1975; 21: 1605-1608.

102. Noma A, Nakayama K. Polarographic method for rapid microdetermination of cholesterol with cholesterol ester and cholesterol oxidase. Clin Chem 1976; 22: 336-340.

103. Pesce MA, Bodourian SH. Enzymatic measurement of cholesterol in serum with the CentrifiChem centrifugal analyzer. Clin Chem 1977; 23: 280-182.

104. Majkic N, Berkes I. Determination of free and esterified cholesterol by a kinetic method. Clin Chim Acta 1977; 80: 121-131.

105. Deacon A, Dawson P. Enzymatic assay of total cholesterol involving chemical or enzymatic hydrolysis a comparison methods. Clin Chem 1979; 25: 976-984.

106. Degg R, Ziegenhorn J. Kinetic enzymic method for automated determination of total cholesterol in serum. Clin Chem 1983; 29: 1798-1802.

107. Bala C, Rotaliu LD, Magearu V. An amperometric sensor for cholesterol determination in bile. J Med Biochem 1997; 1: 143-150.

108. Vidal J, Espuelas J, Ruiz E, Castillo J. Amperometric cholesterol biosensors based on the electropolymerization of pyrrole and the electrocatalytic effect of Prussian-Blue layers helped with self-assembled monolayers. Talanta 2004; 64: 655-664.

109. Gray M, Plant A, Nicholson J, May W. Microenzymatic fluorescent assay for serum cholesterol. Anal Biochem 1995; 224: 286-292.

110. Sasamoto H, Maeda M, Tsuji A. Chemiluminescent enzymatic assay for cholesterol in serum using lucigenin. Anal Chim Acta 1995; 310: 347-353.

111. Iwata T, Yamaguchi M, Nakamura M. Highly sensitive and simple determination of cholesterol and cholestanol in human serum by high-performance liquid chromatography with fluorescence detection. J Chromatogr A 1987; 421: 43-50.

112. Tsuruta Y, Teranishi T, Date Y, Kohashi K. Simultaneous determination of cholesterol and cholestanol in human serum by high-performance liquid chromatography using 3-(5,6-methylenedioxy-2-phthalimidyl)benzoyl azide as precolumn fluorescent labelling reagent. J Chromatogr:Biomed App 1993; 617: 213-220.

113. Driscoll J, Aubuchon D, Descoteaux M, Martin H. Semiautomated, specific routine serum cholesterol determination by gas-liquid chromatography. Anal Chem 1971; 43: 1196-2000.

114. Krug A, Kellner R. Mid-infrared fiber optic determination of cholesterol and triglycerides. J Mol Struct 1993; 294: 211-214.

115. Raghavan V, Ramanathan K, Sundaram P, Danielsson B. An enzyme thermistor-based assay for total and free cholesterol Clin Chim Acta 1999; 289: 145-158.

116. Asanuma H, Kakazu M, Shibata M, Hishiya T, Komiyama M. Molecularly imprinted polymer of beta-cyclodextrin for the efficient recognition of cholesterol. Chem Commun 1997: 1971-1972.

117. Asanuma H, Kakazu M, Shibata M, Hishiya T, Komiyama M. Synthesis of molecularly imprinted polymer of beta-cyclodextrin for the efficient recognition of cholesterol. Supramol Sci 1998; 5: 417-421.

118. Sreenivasan K. Synthesis and evaluation of a beta cyclodextrin-based molecularly imprinted copolymer. J Appl Polym Sci 1998; 70: 15-18.

119. Sreenivasan K. Synthesis and evaluation of a molecularly imprinted polyurethane–poly(HEMA) semi-interpenetrating polymer networks as membrane. Appl Polym Sci 1998; 70: 19-22.

120. Sreenivasan K. Effect of the type of monomers of molecularly imprinted polymers on the interaction with steroids. J Appl Polym Sci 1998; 68: 1863-1866.

121. Piletsky S, Piletskaya E, Sergeyeva T, Panasyuk T, El'skaya A. Molecularly imprinted self-assembled films with specificity to cholesterol. Sensor Actuat B 1999; 60: 216-220.

122. Zhong N, Byun HS , R B. Hydrophilic cholesterol-binding molecular imprinted polymers. Tetra lett 2001; 42: 1839–1841.

123. Sreenivasan K. The use of metal-containing monomer in the preparation of molecularly imprinted polymer to increase the adsorption capacity. J Appl Polym Sci 2001; 80: 2795-2799.

124. Perez N, Whitcombe MJ, Vulfson EN. Surface imprinting of cholesterol on submicrometer core-shell emulsion particles. Macromolecules 2001; 34: 830-836.

125. Hishiya T, Asanuma H, Komiyama M. Spectroscopic anatomy of molecular imprinting of cyclodextrin evidence for preferential formation of ordered cyclodextrin assemblies. J Am Chem Soc 2002; 124: 570-575.

126. Hwang CC, Lee WC. Chromatographic characteristics of cholesterol-imprinted polymers prepared by covalent and non-covalent imprinting methods. J Chromatogr A 2002; 962: 69-78.

127. Gong JL, Gong FC, Zeng GM, Shen GL, Yu RQ. A novel electrosynthesized polymer applied to molecular imprinting technology. Talanta 2003; 61: 447-453.
128. Chou LCS, Liu CC. Development of a molecular imprinting thick film electrochemical sensor for cholesterol detection. Sensor Actuat B 2005; 110: 204-208.
129. Egawa Y, Shimura Y, Nowatari Y, Aiba D, Juni K. Preparation of molecularly imprinted cyclodextrin microspheres. Int J Pharm 2005; 293: 165-170.
130. Spizzirri UG, Peppas NA. Structural analysis and diffusional behavior of molecularly imprinted polymer networks for cholesterol recognition. Chem Mater 2005; 17: 6719-6727.
131. Duncan IL, Mather A, Cooper GR: The procedure for the proposed cholesterol reference method. GA, Center for Disease Control, Atlanta, 1982.
132. Cohen L, Johns RI, Batra KV. Determination of total ester and free cholesterol in serum and serum lipoproteins. Clin Chim Acta 1961; 6: 613-619.
133. Schaffer R, Sneigoski LT, Welch MJ. Comparison of two isotope dilution/ mass spectrometric methods for determination of total serum cholesterol. Clin Chem 1982; 28: 5-8.
134. Cooper GR, Gill JB, Biegeleisen JJ. CDC point of reference for total cholesterol measurements. Clin Chem 1980; 26: 966.
135. Haupt K. Imprinted polymers-tailor-made mimics of antibodies and receptors. Chem Commun 2003; 21: 171-178.
136. Komiyama M, Takeuchi T, Mukawa T, Asanuma H: Molecular imprinting from fundamental to application. Germany, Wiley-Vch, 2003.
137. http://asl.chemistry.gatech.edu/images/mip_principle.gif.
138. Wulff G, Grobe-Einsler R, Vesper W, Sarhan A. Enzyme-analog built polymers, 5. The specificity distribution of chiral cavities prepared in synthetic polymers. Makromolekulare Chemie 1977; 178: 2817-2825.
139. Shea K, Dougherty TK. Molecular recognition on synthetic amorphous surfaces. The influence of functional group positioning on the effectiveness of molecular recognition. J Am Chem Soc 1986; 108: 1091-1093.
140. Arshady R, Mosbach K. Synthesis of substrate-selective polymers by host-guest polymerization. Macromol Chem 1981; 182: 687-692.
141. Vlatakis G, Andersson LI, Muller R, Mosbach K. Drug assay using antibody mimics made by molecular imprinting. Nature 1993; 361: 645-647.

142. Hosoya K, et al. Preparation of uniformly sized polymeric separation media potentially suitable for small-scale high-performance liquid chromatography and/or capillary electrochromatography. J Chromatogr A 1999; 853: 11-20.
143. Allender J, Richardson C, Woodhouse B, Heard CM, Brain KR. Pharmaceutical applications for molecularly imprinted polymers. Int J Pharm 2000; 195: 39-43.
144. Zhu X, Yang J, Su Q, Cai J, Gao Y. Molecularly imprinted polymer for monocrotophos and its binding characteristics for organophosphorus pesticides. Ann Chim 2005; 95: 877-884.
145. Meng Z, Chen W, Mulchandani A. Removal of estrogenic pollutants from contaminated water using molecularly imprinted polymers. Environ Sci Technol 2005; 39: 8958-8962.
146. Joshi VP, Kulkarni MG, Mashelkar RA. Molecularly imprinted adsorbents for positional isomer separation. J Chromatogr A 1999; 849: 319-330.
147. Takeuchi T, Fukuma D, Matsui J. Combinatorial Molecular Imprinting: An Approach to Synthetic Polymer Receptors. Anal Chem 1999; 71: 285-290.
148. Mosbach K, Ramstroem O. The emerging technique of molecular imprinting and its future impact on biotechnology. Biotechnol 1996; 14: 163-170.
149. Peres MN, Mayes AG. Comparative study of imprinted polymer particles prepared by different polymerization methods. Anal Chim Acta 2004; 504: 15-21.
150. Ye L, Cormack P, Mosbach K. Molecularly imprinted monodisperse microspheres for competitive radioassay. Anal Commun 1999; 36: 35-38.
151. Li K, Stöver HDH. Synthesis of monodisperse poly(divinylbenzene) microspheres. J Polym Sci A: Polym Chem 1993; 31: 3257-3263.
152. Hawker CJ, Bosman AW, Harth E. New polymer synthesis by nitroxide mediated living radical polymerizations. Chem Rev 2001; 101: 3661-3688.
153. Fischer H. The persistent radical effect: A principle for selective radical reactions and living radical polymerizations. Chem Rev 2001; 101: 3581-3610.
154. Atsushi G, Takeshi F. Kinetics of living radical polymerization. Prog Polym Sci 2004; 29: 329-385.
155. Studer A, Schulte T. Nitrixide mediated radical process. Chem Rec 2005; 5: 27-35.
156. Otsu T, Yoshida M. Polymer design by organic disulfides as iniferters. Macromol Rapid Commun 1982; 3: 127-132.

157. Otsu T. Iniferter concept and living radical polymerization. J Polym Sci Pol Chem 2000; 38: 2121-2136.

158. Fischer H. The persistent radical effect in controlled radical polymerizations. J Polym Sci Pol Chem 1999; 37: 1885-1901.

159. Ward WW, Cody CW, Hart RC, Cormier MJ. Spectrophotometric identity of the energy transfer chromophores in Renilla and Aequorea green-fluorescent proteins. Photochem Photobiol 1980; 31: 611-615.

160. Prasher DC, Eckenrode VK, Ward WW, Prendergast FG, Cormier MJ. Primary structure of the Aequorea victoria green-fluorescent protein. Gene 1992; 111: 229-233.

161. Ward WW, Cormier MJ. An energy transfer protein in coelenterate bioluminescence. Characterization of the Renilla green-fluorescent protein. J Biol Chem 1979; 254: 781-788.

162. Phillips GN, Jr. Structure and dynamics of green fluorescent protein. Curr Opin Struct Biol 1997; 7: 821-827.

163. Morise H, Shimomura O, Johnson FH, Winant J. Intermolecular energy transfer in the bioluminescent system of Aequorea. Biochemistry 1974; 13: 2656-2662.

164. Shimomura O. Structure of the chromophore of Aequorea green fluorescent protein. FEBS Letters 1979; 104: 220-222.

165. Cubitt AB, et al. Understanding, improving and using green fluorescent proteins. Trends Biochem Sci 1995; 20: 448-455.

166. Cody CW, Prasher DC, Westler WM, Prendergast FG, Ward WW. Chemical structure of the hexapeptide chromophore of the Aequorea green-fluorescent protein. Biochemistry 1993; 32: 1212-1218.

167. Heim R, Prasher DC, Tsien RY. Wavelength mutations and posttranslational autoxidation of green fluorescent protein. Proc Natl Acad Sci USA 1994; 91: 12501-12504.

168. Delagrave S, Hawtin RE, Silva CM, Yang MM, Youvan DC. Red-shifted excitation mutants of the green fluorescent protein. Bio/Technol 1995; 13: 151-154.

169. Lim C, Kimata K, Oka M, Nomaguchi K, Kohno K. Thermosensitivity of a green fluorescent protein utilized to reveal novel nuclear-like compartments. J Biochem (Tokyo) 1995; 118: 13-17.

170. Ward WW, Bokman SH. Reversible denaturation of Aequorea green-fluorescent protein: physical separation and characterization of the renatured protein. Biochemistry 1982; 21: 4535-4540.

171. Inouye S, Tsuji FI. Evidence for redox forms of the Aequorea green fluorescent protein. FEBS Lett 1994; 35: 211-214.

172. Tsien RY. The green fluorescent protein. Annu Rev Biochem 1998; 67: 509-544.

173. Kain SR, et al. Green fluorescent protein as a reporter of gene expression and protein localization. Biotechniques 1995; 19: 650-655.

174. Chalfie M, Tu Y, Euskirchen G, Ward WW, Prasher DC. Green fluorescent protein as a marker for gene expression. Science 1994; 263: 802-805.

175. Hampton RY, Koning A, Wright R, Rine J. In vivo examination of membrane protein localization and degradation with green fluorescent protein. Proc Natl Acad Sci USA 1996; 93: 828-833.

176. Cormack B. Green fluorescent protein as a reporter of transcription and protein localization in fungi. Curr Opin Microbiol 1998; 1: 406-410.

177. Tannahill D, Bray S, Harris WA. A Drosophila E(spl) gene is "neurogenic" in Xenopus: a green fluorescent protein study. Dev Biol 1995; 168: 694-697.

178. Prachayasittikul V, Isarankura Na Ayudhya C, Mejare M, Bulow L. Construction of a chimeric histidine6-green fluorescent protein: role of metal on fluorescent characteristic. Thammasat Int J Sc Tech 2000; 5: 61-68.

179. Garamszegi N, Garamszegi ZP, Rogers MS, Demarco SJ, Strehler EE. Application of a chimeric green fluorescent protein to study protein protein interactions. Biotechniques 1997; 23: 864-866,868-870,872.

180. Morino K, et al. Antibody fusions with fluorescent proteins: a versatile reagent for profiling protein expression. J Immunol Meth 2001; 257: 175-184.

181. Aoki T, Miyashita M, Fujino H, Watabe H. A flexibel single-step detection of blotted antigen using a fusion protein between protein A and green fluorescent protein. Biosci Biotechnol Biochem 2000; 64: 1547-1551.

182. Arai R, Ueda H, Nagamune T. Construction of chimeric proteins between protein G and fluorescence-enhanced green fluorescent protein, and their application to immunoassays. J Ferment Bioeng 1998; 86: 440-445.

183. Prachayasittikul V, Isarankura Na Ayudhya C, Suwanwong Y, Tantimavanich S. Construction of chimeric antibody binding green fluorescent protein for clinical application. Excli J 2005; 4: 91-104.

184. Inouye S, Tsuji FI. Aequorea green fluorescent protein. Expression of the gene and fluorescence characteristics of the recombinant protein. FEBS Lett 1994; 341: 277-280.

185. Yang F, Moss LG, Phillips GN, Jr. The molecular structure of green fluorescent protein. Nat Biotechnol 1996; 14: 1246-1251.

186. Youvan DC, et al. Calibration of fluorescence resonance energy transfer in microscopy using genetically engineered GFO derivatives on nickle chelating beads. Biotechnology et alia 1997; 3: 1-18.

187. Richmond TA, Takahashi TT, Shimkhada R, Bernsdorf J. Engineered metal binding sites on green fluorescent protein. Biochem Biophys Res Comm 2000; 268: 462-465.

188. Isankura Na Ayudhya C: Engineering of chimeric protein for binding to metal ions; Bangkok Thailand, Mahidol University, 2000.

189. Mosbach K. Molecular imprinting. Trends Biochem Sci 1994; 19: 9-14.

190. Ye L, Weiss R, Mosbach K. Synthesis and characterization of molecularly imprinted microspheres. Macromolecules 2000; 33: 8239-8245.

191. Ye L, Surugiu I, Haupt K. Scintillation proximity assay using molecularly imprinted microspheres. Anal Chem 2002; 74: 959-964.

192. Wang J, Cormack PAG, Sherrington DC, Khoshdel E. Monodisperse molecularly imprinted polymer microspheres prepared by precipitation polymerization for affinity separation applications. Angew Chem Int Ed 2003; 42: 5336-5338.

193. Shinkai S, Murata K. Cholesterol-based functional tectons as versatile building-blocks for liquid crystals, organic gels and monolayers. J Mater Chem 1998; 8: 485-495.

194. Sugiyasu K, Fujita N, Shinkai S. Visible-light-harvesting organogel composed of cholesterol-based perylene derivatives. Angew Chem Int Ed 2004; 43: 1229-1233.

195. Andersson HS, et al. Study of the nature of recognition in molecularly imprinted polymers II. Influence of monomer-template ratio and sample load on retention and selectivity. J Chromatogr A 1999; 848: 39-49.

196. Katz A, Davis ME. Investigations into the mechanisms of molecular recognition with Imprinted Polymers. Macromolecules 1999; 32: 4113-4121.

197. Svenson J, Karlsson JG, Nicholls IA. 1H Nuclear magnetic resonance study of the molecular imprinting of (-)-nicotine: template self-association, a molecular basis for cooperative ligand binding. J Chromatogr A 2004; 1024: 39-44.

198. Ye L, Mosbach K. Polymers recognizing biomolecules based on a combination of molecular imprinting and proximity scintillation: A new sensor concept. J Am Chem Soc 2001; 123: 2901-2902.

199. Ansell RJ. Molecularly imprinted polymers in pseudoimmunoassay. J Chromatogr B 2004; 804: 151-165.

200. Pap T, Horvai G. Binding assays with molecularly imprinted polymers-why do they work? J Chromatogr B 2004; 804: 167-172.

201. Zimmerman SC, Wendland MS, Rakow NA, Zharov I, Suslick KS. Synthetic hosts by monomolecular imprinting inside dendrimers. Nature 2002; 418: 399-403.

202. Patel A, Fouace S, Steinke JHG. Enantioselective molecularly imprinted polymers via ring-opening metathesis polymerization. Chem Commun 2003: 88-89.

203. Matyjaszewski K, Xia J. Atom transfer radical polymerization. Chem Rev 2001; 101: 2921-2990.

204. Wei X, Li X, Husson SM. Surface molecular imprinting by atom transfer radical polymerization. Biomacromolecules 2005; 6: 1113-1121.

205. Chiefari J, et al. Living free-radical polymerization by reversible addition-fragmentation chain transfer: The RAFT process. Macromolecules 1998; 31: 5559-5562.

206. Benoit D, Chaplinski V, Braslau R, Hawker CJ. Development of a universal alkoxyamine for "living" free radical polymerizations. J Am Chem Soc 1999; 121: 3904-3920.

207. Hintermann T, Kramer A, Nesvadba P, Fink J. Novel high performance nitroxides for controlled low temperature radical polymerization. Polym Prepr 2002; 43: 86-87.

208. Boonpangrak S, Prachayasittikul V, Bulow L, Ye L. Molecularly imprinted polymer microspheres prepared by precipitation polymerization using a sacrificial covalent bond. J Appl Polym Sci 2006; 99: 1390-1398.

209. Shimomura O, Johnson FH, Saiga Y. Extraction, purification, and properties of aequorin, a bioluminescent protein from the luminous hydromedusan, Aequorea. J Cell Compar Physl 1962; 59: 223-239.

210. Bokman SH, Ward WW. Renaturation of Aequorea green-fluorescent protein. Biochem Bioph Res Co 1981; 101: 1372-1380.

211. Crameri A, Whitehorn EA, Tate E, Stemmer WP. Improved green fluorescent protein by molecular evolution using DNA shuffling. Nat biotechnol 1996; 14: 315-319.

212. Cha HJ, et al. Insect larval expression process is optimized by generating fusions with green fluorescent protein. Biotechnol Bioeng 1999; 65: 316-324.

213. Yang TT, Cheng L, Kain SR. Optimized codon usage and chromophore mutations provide enhanced sensitivity with the green fluorescent protein. Nucl Acids Res1996; 24: 4592-4593.

214. Kimata Y, Iwaki M, Lim CR, Kohno K. A novel mutation which enhances the fluorescence of green fluorescent protein at high temperatures. Biochem Biophys Res Commun 1997; 232: 69-73.

215. Yang TT, et al. Improved fluorescence and dual color detection with enhanced blue and green variants of the green fluorescent protein. J Biol Chem 1998; 273: 8212-8216.

216. Kojima S, Hirano T, Niwa H, Ohashi M, Inouye S, Tsuji FI. Mechanism of the Redox Reaction of the Aequorea Green Fluorescent Protein (GFP). Tetrahedron Lett 1997; 38: 2875-2878.

217. Mejare M, Lilius G, Bulow L. Evaluation of genetically attached histidine affinity tails for purification of lactate dehydrogenase from transgenic tobacco. Plant Sci 1998; 134 103-114.

218. Maniatis T, Fritsch, E., Sambrook, J. Molecular Cloning, A Laboratory Manual. Cold Spring Harbour Laboratory Press, New York 1989.

219. Cha HJ, Dalal NG, Pham M-Q, Bentley WE. Purification of human interleukin-2 fusion protein produced in insect larvae is facilitated by fusion with green fluorescent protein and metal affinity ligand. Biotechnol Prog 1999; 15: 283-286.

220. Cha HJ, Wu CF, Valdes JJ, Rao G, Bentley WE. Observations of green fluorescent protein as a fusion partner in genetically engineered Escherichia coli: monitoring protein expression and solubility. Biotechnol Bioeng 2000; 67: 565-574.

221. Woodman SE, Schlegel A, Cohen AW, Lisanti MP. Mutational analysis identifies a short atypical membrane attachment sequence (KYWFYR) within caveolin-1. Biochemistry 2002; 41: 3790-3795.

222. Dorn IT, Pawlitschko K, Pettinger SC, Tampe R. Orientation and two-dimensional organization of proteins at chelator lipid interfaces. Biol Chem 1998; 379: 1151-1159.

223. Wang QJ, Bhattacharyya D, Garfield S, Nacro K, Marquez VE., Blumberg, P.M. Differential localization of protein kinase C delta by phorbol esters and related compounds using a fusion protein with green fluorescent protein. J Biol Chem 1999; 274: 37233-37239.

224. Oancea E, Teruel MN, Quest AF, Meyer T. Green fluorescent protein (GFP)-tagged cysteine-rich domains from protein kinase C as fluorescent indicators for diacylglycerol signaling in living cells. J Cell Biol 1998; 140: 485-498.

225. Hurley JH, Meyer T. Subcellular targeting by membrane lipids. Curr Opin Cell Biol 2001; 13: 146-152.

226. Razzini G, et al. Different subcellular localization and phophoinositides binding of insulin recepter substrate protein pleckstrin homology domains. Mol Endocrinol 2000; 14: 823-836.

227. Obrdlik P, Neuhaus G, Merkle T. Plant heterotrimeric G protein beta subunit is associated with membranes via protein interactions involving coiled-coil formation. FEBS Lett 2000; 476: 208-212.

228. Klee B, Duveneck GL, Oroszlan P, Ehrat, M, Widmer HM. A model system for the development of an optical biosensor based on lipid membranes and membrane-bound receptors. Sensors and Actuators B 1995; 29: 307-311.

229. Dietrich C, Boscheinen O, Scharf KD, Schmitt, L., Tampe, R. Functional immobilization of a DNA-binding protein at a membrane interface via histidine tag and synthetic chelator lipids. Biochemistry 1996; 35: 1100-1105.

230. Nock S, Spudich JA, Wagner P. Reversible, site-specific immobilization of polyarginine-tagged fusion proteins on mica surfaces. FEBS Lett 1997; 414: 233-238.

231. Kostov Y, Albano CR, Rao G. All solid-state GFP sensor. Biotechnol Bioeng 2000; 70: 473-477.

232. Tvarozek V, Hianik T, Novotny I, Rehacek V, Ziegler W, Ivanic R. Thin films in biosensors. Vacuum 1998; 50: 251-262.

233. Vallee B, Falchuk K. The biochemical basis of zinc physiology. Physiol Rev 1993; 73: 79-118.

234. Rudolf E, Cervinka M. Depletion of endogenous zinc stores induces oxidative stress and cell death in human melanoma cells. Acta Medica (Hradec Kralove) 2004; 47: 91-96.

235. Prasad A. Recognition of Zinc-Deficiency Syndrome. Nutrition 2001; 17: 67-69.

236. Liuzzy J, Counsins R. Mammalian zinc transporters. Annu Rev Nutr 2004; 24: 151-172.

237. Patzer SI, Hantke K. The ZnuABC high-affinity zinc uptake system and its regulator Zur in Escherichia coli. Mol Microbiol 1998; 28: 1199-1210

238. Brocklehurst K, et al. ZntR is a Zn(II)-responsive MerR-like transcriptional regulator of zntA in Escherichia coli. Mol Microbiol 1999; 31: 893-902.

239. Outen C, O Halloran T. Femtomolar sensitivity of metalloregulatory proteins controlling zinc homeostasis. Science 2001; 292: 2488-2492.

240. Sensi S, et al. Measurement of intracellular free zinc in living cortical neurons: routes of entry. J Neurosci 1997; 17: 9554-9564.

241. Devergnas S, et al. Differential regulation of zinc efflux transporters ZnT-1, ZnT-5 and ZnT-7 gene expression by zinc levels: a real-time RT–PCR study. Biochem Pharmacol 2004; 68: 699-709.

242. Duffy J, et al. A decrease in intracellular zinc level precedes the detection of early indicators of apoptosis in HL-60 cells. Apoptosis 2001; 6: 161-172.

243. Frederickson CJ, et al. Depletion of intracellular zinc from neurons by use of an extracellular chelator in vivo and in vitro. J Histochem Cytochem 2002; 50: 1659-1662.

244. Mejare M, Ljung S, Bulow L. Selection of cadmium specific hexapeptides and their expression as OmpA fusion proteins in *Escherichia coli.* Protein Eng 1998; 11: 489-494.

245. Kjaergaard K, Schembri M, Klemm P. Novel Zn^{2+}-chelating peptides selected from a fimbria-displayed random peptide library. Appl Environ Microbiol 2001; 67: 5467-5473.

246. Xu Z, Lee S. Display of polyhistidine peptides on the Escherichia coli cell surface by using outer membrane protein C as an anchoring motif. Appl Environ Microbiol 1999; 65: 5142-5147.

247. Sousa C, Cebolla A, de Lorenzo V. Enhanced metalloadsorption of bacterial cells displaying poly-His peptides. Nat biotechnol 1996; 14: 1017-1020.

248. Beveridge T, Koval S. Binding of metals to cell envelopes of Escherichia coli K-12. Appl Environ Microbiol 1981; 42: 325-335.

249. Isarankura Na Ayudhya C. Engineering of chimeric protein for binding to metal ions. PhD Thesis. Bangkok, Thailand: Mahidol University. 2000.

250. Prachayasittikul V, et al. Interaction analysis of chimeric metal-binding green fluorescent protein and artificial solid-supported lipid membrane by quartz crystal microbalance and atomic force microscopy. Biochem Biophys Res Commun 2005; 327: 174-182.

251. Prachayasittikul V, Isarankura Na Ayudhya C, Tantimongcolwat T, Galla H-J. Nanoscale orientation and lateral organization of chimeric metal-binding green fluorescent protein on lipid membrane determined by epifluorescence and atomic force microscopy. Biochem Biophys Res Commun 2005; 326: 298-306.

252. Bae W, Chen W, Mehra R, Mulchandani A. Heavy metal removal using bacteria displaying synthetic phytochelatins. Preprints of Extended Abstracts presented at the ACS National Meeting, American Chemical Society, Division of Environmental Chemistry 2000; 40: 793-794.

253. Lee S, et al. Functional analysis of the Escherichia coli zinc transporter ZitB. FEMS Microbiol Lett 2002; 215: 273-278.

254. Moreau S, et al. GmZIP1 encodes a symbiosis-specific zinc transporter in soybean. J Biol Chem 2002; 277: 4738-4746.

255. Kirschle C, Huang L. ZnT7, a novel mamalian zinc transporter, accumulates zinc in the golgi apparatus. J Biol Chem 2003; 278: 4096-4102.

256. Baubet V, et al. Chimeric green fluorescent protein-aequorin as bioluminescent Ca2+ reporters at the single-cell level. PNAS 2000; 97: 7260-7265.

257. Nagai T, Sawano A, Park ES, Miyawaki A. Circularly permuted green fluorescent proteins engineered to sense Ca2+. PNAS 2001; 98: 3197-3202.

258. Battistoni A, et al. A histidine-rich metal binding domain at the N terminus of Cu, Zn-superoxide dismutases from pathogenic bacteria: a novel strategy for metal chaperoning. J Biol Chem 2001; 276: 30315-30325.

BIOGRAPHY

NAME	Mr. Somchai Boonpangrak
DATE OF BIRTH	21 July 1975
PLACE OF BIRTH	Bangkok, Thailand
EDUCATION	Mahidol University, 1994-1997 B.Sc. (Medical Technology) Second class honor Mahidol University, 1998-2006 Ph.D. (Medical Technology)
GRANTING SUPPORT	Royal Golden Jubilee Ph.D. Scholarship
ADDRESS	61/397 Preuksa 8 Lantakpha Nakornchisri Nakornprathom 73120 e-mail: g4136468@yahoo.com